DESIGN OF SERVO SYSTEM FOR ROTATIONAL INVERTED PENDULUM BY CDM APPROACH

ADHA IMAM CAHYADI

A THESIS SUBMITTED IN PARTIAL FULFILLMENT OF
THE REQUIREMENTS FOR THE DEGREE OF
MASTER OF ENGINEERING IN CONTROL ENGINEERING
SCHOOL OF GRADUATE STUDIES
KING MONGKUT'S INSTITUTE OF TECHNOLOGY LADKRABANG
2005

ISBN 974-15-1435-2

Thesis Title	Design of Servo System for Rotational Inverted Pendulum by CDM Approach
Student	Adha Imam Cahyadi
Student ID	46067014
Degree	Master of Engineering
Programme	Control Engineering
Year	2005
Thesis Advisor	Assoc. Prof. Dr. Jongkol Ngamwiwit

ABSTRACT

This thesis presents a design of controller by Coefficient Diagram Method (CDM) for a servo type system which is an augmented system constructed from a linearized rotational inverted pendulum with an integrator added to its arm. In order to apply the CDM concept, the augmented system must be converted into controllable canonical form. Then, the controller consisting of the state feedback gain matrix and an integral gain in sense of CDM can be obtained. This shows that design procedure for the proposed controller is easy when compared to the existing methods. The experimental results obtained from the rotational inverted pendulum controlled by the proposed controller show that the system response has no steady-state error while the amplitude of the oscillation of the arm angle is still remarkable. Therefore, in this thesis, the friction compensation using a simple method of Coulomb friction with stiction is also added to the controller. Consequently, the amplitude of the oscillation of the arm angle can be reduced as shown in the experimental results.

The swinging-up of the rotational inverted pendulum will also be presented in this thesis. In order to swing the pendulum up, the position control of the arm angle using proportional plus derivative (PD) control will be used in accordance with the sign of the injected energy to the pendulum. The experimental results show that the pendulum can be brought to the inverted position effectively.

ACKNOWLEDGEMENTS

The process in finishing this thesis is long, hefty and not easy. I will never complete this works without assistances. Therefore, I would like to express sincere appreciation to:

1. My advisor Ajarn Jongkol Ngamwiwit who has been allocated so much time and energy with her extra patience for my research works.
2. My co-advisor Noriyuki Komine Sensei who suggested me some ideas in completing and enhancing my thesis.
3. Ajarn Taworn Benjanarasuth who assisted me some introduction in many mathematical relations, Matlab and simulink tutorials, which I had never known before.
4. Songmoung who helped me in technical matter of my experimental apparatus, thanks for your warm friendship.
5. Pe' Don, Oil, Pe' Noom, Pe' Ekachai and all of the alumni of Control and Mechatronics Laboratory in Research Center for Communication and Information Technology (ReCCIT), KMITL.
6. All of my brothers in Muslim Club who always refresh my lost of soul so that I still keep my *"dien"* tightly with me.
7. My beloved Fafa, for her endless love and encouragements.
8. My Parents, of course, who take care of me a lot even tough they are not with me physically.

I also thank to everybody who had given their assistance to me which I can not mention one by one. Finally, I should give my best gratitude to the AUN-SEED/Net program for their kind full support for the budget and assistance.

CONTENTS

CONTENTS (Cont.)

CONTENTS (Cont.)

LIST OF TABLES

LIST OF FIGURES

LIST OF FIGURES (Cont.)

NOMENCLATURE

a	Acceleration of the pendulum's pivot
a_i	Coefficient of the characteristic polynomial
A	State variable matrix
A_a	State variable matrix of the augmented system
$A_c(s)$	Denominator polynomial of the controller
A_{cl}	Closed-loop state variable matrix
$A_p(s)$	Denominator polynomial of the plant
b	Viscous damping coefficient
B	Input matrix
B_a	Input matrix of the augmented system
$B_a(s)$	Pre-filter
$B_c(s)$	Numerator polynomial of the controller
$B_p(s)$	Numerator polynomial of the plant
c, d	Constants
C	Output matrix
$C(s)$	Output of the system
C_a	Output matrix of the augmented system
$D(s)$	Disturbance entering the system
E_d	Desired energy level in the swing-up control
E_k	Kinetic energy
E_{kc}	Kinetic energy of the centre pillar
E_{km}	Kinetic energy of the pendulum
E_{kt}	Total of the kinetic energy
E_p	Potential energy
E_{pc}	Potential energy of the centre pillar
E_{pm}	Potential energy of the pendulum
E_{pt}	Total of the potential energy
E_t	Total energy
$f(\cdot,\cdot)$	First order nonlinear ordinary differential equation

NOMENCLATURE (Cont.)

F	Torque generated by the friction
$\hat{F}$	Approximation of torque generated by the friction
F_c	Coulomb friction constant
F_s	Stiction constant
$\bar{F}$	Resultant forces acting at the friction joint
g	Gravitational acceleration
G	Matrix of the reference signal
$G(s)$	Plant
H	Output matrix of the augmented system
J	Moment of inertia of the DC motor
J_p	Moment of inertia of the pendulum
k_i	Integral gain
k_j	Coefficient of the denominator of the controller
$\hat{k}_j$	Gains of the transformed system
K	Feedback gain
$\hat{K}$	Augmented feedback gain
l	Length of the pendulum
l_i	Coefficient of the numerator of the controller
L	Lagrangian
m	Mass of the pendulum
n_o	Noise on the output
n	Degree of the system
$P(s)$	Characteristic polynomial
$P_{l1}(s)$	Denominator polynomial
$P_k(s)$	Numerator polynomial
r_x, r_y, r_z	Position of the pendulum in Cartesian coordinate
R	Length of the arm
$r(t), R(s)$	Reference
$S(s)$	Sensitivity function

NOMENCLATURE (Cont.)

t_s	Settling time
$T(s)$	Complementary sensitivity function
T	Transformation matrix
T_s	Sampling period
$u(t)$, $U(s)$	Control signal
$\hat{u}$	Control signal with friction compensation signal
v	Velocity of the pendulum w.r.t. fixed base position
x	State variable of the system
x_a	State variable of the augmented system
x_o	Initial value of the state variable of the system
y	Output of the system
$\overline{y}, \overline{Y}(s)$	Selected output of the system
y_r	Reference input
$z(t)$	Transformed state variable
β	Arm angle
θ	Pendulum angle
δ_i	Coefficient of the open loop characteristic polynomial
γ_i	Stability index
γ_i^*	Stability limit
$\eta(k)$	Angle of the arm or the pendulum at current sampling
Ψ	Swing-up control gain
τ	Equivalent time constant
τ_m	Total torque produced by DC motor
τ_β	External forces applied to the horizontal arm joint
τ_θ	External forces applied to the pendulum joint
ζ	Damping factor

Chapter 1

Introduction

1.1 Statement and Significance of the Problem

Inverted pendulum is a famous tool for testing the effectiveness of many control schemes. Owing to their nonlinearity and unstable characteristic, its controller development had been a great interest of many researchers [1-9]. So far, many controllers had been implemented either linear or nonlinear controllers. The nonlinear controllers guarantee a wide range operation and overcome the hard nonlinearity [3]. In spite of having some drawbacks, a linear controller, however, is easier to be designed and implemented [7-8]. As proposed in [7], a linear controller based on linear quadratic regulator (LQR) with an integrator augmented to the rotating arm angle can satisfy the required specifications. The integrator was needed to reject the steady-state error in controlling the inverted pendulum system due to the disturbance generated by the hardware. Unfortunately the choice in selecting the proper weighting matrix was still trial and error. Furthermore, when the inverted pendulum is linearized by simply neglecting the friction, it will lead to limit cycles, which implies to somewhat oscillatory results [8-9]. As reported in [18], coefficient diagram method (CDM) can satisfy time domain specification and the design is simple. In CDM the stability and speed of the closed-loop system are related to the stability index and the equivalent time constant respectively. Consequently, the desired characteristic polynomial based on these parameters can be composed.

In this thesis, a design of a controller to stabilize the inverted pendulum in upright position while maintaining the arm position angle in certain position using CDM will be presented. As the responses exhibit remarkable oscillation, friction compensation using Coulomb friction with stiction will also be introduced.

The rotational inverted pendulum is a SIMO system with motor torque input and two outputs i.e. the pendulum angle θ and the arm angle β. By employing the Euler-Lagrange method, a nonlinear model of the inverted pendulum system can be obtained. As CDM is applicable to the linear system, the model must be linearized about upright position. After representing the linear model including one augmented integrator in state space form, it will be transformed into controllable canonical form utilizing a transformation matrix [25] so that the CDM concept can be applied. Then, each element of the state feedback gain matrix and the

integral gain can be designed by matching the closed-loop characteristic polynomial of the system to those obtained from the CDM concept.

As an interesting problem faced by almost researchers in inverted pendulum, the swinging-up control of the inverted pendulum will also be presented in this thesis. Some swinging-up ideas recently proposed including sliding-mode control incorporated with arm control [3], feedback linearization [4] and energy control [5]. The energy control [5] will be adopted as an approach in this thesis due to its simplicity. However, the saturation function in its control law could make undesirable hazard in the experimental apparatus. In addition, this swinging-up method did not consider limited sector of the arm angle to avoid the twisted cable in the apparatus. Therefore, in this thesis the position control of the arm angle using PD control designed by CDM in accordance with the energy control is proposed to replace the saturation function in [5]. Consequently, the limited arm sector angle can be achieved and the saturation function can also be replaced effectively by choosing small equivalent time constant τ in designing the arm position control.

1.2 Objective and Research Methodology

Being a famous tool for benchmarking of many control schemes, the study of stabilizing the inverted pendulum is very challenging. The goal is twofold; firstly testing the effectiveness of the controller itself, secondly studying the dynamics of the inverted pendulum control system and possible application of the controller into various field. Moreover, this research become more interesting as

1. The concept of Coefficient Diagram Method will be used as an approach to design the controller. The controller itself will not be in CDM controller but rather than the design of state feedback controller by the concept of CDM. It will be shown that using the same design specifications with the CDM usual controller namely: the equivalent time constant τ and the stability index γ_i we can construct the state-feedback controller which satisfy the stability and responses speed as the CDM.
2. The concept of CDM is applicable for linear system and the design will be more challenging as some problems met in applying the controller to the real system. As the limit cycle caused by the friction is significant, the linearization around the upright position cannot be performed perfectly. Then another type of controller so called the friction compensator must be used in order to reduce the effect of the friction.

In doing the research, three stages were conducted. The first stage is the theoretical phase. In theoretical phase several concepts on control engineering are studied such as the mathematical modelling, modern control system theory, CDM concept and another control design issue obtained from some publications. In this phase, the model of inverted pendulum is also constructed. Assigning Euler-Lagrange method the set of nonlinear first order differential equation of the inverted pendulum representation can be obtained, and then the linearization method is performed to obtain the linear model in the neighborhood of the upright position. From here, the CDM concept is applicable to design either the state feedback or integral controller which is linear controller.

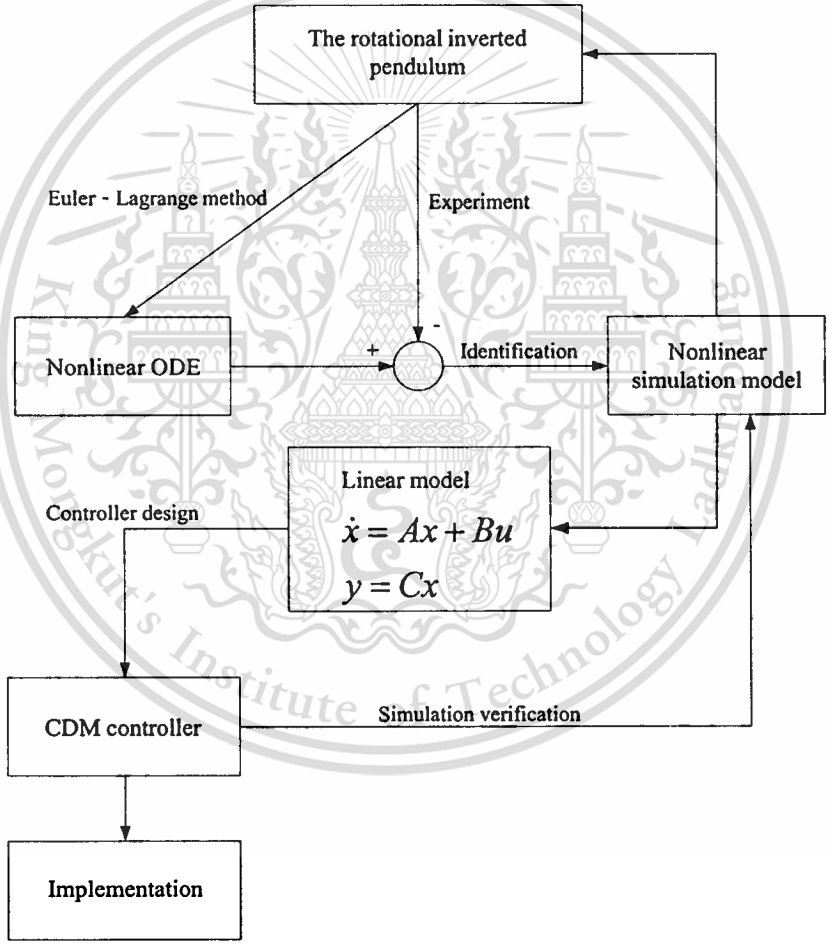

Figure 1.1 Research stages

The next stage is the simulation phase. In this stage, the identification of the inverted pendulum model is done by testing the constructed model in order to minimize the difference between the model and the system output, for the same applied input. The controller is also verified before entering to the next stage. Therefore, the unnecessary loss in time, cost and hazard

can be avoided. Using the results of this stage, the decision can be made whether the controller is well enough or not to be applied to the physical system.

Finally the last stage is the experimental phase where the last test of the controller is performed. The experimental results are then obtained in order to show the effectiveness of the proposed control method. In this stage several problems will arise as the real is always different with the theoretical. This comes from the fact that all practical control problems have a certain amount of uncertainty because of the lack of knowledge.

1.3 Scope

This thesis is organized in 6 chapters including reference and appendices.

Chapter 2 describes about the concept of CDM. The performance specifications in designing a controller by CDM will be explained. Also the stability, speed of the responses and the robustness of the control system will be evaluated by means of coefficient diagram. To get a good insight an example about how to use the coefficient diagram will be presented.

Chapter 3 explains the inverted pendulum. It begins with a kind of inverted pendulum extensively used. Then the model of the rotational inverted pendulum will be formulated using Euler-Lagrange method to get the nonlinear ODE (Ordinary Differential Equation). From here, the linearization will be used to obtain the linear model around the upright position. The friction which is the one of the important factor of many electromechanical designs will also be presented in brief. Finally the identification of the unmeasured parameters will be presented in the end of this chapter.

Chapter 4 is the controller design using CDM approach which is the main chapter in this thesis. The augmented system is derived from the original system by augmenting an integrator in order to achieve the zero steady state-error. As the friction term is significant then a compensation based friction model is presented to reduce the limit cycle. The chapter ends with the swinging-up control of the rotational inverted pendulum, using simple method: position control of the arm angle incorporated with energy control.

In Chapter 5 the simulation and the experimental results will be presented and evaluated. This Chapter will describe the experimental apparatus and their parameters used in experiment. Then the simulation and the experimental results will be presented concurrently. The stability investigation will also be presented using the coefficient diagram.

At last, Chapter 6 will conclude the results of this research and the future works.

Chapter 2

Coefficient Diagram Method

In the present day, basically there are three control approaches i.e. classical control, modern control and polynomial method. The classical control is simple and reliable design approach for the ordinary control design problems, but it is very difficult for the more complex plants. Then the modern control has been developed to answer to this weakness. However, it has not reached to the satisfactory state yet. Another method is polynomial method (or algebraic design approach). In this method, the controller is algebraically obtained from the characteristic polynomial by solving the Diophantine equation. Hence, it is not difficult to define the characteristic polynomial from stability and response specification, but it is very difficult to choose it with guarantee of robustness.

Coefficient Diagram Method (CDM) [18] is one of the polynomial methods in control system design. It has been developed to obtain the easiness in designing the controller. Initially the CDM is not well-known, but its promising results as shown in the application of robotics [11], process control [12-13], space craft altitude control [14] and vibration control [21] have been making some interests for some researchers.

The effectiveness of CDM is mainly obtained from the usage of a diagram called as "Coefficient Diagram". Coefficient diagram shows the coefficient of characteristic polynomial and those of numerator polynomials corresponding to sensitivity and complementary sensitivity function in logarithmic scale, where abscissa is the order of the characteristic polynomial in descending order. From the shape the designer can visualize the stability, response and the robustness. Also the frequency response of the sensitivity and complementary sensitivity function can also be visualized.

2.1 Basic of CDM

2.1.1 Basic Philosophy of CDM

The CDM is an algebraic control design approach with the following five features

1. Polynomials and polynomials matrix are used for system representation
2. Characteristic polynomial and the controller are simultaneously designed
3. Coefficient diagram is effectively utilized

4. The sufficient condition for stability by Lipatov constitutes the theoretical basis of CDM
5. Kessler standard form [3] is improved and used as the standard form of CDM.

CDM design is based on the stability index and equivalent time constant as defined later. Thus for the specified settling time, a controller of the lowest order with the narrowest bandwidth and of no overshoot can be easily designed.

2.1.2 Mathematical Model of CDM

The standard block diagram for the CDM design for a single input single output is shown in Fig. 2.1. The extension to multi input multi output can be made with proper interpretation. The plant equation is given as

$$A_p(s)x = u + d \tag{2.1}$$

$$y = B_p(s)x \tag{2.2}$$

where u, y and d are input, output and disturbance respectively. The symbol x is called the basic state variable. $A_p(s)$ and $B_p(s)$ are denominator and numerator of the plant transfer function respectively. It can be easily seen that this expression has direct correspondence with the control canonical form of the state space expression and x corresponds to the state variable of the lowest order. All the other states are expressed as the derivatives of x of high order. Controller equation is given as

$$A_c(s)u = B_a(s)y_r - B_c(s)(y+n) \tag{2.3}$$

where y_r and n are reference input and noise on the output. $A_c(s)$ is the denominator of the controller transfer function, $B_c(s)$ and $B_a(s)$ are called the reference numerator and the feedback numerator of the controller transfer function. Because this controller has two numerators, it is called two degree of freedom control system. Elimination of y and u of equation (2.3) by equation (2.1) and (2.2) gives

$$P(s)x = B_a(s)y_r + A_c(s)d - B_c(s)n \tag{2.4}$$

where $P(s)$ is the characteristic polynomial and given as

$$P(s) = A_c(s)A_p(s) + B_c(s)B_p(s) \tag{2.5}$$

In a similar manner, equation for y and u can be obtained. Because the system has 3 inputs and 3 outputs, there are 9 transfer functions.

For CDM design, the following four basic relations are selected as standard, namely

$$P(s)x = P(0)y_r, \tag{2.6}$$

$$P(s)y = B_p(s)B_a(s)y_r, \tag{2.7}$$

$$P(s)y = B_p(s)A_c(s)d, \tag{2.8}$$

$$P(s)(-y) = B_p(s)B_c(s)n. \tag{2.9}$$

Equation (2.6) is the response of x to y_r when $B_a(s) = P(0)$, and it is the 0-th order canonical transfer function of $P(s)$. It is a good measure of the stability and the response speed. Equation (2.7) is command following characteristics. Equation (2.8) is for the disturbance rejection characteristics. Equation (2.9) corresponds to the complementary sensitivity function $T(s)$, and it is useful for checking the robustness. In the CDM design, these four basic relations are used as performance specification. The design of $P(s)$ is first made to satisfy specification on equation (2.6), (2.8) and (2.9) and then $B_a(s)$ is adjusted to satisfy the specification on equation (2.7).

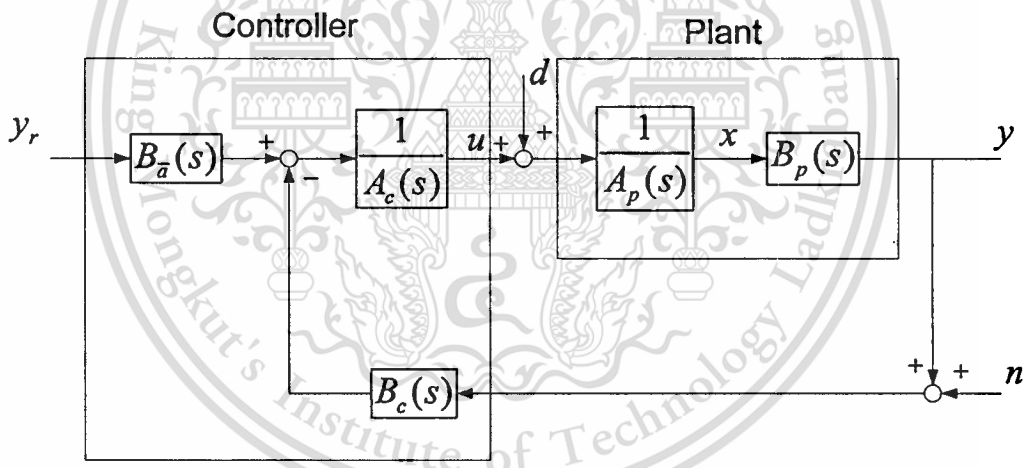

Figure 2.1 Standard CDM block diagram

2.2 Mathematical Relation of CDM

In CDM, the characteristic polynomial is given in the following form

$$P(s) = a_n s^n + \cdots + a_1 s^1 + a_0 = \sum_{i=0}^{n} a_i s^i. \tag{2.10}$$

Based on equation (2.10) the performance specification known as stability index γ_i, equivalent time constant τ and stability limit γ_i^* can be synthesized as these equations

$$\gamma_i = \frac{a_i^2}{a_{i-1}a_{i+1}}, \quad (i = 1,2,\cdots,n-1) \tag{2.11}$$

$$\tau = \frac{a_1}{a_0}, \tag{2.12}$$

$$\gamma_i^* = \frac{1}{\gamma_{i-1}} + \frac{1}{\gamma_{i+1}}, \tag{2.13}$$

where $i = 1 \sim n-1, \quad \gamma_1 = \gamma_n = \infty$.

Then the characteristic polynomial in term of γ_i, τ and a_0 can be expressed back as follows

$$P(s) = a_0 \left[\left\{ \sum_{i=2}^{n} \left(\prod_{j=1}^{i-1} \frac{1}{\gamma_{i-j}^{j}} \right) (\tau s)^i \right\} + \tau s + 1 \right]. \tag{2.14}$$

Notice that $P(s)$ is expressed in $(\tau s)^i$ and its coefficients are function of γ_i. Thus for given γ_i the response shape of the control system is similar irrespective of τ. For different τ, the response speed changes while the response shape remain similar.

2.3 Coefficient Diagram

2.3.1 Motivating Example

In order to visualize the use of coefficient diagram, the example is given. Let the plant and the controller polynomial are as follows

$$A_p(s) = 0.25s^4 + s^3 + 2s^2 + s + 0.2, \quad B_p(s) = 1, \quad A_c(s) = l_1 s, \quad B_c(s) = k_2 s^2 + k_1 s + k_0$$

$$l_1 = 1, \quad k_2 = 1.5, \quad k_1 = 1, \quad k_0 = 0.2, \tag{2.15}$$

then the characteristic polynomial is expressed as

$$P(s) = 0.25s^5 + s^4 + 2s^3 + 2s^2 + s + 0.2. \tag{2.16}$$

Hence,

$$a_i = [a_5 \quad \cdots \quad a_1 \quad a_0] = [0.25 \quad 1 \quad 2 \quad 2 \quad 1 \quad 0.2] \tag{2.17a}$$

$$\gamma_i = [\gamma_4 \quad \cdots \quad \gamma_2 \quad \gamma_1] = [2 \quad 2 \quad 2 \quad 2.5] \tag{2.17b}$$

$$\tau = 5 \tag{2.17c}$$

$$\gamma_i^* = [\gamma_4^* \quad \cdots \quad \gamma_2^* \quad \gamma_1^*] = [0.5 \quad 1 \quad 0.9 \quad 0.5]. \tag{2.17d}$$

The coefficient diagram is shown as in Fig. 2.2, where coefficient a_i is read by the left side scale, and stability index γ_i, equivalent time constant τ and stability limit γ_i^* are read by the right side scale. The τ is expressed by the line connecting 1 to τ. The stability index γ_i can be graphically obtained (Fig. 2.3a). If the curvature of the a_i become larger, the system become more stable,

corresponding to larger stability index γ_i. If the a_i curve is left-end down (Fig. 2.3b), the equivalent time constant τ become small and the response is fast.

The coefficient diagram is also used for parameter sensitivity analysis and robustness analysis. In this example, the characteristic polynomial $P(s)$ is composed of two component polynomials: denominator polynomial $P_{l1}(s)$ and numerator polynomial $P_k(s)$.

$$P(s) = P_{l1}(s) + P_k(s) \tag{2.18}$$

$$P_{l1}(s) = l_1(0.25s^5 + s^4 + 2s^3 + 0.5s^2) \tag{2.19}$$

$$P_k(s) = k_2 s^2 + k_1 s + k_0 . \tag{2.20}$$

The sensitivity and complementary sensitivity functions, $S(s)$ and $T(s)$ are expressed as

$$S(s) = P_{l1}(s)/P(s) \tag{2.21}$$

$$T(s) = P_k(s)/P(s) . \tag{2.22}$$

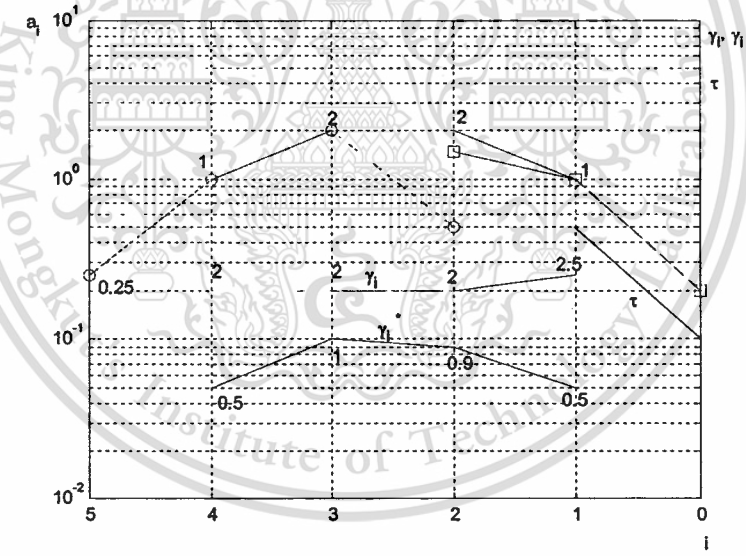

Figure 2.2 Coefficient diagram

Equation (2.19) is shown in Fig. 2.2 with small circles and dash–dot lines. Equation (2.20) is shown with small squares with broken lines. Designer can visually asses the deformation of the coefficient diagram due to the variation of k_2, k_1, k_0. Then he can visualize the variation of stability and response. Also from equation (2.22) it is clear that the robustness can be analyzed by comparison of coefficients a_i and k_i at the coefficient diagram.

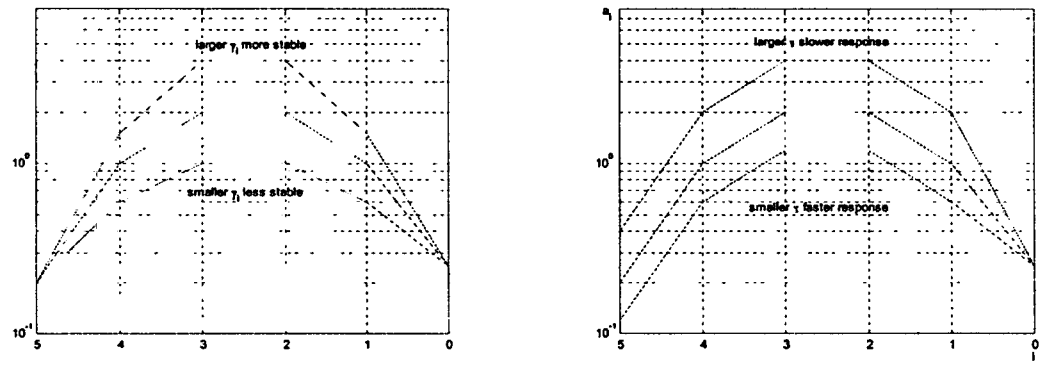

(a) (b)

Figure 2.3 Use of coefficient diagram

Thus the coefficient diagram indicates stability, response and robustness which are three major properties in control system design in a single diagram. It is enabling the designer to grasp the total picture of control system.

2.3.2 Stability Condition

From the Routh-Hurwitz stability criterion, the stability condition for 3rd order system is given as

$$a_2 a_1 > a_3 a_0 . \tag{2.23}$$

If it is expressed by stability index

$$\gamma_2 \gamma_1 > 1 , \tag{2.24}$$

the stability condition for the fourth order is given as

$$a_2 > (a_1 / a_3) a_4 + (a_3 / a_1) a_0 , \tag{2.25}$$

$$\gamma_2 > \gamma_2^* . \tag{2.26}$$

For the system higher than or including 5th degree, Lipatov gave the sufficient condition for stability and instability in several forms [18], [19]. The conditions most suitable for CDM can be stated as follows:

"The system is stable if all the partial 4th order polynomial are stable with the margin of 1.12. The system is unstable if some partial 3rd order polynomial is unstable."

Thus the sufficient condition for stability is given as

$$a_i > 1.12 \left[\frac{a_{i-1}}{a_{i+1}} a_{i+2} + \frac{a_{i+1}}{a_{i-1}} a_{i-2} \right], \tag{2.27}$$

$$\gamma_i > 1.12\gamma_i^*, \text{ for all } i = 2 \sim n-2. \tag{2.28}$$

The sufficient condition for instability is given as

$$a_{i+1}a_i \le a_{i+2}a_{i+1}, \tag{2.29}$$

$$\gamma_{i+1}\gamma_i \le 1, \text{ for some } i = 1 \sim n-2. \tag{2.30}$$

2.4 Standard Form of CDM

Kessler proposed stability index γ_i to be 2 for all i in order to decrease the oscillation and overshoot in the ITAE (Integral Time Absolute Error) form. But it was later found that better response, no overshoot and shorter settling time can be obtained by increasing γ_1 to 2.5. Thus the standard value of CDM is

$$\gamma_{n-1} = \ldots = \gamma_3 = \gamma_2 = 2, \gamma_1 = 2.5. \tag{2.31}$$

and the CDM design has settling time

$$t_s = 2.5\tau \sim 3\tau. \tag{2.32}$$

The feature of the CDM standard form can be summarized as follows:

(1) No overshoot of the type 1 system, and proper overshoot about 40 percent for the type 2 system

(2) The shortest settling time for the same equivalent time constant τ

(3) The similar wave form irrespective to the order of system

(4) The low order poles are of the equal decay. The high order poles are in the sector ±50 degrees from the negative real axis. The damping ratio ζ is 0.65

In the actual design, the choice of the standard stability index is strongly recommended due to the stability and response requirements. However it is not necessary to make $\gamma_4 \sim \gamma_{n-1}$ equal to 2. The condition can be relaxed to

$$\gamma_i > 1.5\gamma_i^*. \tag{2.33}$$

Therefore, the designer has a freedom in designing the controller. Sometimes it is advisable to select the larger stability index, in order to improve the robustness related to the parameters change. From the sufficient condition by Lipatov, stability is guaranteed when all γ_i's are larger than 1.5. Also it was proved that if all γ_i's are greater than 4, all the roots are negative real. Thus, γ_i's are usually chosen between 1.5 to 4. Sometimes the system is built in such manner that some γ_i is larger than the standard value.

Chapter 3

Rotational Inverted Pendulum

Inverted pendulum is a classical example in studying the control system [25], [26]. The motivations are it is simple and not so complex plant; however it is nonlinear and unstable system. Therefore, the development of a controller either for stabilizing or swinging-up the inverted pendulum has been a great interest for many researchers for many years.

3.1 Types of Inverted Pendulum

Basically there are two types of inverted pendulum that is inverted pendulum on cart which is translational, and rotational inverted pendulum as shown in Fig. 3.1.

Figure 3.1 Two basic types of inverted pendulum

As seen in several literatures in order to increase the degree of complexity, some authors extended the inverted pendulum into some types of inverted pendulum namely n-link inverted pendulum which most common example are double inverted pendulum or triple inverted pendulum as depicted in Fig. 3.2. One kind of inverted pendulum which is also developed is dual inverted pendulum as shown in Fig. 3.3.

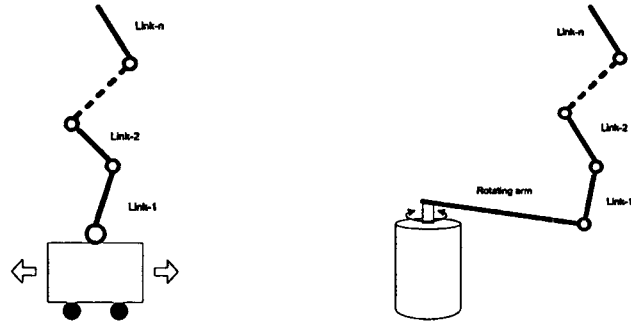

Figure 3.2 Multilink inverted pendulums

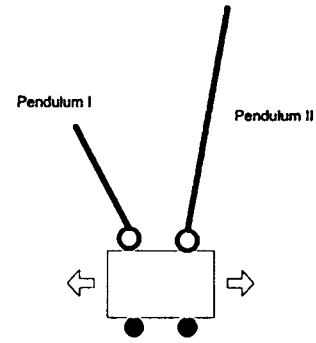

Figure 3.3 Dual inverted pendulums on cart

However, in this thesis the discussion is only focused to stabilize the single rotational inverted pendulum which is controlled by a controller designed using CDM.

3.2 Modelling of the Rotational Inverted Pendulum

The modelling of the inverted pendulum will be presented in this subsection. The inverted pendulum in the laboratory is shown in Fig. 3.4 while its notations and units of parameters are shown in Table 1.

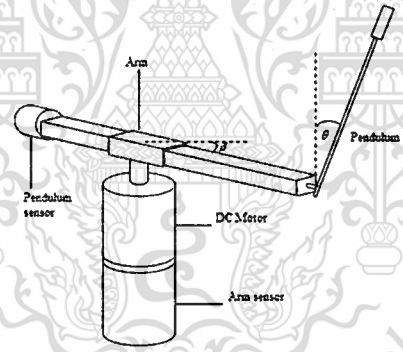

Figure 3.4 Inverted pendulum structure used in laboratory

Table 3.1 Notations and units of the rotational inverted pendulum parameters

Quantity	Symbol	Unit
Arm angle	β	rad
Pendulum angle	θ	rad
Pendulum mass	m	kg
Pendulum length	l	m
Arm length	R	m
Moment of inertia	J	$kg \cdot m^2$
Viscous coefficient	b	$kg \cdot m^2 / s$

In order to derive the dynamics equation of the inverted pendulum, the Lagrange method will be employed. The orientations of the inverted pendulum either the rotating arm or the pendulum are shown in Fig. 3.5. Note that the angles are measured counter clockwise and the zero degree for the inverted pendulum is chosen at the upright position.

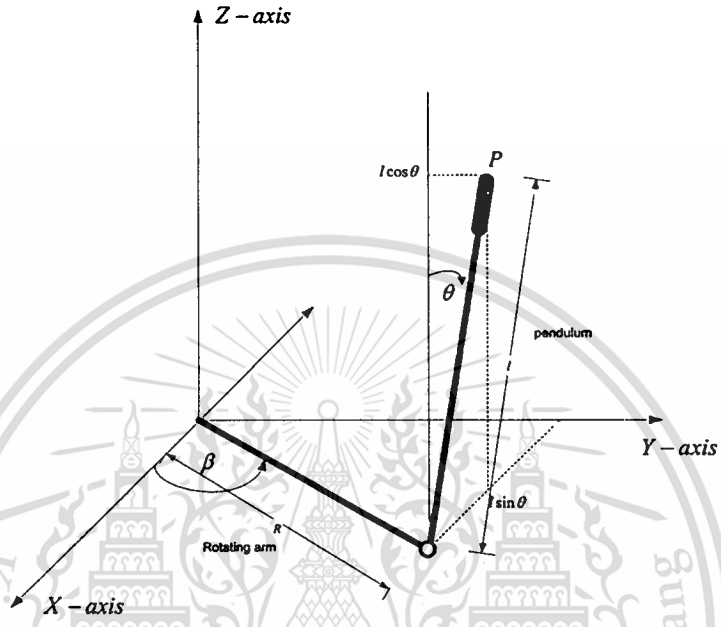

Figure 3.5 Inverted pendulum orientation

3.2.1 Kinematics

For the sake of illustration, as shown in Fig. 3.5 the position of point P in the tip of the rotational inverted pendulum is given as follows

$$r(\beta,\theta)=\left[r_x(\beta,\theta),r_y(\beta,\theta),r_z(\beta,\theta)\right]^T \tag{3.1}$$

where

$$r_x(\beta,\theta)=R\cos\beta-l\sin\beta\sin\theta$$

$$r_y(\beta,\theta)=R\sin\beta+l\cos\beta\sin\theta$$

$$r_z(\beta,\theta)=l\cos\theta\,.$$

The velocity of this point can be obtained by taking the partial derivative of equation (3.1) with respect to the variables which are the arm angle β and the pendulum angle θ as

$$v(\beta,\theta)=\left[v_x(\beta,\theta),v_y(\beta,\theta),v_z(\beta,\theta)\right]^T \tag{3.2}$$

where

$$v_x(\beta,\theta) = -R\sin\beta\dot{\beta} - l\cos\theta\sin\beta\dot{\theta} - l\sin\theta\cos\beta\dot{\beta}$$

$$v_y(\beta,\theta) = R\cos\beta\dot{\beta} + l\cos\theta\cos\beta\dot{\theta} - l\sin\theta\sin\beta\dot{\beta}$$

$$v_z(\beta,\theta) = -l\sin\theta\dot{\theta}.$$

In order to express the kinetic energy expression which will be used later, the square of the velocity of point P is derived as

$$v^2(\beta,\theta) = (R^2 + l^2\sin^2\theta)\dot{\beta}^2 + 2Rl\cos\theta\dot{\beta}\dot{\theta} - l^2\dot{\theta}^2. \tag{3.3}$$

The position, velocity and the square of velocity of any points in the inverted pendulum can also be found accordingly by proper interpretation.

3.2.2 Energy Expression

From Fig. 3.5 it is clear that the energy can be found from its position and velocity of every point of the inverted pendulum control system by these following two equations

$$E_k = \frac{1}{2}\int v^2 dm \tag{3.4}$$

$$E_p = g\int r_z dm. \tag{3.5}$$

Equation (3.4) corresponds to the kinetic energy expression while equation (3.5) is the potential energy expression. Using these two equations the energy expression of each part of the rotational inverted pendulum can be found respectively. It should be noted that the reference of the potential energy is chosen in the level of the inverted pendulum arm. Therefore, any position below the inverted pendulum arm will have negative potential energy and vice versa.

Centre pillar is the junction between the actuator which is the DC motor and the arm of the pendulum. In the center pillar, the effect of friction from the coupled DC motor is ineligible. The moment of inertia is also significant. However, for the sake of linearity, the friction term will be omitted and treated separately in the next subsection. In this part, the energy expression then can be written as

$$E_{kc} = \frac{1}{2}J\dot{\beta}^2 \tag{3.6}$$

$$E_{pc} = 0. \tag{3.7}$$

The arm and the rod of the pendulum are made from aluminum. Compared to the inverted pendulum load, the weight of this part is small; this implies the small moment of inertia. As the energy is a function of both mass and moment of inertia, the energy in this part could be neglected.

Our attention now is to the mass of the inverted pendulum which has ineligible potential and kinetic energy. In this part the kinetic and potential energy can be formulated from equation (3.4) and (3.5) as

$$E_{km} = \frac{1}{2}\left[m(R^2 + l^2\sin^2\theta)\dot{\beta}^2 + 2mRl\cos\theta\dot{\beta}\dot{\theta} + ml^2\dot{\theta}^2\right] \tag{3.8}$$

$$E_{pm} = mgl\cos\theta\,. \tag{3.9}$$

Therefore, the total kinetic energy and the total potential energy from every part of the inverted pendulum system are respectively as follows

$$E_k = E_{kc} + E_{km} \tag{3.10}$$

$$E_p = E_{pc} + E_{pm} \tag{3.11}$$

3.2.3 Equation of Motion

Using the computed energy, either potential energy or kinetic energy, the Lagrangian of the rotational inverted pendulum can be written down as

$$L = E_k - E_p\,. \tag{3.12}$$

Then the following relations must hold

$$\frac{d}{dt}\frac{\partial L}{\partial \dot{\beta}} - \frac{\partial L}{\partial \beta} = \tau_\beta \tag{3.13}$$

$$\frac{d}{dt}\frac{\partial L}{\partial \dot{\theta}} - \frac{\partial L}{\partial \theta} = \tau_\theta = 0\,, \tag{3.14}$$

with τ_β and τ_θ being the external forces applied to the horizontal arm joint and the pendulum joint respectively. The external forces acting on the horizontal arm joint τ_β is the acting torque produced by the DC motor, and it can be formulated by

$$\tau_\beta = \tau_m - b\dot{\beta} - \text{N.F.T.} \tag{3.15}$$

where N.F.T. stands for the nonlinear friction term and τ_m is total torque produced by the DC motor. On the other hand, τ_θ can be assumed to be zero as no external force exerts on the vertical joint. Then the partial derivatives are as follows

$$\frac{\partial L}{\partial \beta} = 0 \tag{3.16}$$

$$\frac{\partial L}{\partial \dot{\beta}} = m(R^2 + l^2 \sin^2\theta)\dot{\beta} + mRl\cos\theta\dot{\theta} + J\dot{\beta} \tag{3.17}$$

$$\frac{\partial L}{\partial \theta} = ml^2 \sin\theta\cos\theta\dot{\beta}^2 - mRl\sin\theta\dot{\beta}\dot{\theta} + mgl\sin\theta \tag{3.18}$$

$$\frac{\partial L}{\partial \dot{\theta}} = mRl\cos\theta\dot{\beta} + ml^2\dot{\theta}. \tag{3.19}$$

Substituting equation (3.16)-(3.19) to equation (3.13)-(3.14), we have

$$(J + mR^2 + ml^2\sin^2\theta)\ddot{\beta} + 2ml^2\sin\theta\cos\theta\dot{\beta}\dot{\theta} + mRl\cos\theta\ddot{\theta} - mRl\sin\theta\dot{\theta}^2 = \tau_\beta \tag{3.20}$$

$$mRl\cos\theta\ddot{\beta} + ml^2\ddot{\theta} - ml^2\sin\theta\cos\theta\dot{\beta}^2 - mgl\sin\theta = \tau_\theta = 0. \tag{3.21}$$

Equation (3.20) and (3.21) can be rewritten in the form of first order system of differential equations as

$$\frac{d\theta}{dt} = \dot{\theta} \tag{3.22}$$

$$\frac{d\dot{\theta}}{dt} = \frac{1}{J + (mR^2 + ml^2)\sin^2\theta}\Big[-2ml^2\sin\theta\cos\theta\dot{\beta}\dot{\theta} - mlR\sin\theta\cos^2\theta\dot{\beta}^2 - mRg\sin\theta\cos\theta + mRl\sin\theta\dot{\theta} + \tau_\beta\Big] \tag{3.23}$$

$$\frac{d\beta}{dt} = \dot{\beta} \tag{3.24}$$

$$\frac{d\dot{\beta}}{dt} = \frac{1}{J + (mR^2 + ml^2)\sin^2\theta}\Big[\frac{J + mR^2 + ml^2\sin^2\theta}{R\cos\theta}\left(l\sin\theta\cos\theta\dot{\beta}^2 + g\sin\theta\right) - 2ml^2\sin\theta\cos\theta\dot{\beta}\dot{\theta} - mRl\sin\theta\dot{\theta}^2 - \tau_\beta\Big]. \tag{3.25}$$

In the compact form those can be expressed as

$$\dot{x} = f(x,u) \tag{3.26}$$

where $x = \begin{bmatrix}\theta & \dot{\theta} & \beta & \dot{\beta}\end{bmatrix}^T$ and $u = \tau_\beta$.

3.2.4 Equilibrium Points

The equilibrium points are defined as the roots of the equation $f(x,u) = 0$. Hence, the equilibrium points of system (3.26) can be obtained by inserting $\dot{\theta} = \ddot{\theta} = \dot{\beta} = \ddot{\beta} = 0$ which implies to $x = \begin{bmatrix}2n\pi & 0 & c & 0\end{bmatrix}^T$ or $x = \begin{bmatrix}(2n+1)\pi & 0 & c & 0\end{bmatrix}^T$ with $u = \tau_\beta = 0$ where n is any integer greater than or equal to zero. The first equilibrium points correspond to the upright position, while

the second are the hanging position. As $\ddot{\beta}$ is connected equilibrium point, the characteristic of equilibrium points θ in our system can be visualized by drawing its phase portrait. The phase portrait of the inverted pendulum using only θ and $\dot{\theta}$ are shown in Fig. 3.6. It is seen from the figure that the first equilibrium points are saddle point which is unstable while the second are stable focus. Therefore the upright positions are unstable equilibrium points.

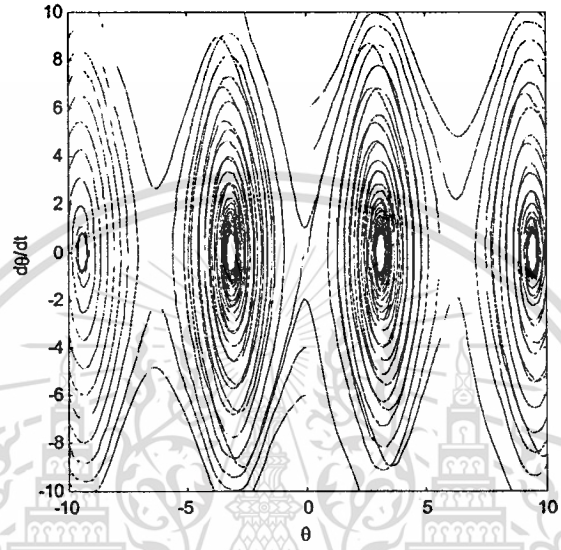

Figure 3.6 Phase portrait of θ and $\dot{\theta}$

3.2.5 Linearization

As we only interest to design the controller on upright position i.e. $\theta = 0$ for $x_o = [0 \quad 0 \quad 0 \quad 0]^T$ and $u = 0$, by neglecting the nonlinear friction term on τ_β to be

$$\tau_\beta = \tau_m - b\dot{\beta} \tag{3.27}$$

then the linearized state equation can be obtained as

$$\frac{dx}{dt} = \left.\frac{\partial f(x,u)}{\partial x}\right|_{x=0} + \left.\frac{\partial f(x,u)}{\partial u}\right|_{u=0} = Ax + Bu \tag{3.28}$$

where the system matrix A and input vector B are

$$A = \begin{bmatrix} 0 & 1 & 0 & 0 \\ \frac{g(J+mR^2)}{Jl} & 0 & 0 & \frac{Rb}{Jl} \\ 0 & 0 & 0 & 1 \\ -\frac{mRg}{J} & 0 & 0 & -\frac{b}{J} \end{bmatrix} \text{ and } B = \begin{bmatrix} 0 \\ -\frac{R}{Jl} \\ 0 \\ \frac{1}{J} \end{bmatrix}.$$

Respectively, the characteristic polynomial of (3.28) is then given as follows

$$P(s) = sI - A$$

$$= s^4 + \frac{bl - Jl}{Jl}s^3 + \frac{(-gJ - gmR - bl)}{Jl}s^2 - \frac{gb}{Jl}s, \tag{3.29}$$

which can be seen that there is one integrator in the plant. From Routh –Hurtwitz stability criterion the system is also unstable as one of the coefficients of the polynomial is negative. Therefore, at least one of the roots is unstable root.

As the main interests are the rotating arm angle β and the pendulum angle θ then the output equation can be given by

$$y = Cx \tag{3.30}$$

where $C = \begin{bmatrix} 1 & 0 & 0 & 0 \\ 0 & 0 & 1 & 0 \end{bmatrix}^T$.

3.3 Frictions

As described in [16] and [17], friction can generate limit cycles with cannot be simply neglected otherwise it will lead to the oscillatory system. However, except the viscous friction, the other friction components such as coulomb friction and stiction friction are nonlinear quantities that cannot be linearized. Therefore, the effect of the friction will be treated separately by the so called friction compensation. Some of friction models extensively used will be described in the following parts.

3.3.1 Coulomb Friction

The Coulomb friction, which is the most commonly used friction model, can be expressed in mathematical form as

$$F = F_c \operatorname{sgn}(\dot{\beta}). \tag{3.31}$$

A friction estimation used for compensation is obtained from this mathematical model as

$$\hat{F} = \begin{cases} F_c \operatorname{sgn}(\dot{\beta}) & \text{if } |\dot{\beta}| > \delta v \\ F_c v / \delta v & \text{if } |\dot{\beta}| \le \delta v \end{cases}. \tag{3.32}$$

The friction estimation however is non-smooth, which can be a problem in certain applications. The constant δv is used to avoid the discontinuity at $\dot{\beta} = 0$. Although very simple, this model captures the essential behavior of friction and has been shown in many applications. Fig. 3.7a shows the representation of the coulomb friction.

3.3.2 Coulomb Friction with Stiction

Stiction is the phenomenon that initiating a motion requires a larger force than retaining it. The simplest memoriless friction model with stiction is as follows

$$\hat{F} = \begin{cases} F_c \operatorname{sgn}(\dot{\beta}) & \text{if } \dot{\beta} \neq 0, \\ \bar{F} & \text{if } \dot{\beta} = 0 \text{ and } |\bar{F}| < F_s, \\ F_s \operatorname{sgn}(\bar{F}) & \text{otherwise} \end{cases} \tag{3.33}$$

with $\bar{F}$ being the resultant forces acting at the friction joint. It should be noted that this friction model is a function of $\dot{\beta}$ and $\bar{F}$. This model effectively removes the friction. However, the control signal becomes discontinuous and chattering at velocities close to zero.

There are numbers of more complicated friction models such as friction observer and coulomb friction with Stibeck effect which is used to compensate the friction more effectively. However in this thesis, only the above two models will be applied as the friction is not the main emphasis of this thesis.

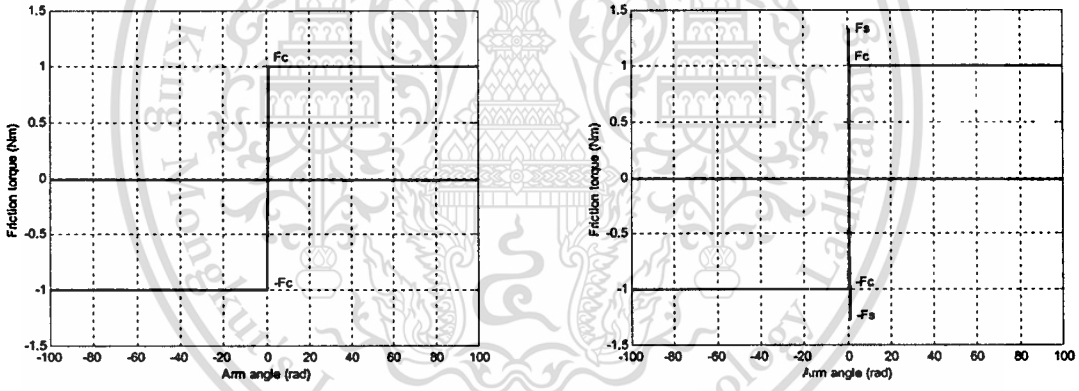

(a) Coulomb friction (b) Coulomb friction with stiction

Figure 3.7 Friction models

3.4 Parameters Identification

As several parameters of inverted pendulum cannot be obtained directly by measurement, the offline identification is done in order to find the values of the parameters. Firstly, the first order differential equation model of inverted pendulum model is composed by using the Matlab's m-file and simulink as shown in Appendix A. Then the open-loop response of the inverted pendulum is measured. Finally, utilizing the Matlab optimization toolbox whose source code is also attached in Appendix A, the unknown parameter is optimized by fitting the simulation result to the plant's measurement data.

The step of the plant parameters identification is depicted in Fig. 3.8. The plant parameters that need to be identified are the DC motor moment of inertia J, the viscous friction coefficient b and the Coulomb and stiction constant F_c and F_s respectively. The results of parameter identification are compared to the real experiment and will be presented at chapter 5.

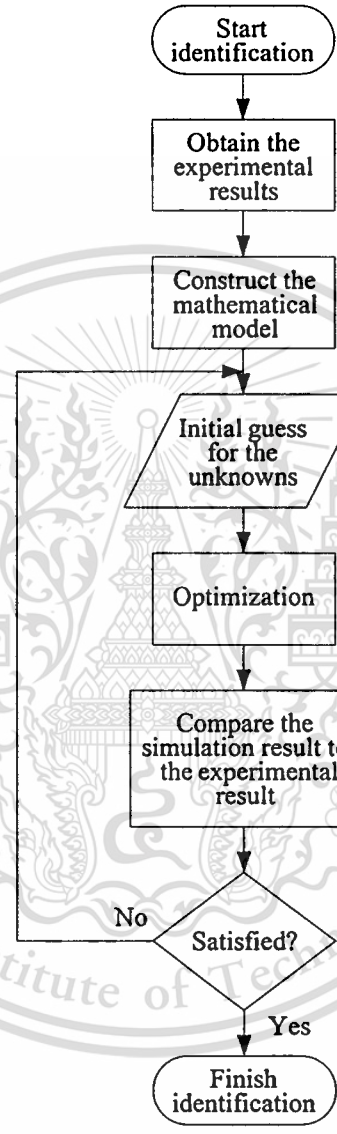

Figure 3.8 Process of parameters identification

Chapter 4

Controller Design

In this Chapter, the controller design procedure will be described. The stabilizing control designed using CDM approach including friction compensation will be presented first. Then the swinging-up control will also be presented in spite of not the main interest in this thesis. As mentioned in the previous chapter, the linearization around upright position cannot be performed easily due to the significant friction term. Therefore, in the linearized model the friction term is treated separately by using compensator. For CDM which is developed for a class of linear system, in order to design the controller, the nonlinear model (3.26) will be suppressed and represented only by its linearized model around upright position as given in (3.28). For the swinging-up control, the inverted pendulum at upright position cannot be stabilized by using only swinging-up control. Consequently, around the upright position the swinging-up control law must be switched into stabilizing control law. The control strategy for the swinging-up and the stabilizing control is shown in Fig. 4.1.

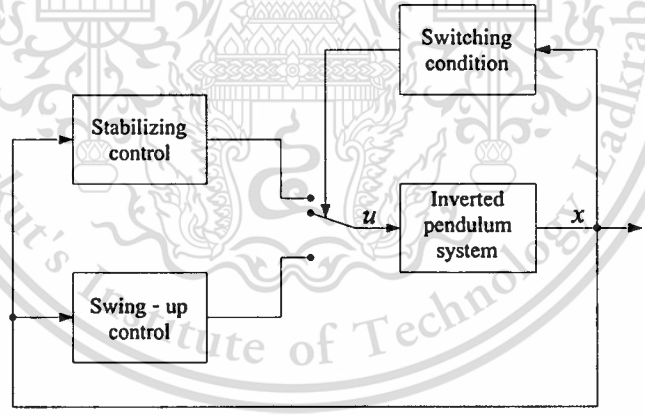

Figure 4.1 Control strategy

4.1 Stabilizing Control Structure

The control system structure with the state feedback gain matrix and compensation is depicted in Fig. 4.2. As shown later, this control system structure has main drawback i.e. the offset appeared in the output mainly the rotating arm angle β. This error occurs as we do not really know the parameters of the system. In order to achieve the asymptotic stability these errors need to be rejected. As stated by Khalil in [26], integral control approach can be used to ensure asymptotic regulation under all parameter perturbations that do not destroy the stability of the

closed-loop system. Hence, an integrator is augmented to the system as shown in Fig. 4.3 and it is called as the augmented system.

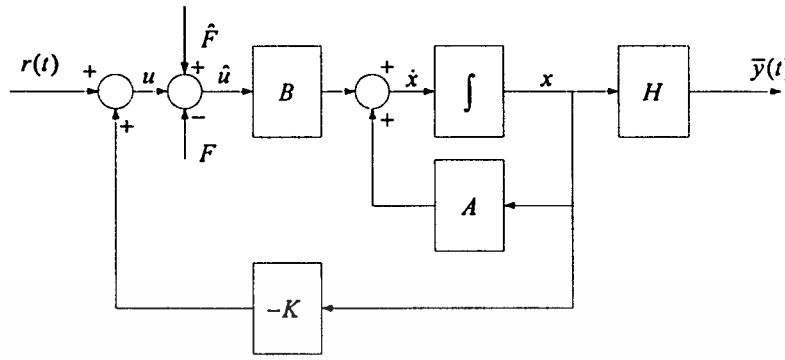

Figure 4.2 State feedback system with compensation

Using the augmented system, the offset appeared in the outputs could be rejected effectively; however the order of the system will be increased by one, which implies to a higher order controller.

Defining

$$\dot{x}_i(t) = r(t) - Hx(t) \tag{4.1}$$

then the state equation and output equation of the augmented system shown in Fig. 4.3 can be given as follows:

$$\dot{x}_a(t) = A_a x_a(t) + B_a u(t) + Gr(t) \tag{4.2}$$

$$y(t) = C_a x_a(t), \tag{4.3}$$

where

$x_a = \begin{bmatrix} x \\ x_i \end{bmatrix}, A_a = \begin{bmatrix} A & 0 \\ -H & 0 \end{bmatrix}, B_a = \begin{bmatrix} B \\ 0 \end{bmatrix}, G = \begin{bmatrix} 0 \\ 1 \end{bmatrix}$ and $C_a = \begin{bmatrix} C \\ 0 \end{bmatrix}^T$, $r(t)$ is the reference signal to the arm angle, $H = \begin{bmatrix} 0 & 0 & 1 & 0 \end{bmatrix}$ is derived from the second row of C matrix and $x_i(t)$ is the state variable obtained by augmenting an integrator to the arm angle.

If the pair of A and B in (3.28) is controllable and $A_a = \begin{bmatrix} A & B \\ -H & 0 \end{bmatrix}$ is full rank, then the augmented system is completely state controllable. Therefore, the control law $u(t)$ can be assigned as

$$u(t) = -K_a x_a(t) \tag{4.4}$$

where $K_a = [K \quad -k_i]$ and where $K = [k_1 \quad k_2 \quad \ldots \quad k_{n-2} \quad k_{n-1}]$ is the state feedback gains matrix and $k_i = -k_n$ is the integral gain. Then the following relation can be obtained as

$$\dot{x}_a(t) = (A_a - B_a K_a) x_a(t) + Gr(t) = A_{cl} x_a(t) + Gr(t). \tag{4.5}$$

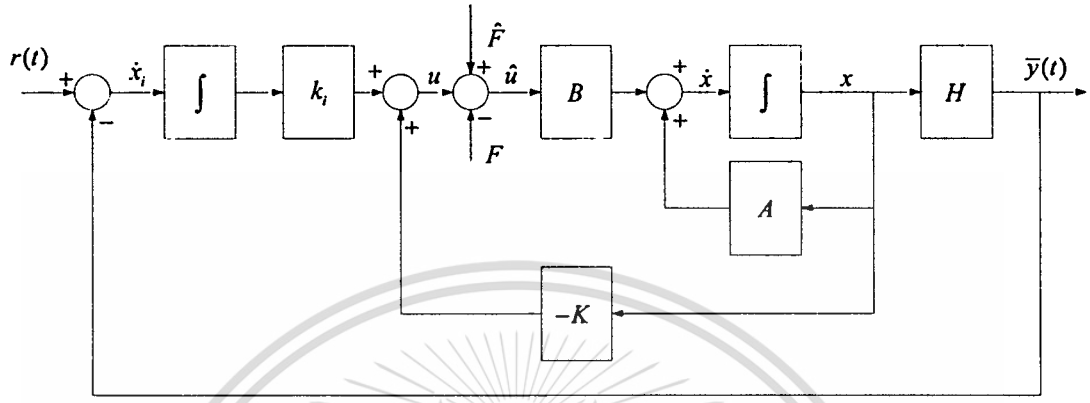

Figure 4.3 Control system structure

Therefore, the origin of system (3.26) using equation (4.5) can be made locally stable around the upright position by choosing the state feedback gains matrix K and the integral gain k_i such that $A_a - B_a K_a$ is Hurwitz.

4.2 CDM Controller

In this sub-section, the design procedure for assigning the feedback gain matrix K and integral gain k_i of the system shown in Fig. 4.3 by CDM is proposed. It can be done by matching the closed-loop characteristic polynomial of equation (4.5) to the characteristic polynomial designed by CDM. The generalized controller design can be characterized as the following procedure:

1. Transform the closed-loop system (4.5) into controllable canonical form as

$$\dot{z}(t) = T^{-1} A_{cl} T z(t) + T^{-1} G r(t) \tag{4.6}$$

by introducing a new state $z(t) = T^{-1} x_a(t)$. The transformation matrix T is defined as $T = MW$, where M and W are given by [25]

$$M = [B_a \quad A_a B_a \quad A_a^2 B_a \quad \cdots \quad A_a^{n-1} B_a]$$

$$W=\begin{bmatrix} \delta_1 & \delta_2 & \cdots & \delta_{n-1} & 1 \\ \delta_2 & \delta_3 & \cdots & 1 & 0 \\ \vdots & \vdots & & 0 & 0 \\ \delta_{n-1} & 1 & \cdots & 0 & 0 \\ 1 & 0 & \cdots & 0 & 0 \end{bmatrix},$$

and where $\delta_{n-1},\delta_{n-2},...,\delta_1$ are the coefficient of the open-loop characteristic polynomial $P_o(s)=|sI-A_a|=s^n+\delta_{n-1}s^{n-1}+\ldots+\delta_1 s+\delta_0$.

2. Find the closed-loop characteristic polynomial of system (4.6) as

$$P_{cl}(s)=|sI-T^{-1}A_{cl}T|$$

$$=s^n+(\delta_{n-1}+\hat{k}_n)s^{n-1}+(\delta_{n-2}+\hat{k}_{n-1})s^{n-2}+\ldots+(\delta_0+\hat{k}_1), \tag{4.7}$$

where

$$K_aT=\begin{bmatrix}\hat{k}_1 & \hat{k}_2 & \cdots & \hat{k}_{n-1} & |\hat{k}_n\end{bmatrix}. \tag{4.8}$$

3. Choose the equivalent time constant τ and the stability index γ_i and derive the desired characteristic polynomial

$$P(s)=s^n+\sum_{i=2}^{n-1}\left(\prod_{j=i}^{n-1}\gamma_j^{n-j}\prod_{k=1}^{i-1}\gamma_k^{n-i}\frac{1}{\tau^{n-i}}s^i\right)+\sum_{i=0}^{1}\left(\prod_{j=1}^{n-1}\gamma_{n-j}^{j}\frac{1}{\tau^{n-i}}s^i\right)$$

$$=s^n+a_{n-1}s^{n-1}+\cdots+a_1s^1+a_0 \tag{4.9}$$

from the characteristic polynomial in equation (2.14) which is assumed to be monic (i.e. $a_n=1$) so that $a_0=(\prod_{j=1}^{n-1}\gamma_{n-j}^{j})/\tau^n$. The derivation of equation (4.9) is shown in Appendix B.

4. Finally we can equate the closed-loop characteristic polynomial (4.7) with the desired characteristic polynomial (4.9) to obtain

$$K_a=\begin{bmatrix}a_0-\delta_0 & a_1-\delta_1 & \ldots & a_{n-2}-\delta_{n-2} & |a_{n-1}-\delta_{n-1}\end{bmatrix}T^{-1}. \tag{4.10}$$

By using the CDM concept the poles can be located in favorable region according to the design specification. In case of the rotational inverted pendulum, using the model given in Chapter 3, the state feedback gains matrix and the integral gain can be obtained by setting n to 5. If we do not want to augment the integrator to the system then $n=4$ will be used. In the next chapter the closed-loop pole location from the real experiment and the coefficient diagram will be shown.

4.3 Friction Compensation

The friction compensation is introduced because of the ineligible limit cycles generated mainly by motor driving the arm. Some methods for friction compensation have been described in [8]. However, a simple method of Coulomb friction with stiction $\hat{F}$ which can effectively reduce the oscillation amplitude is rewritten from equation (3.33) as

$$\hat{F} = \begin{cases} F_c \operatorname{sgn}(\dot{\beta}) & \text{if } \dot{\beta} \neq 0, \\ \bar{F} & \text{if } \dot{\beta} = 0 \text{ and } |\bar{F}| < F_s, \\ F_s \operatorname{sgn}(\bar{F}) & \text{otherwise} \end{cases} \tag{4.11}$$

where F_c is the coulomb friction constant, F_s is the stiction constant and $\bar{F}$ is the resultant forces acting on the slip ring. In this case $\bar{F} = \frac{-mgR}{J}x_1(t) + \frac{-b}{J}x_4(t) + \frac{1}{J}u(t)$ which is the unit of arm angle angular acceleration.

The friction compensation added to the system is shown in Fig. 4.3 and then is applied to the control law as

$$\hat{u} = K_a x_a + \hat{F}. \tag{4.12}$$

It should be noted here that the friction in this case is treated as disturbance entered to the control system and it is compensated by adding the signal generated by the friction model. As the friction model used is discontinue then there is some scattering appeared in the control law $\hat{u}$.

4.4 Swinging-up Control

The swinging-up of the rotational inverted pendulum is the minor issue of this thesis. It is described because of the interesting problem faced by most researchers of the inverted pendulum. Some swinging-up ideas recently proposed including sliding-mode control incorporated with arm control [3], feedback linearization [4] and energy control [5]. The simplest method is the swinging-up control of the inverted pendulum using energy control scheme proposed by Astrom and Furuta [5] which will be used as an approach in this thesis.

The swinging-up strategy using energy control is simple. First the energy is pumped to the system to collect the energy until the desired energy level of the upright position then switch the control law to u to catch and stabilize the inverted pendulum into upright position. The way of pumping the energy is by giving some acceleration to the pendulum pivot, which is the arm angle, based on the information of the sign of the injected energy. The swinging-up control is performed until the prescribed energy level can be achieved. On the other words, when the

pendulum angle θ can be brought into prescribed sector of angle, the swinging-up control of the pendulum is then switched to stabilizing control as described in section 4.1 and 4.2.

Although our inverted pendulum is rotational, for the sake of computation simplification, we will use the pendulum on cart model instead of the complete model developed in the previous chapter. If we fix the base of the pendulum into its arm as shown in Fig. 4.4 then the model can be simplified to be [5]

$$J_p \frac{d^2\theta}{dt^2} = \frac{1}{2}(mgl\sin\theta - mla\cos\theta) \tag{4.13}$$

where J_p is the moment of inertia of the pendulum and a is the acceleration of the rotating arm or in this case

$$R\frac{d^2\beta}{dt^2} = a. \tag{4.14}$$

Figure 4.4 Inverted pendulum when the base is fixed to its arm

It should be noted here that in designing the state feedback gains and the integral gain, the pendulum's moment of inertia J_p is neglected. However, in the swinging-up control it is considered otherwise the equation of motion (4.13) will be meaningless without considering the pendulum's moment of inertia J_p.

The total energy of equation (4.13) is given by

$$E = \frac{1}{2}J_p\dot{\theta}^2 + mgl\cos\theta. \tag{4.15}$$

It should be noticed that the potential energy is still chosen such that the arm position has zero energy level. In order to know the energy is pumped correctly we must obtain the direction whether the energy is injected or removed from the system. It can be determined from the rate of energy as

$$\dot{E} = J_p \dot{\theta}\ddot{\theta} - mgl\dot{\theta}\sin\theta = -mal\dot{\theta}\cos\theta . \tag{4.16}$$

The last equation tells us that the energy can be pumped to the system when the arm acceleration a is in the opposite direction of $\dot{\theta}\cos\theta$. If the acceleration is enough, we can drive the energy to desired level then we set acceleration to zero, at which the inverted pendulum can be swung up in one swing. If the acceleration is not enough, we can apply the maximum arm angle acceleration, however multiple swings will be needed to bring the pendulum to the inverted position. As described in Appendix C, the appropriate control law is chosen as follows

$$u = mRa = mR \cdot sat(\Psi(E - E_d) \cdot \mathrm{sgn}(\dot{\theta}\cos\theta)) . \tag{4.17}$$

where Ψ is a constant gain, E_d is the desired energy level, sgn is the sign function and sat is the saturation function as explained in Appendix C.

However, the main drawback of this control law is the safety of the experiment. As the energy is computed using information of state equations, the accuracy of its information relies on the accuracy of the state variables as well. Therefore, it is very difficult to achieve desired energy level even some tolerance is given. Moreover, the saturation function will sense whatever small it is. This situation will lead to harm the apparatus as the DC motor using maximum torque will always be applied.

In our case, it is very difficult to apply the control law (4.17), because some of the state variables cannot be measured and are only obtained by the approximation using backward difference which will be mentioned in section 4.5. Therefore, the desired energy level will be almost impossible to be reached by the energy computation. Instead, here we propose position control of the arm angle to replace the saturation function in (4.17). The advantage of this method is the arm angle always swings in restricted sector of angles or never rotates in full rotation. Therefore, some kinds of harm like twisted cable in the experiment can be avoided.

In order to swing the pendulum up, let's consider the arm angle equation of motion (3.25) which is also the 4th row of the inverted pendulum equation of motion (3.26) as

$$\frac{d\dot{\beta}}{dt} = \frac{1}{J + (mR^2 + ml^2)\sin^2\theta}\left[\frac{J + mR^2 + ml^2\sin^2\theta}{R\cos\theta}\left(l\sin\theta\cos\theta\dot{\beta}^2 + g\sin\theta\right)\right. \\ \left. - 2ml^2\sin\theta\cos\theta\dot{\beta}\dot{\theta} - mRl\sin\theta\dot{\theta}^2 - \tau_\beta\right]. \tag{4.18}$$

In the swinging-up stage it is reasonable to assume that all of the inertia factors of the inverted pendulum are small compared with the DC motor moment of inertia. Then equation (4.18) can be simplified to be

$$\frac{d\dot{\beta}}{dt} = \ddot{\beta} = \frac{1}{J}(-\tau_m + b\dot{\beta}), \tag{4.19}$$

which is linear. Therefore, the transfer function of the arm angle β to the DC motor torque τ_m is given by

$$\frac{\bar{Y}(s)}{U(s)} = -\frac{1}{Js^2 - bs}. \tag{4.20}$$

In order to control the position of the rotating arm angle, the PD controller is going to be employed. As shown in Fig. 4.5 the control law then is given by

$$u = k_p(r - \beta) - k_d\dot{\beta}, \tag{4.21}$$

or in the frequency domain it can be rewritten as

$$U(s) = k_p\left(R(s) - \bar{Y}(s)\right) - k_d s\bar{Y}(s). \tag{4.22}$$

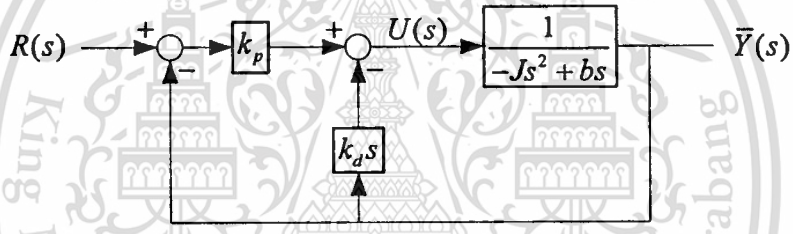

Figure 4.5 Position control of the arm angle

Therefore, the closed-loop transfer function from $\bar{Y}(s)$ to $R(s)$ is as follows

$$\frac{\bar{Y}(s)}{R(s)} = \frac{k_p}{-Js^2 + (b + k_d)s + k_p}. \tag{4.23}$$

It is proposed that the proportional and the derivative gains will be designed by CDM. Using equation (2.14) as described in Chapter 2, the desired characteristic polynomial is composed as follows

$$P(s) = a_0\left(\frac{\tau^2}{\gamma_1}s^2 + \tau s + 1\right). \tag{4.24}$$

By matching the coefficient of the polynomial in equation (4.23) and equation (4.24) the proportional gain k_p and the derivative gain k_d can be obtained respectively as follows

$$k_p = -J\frac{\gamma_1}{\tau^2}, \tag{4.25}$$

$$k_d = k_p \tau - b \,. \tag{4.26}$$

In order to swing the inverted pendulum up, this arm angle position control is combined with the energy control. The direction of the energy term $\dot{\theta}\cos\theta$ in equation (4.16) is incorporated to the direction of reference angle in the control law (4.22) to be

$$r = -r_c \,\mathrm{sgn}(\dot{\theta}\cos\theta) \tag{4.27}$$

where r_c is the positive reference constant. Consequently, the control law proposed by [5] in equation (4.17) can be replaced using position control of the arm angle and its energy rate information in equation (4.21) and (4.27). The complete swinging-up control of the inverted pendulum is depicted in Fig. 4.6.

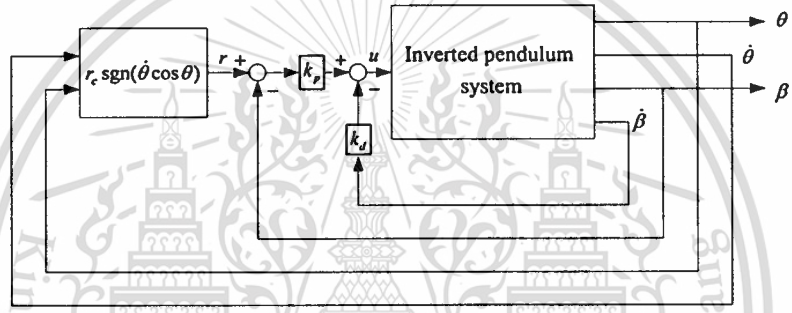

Figure 4.6 Swinging-up control of the inverted pendulum

4.5 Approximation of the Velocity

In order to implement the controller the information of the full state is needed. However, not all the state variables are available from the measurement. Therefore, an observer or at least the approximation of the unmeasured state variables must be provided. The linear observer unfortunately risky to be applied as the responses is oscillatory. Hence, the backward different method is used to approximate the angular velocity of the arm angular velocity and the pendulum angular velocity as

$$\dot{\eta}(k) \approx \frac{\eta(k) - \eta(k-1)}{T_s} \tag{4.17}$$

where $\dot{\eta}(k)$ is the angular velocity of the arm or the pendulum, T_s is the sampling period, $\eta(k)$ and $\eta(k-1)$ is the angle of the arm or the pendulum at current sampling and last sampling respectively.

Chapter 5

Results and Discussions

In this chapter the effectiveness of the controller is going to be evaluated. First the experimental arrangement of the inverted pendulum apparatus will be presented, and then the simulation and experiment will be performed.

5.1 Experimental Setup

The physical parameters of the rotational inverted pendulum used in the experiments either obtained from measurement or identification process are shown in Table 5.1. The moment of inertia of the DC motor and its viscous friction coefficient were obtained from offline identification as described in Chapter 3 while the pendulum mass, the pendulum length and the arm length can be obtained directly from measurement. The comparison of the open-loop responses of the model using identified parameter to the real experimental data using the initial value of the state variable $\left[\frac{3}{2}\pi \quad 0 \quad 0 \quad 0\right]^T$ is depicted in Fig. 5.1. It is seen that the oscillation of the identified parameter model is suspended with its amplitude approximately 0.3 rad. The model of the real plant thus can be obtained and will be used to design the controller by CDM.

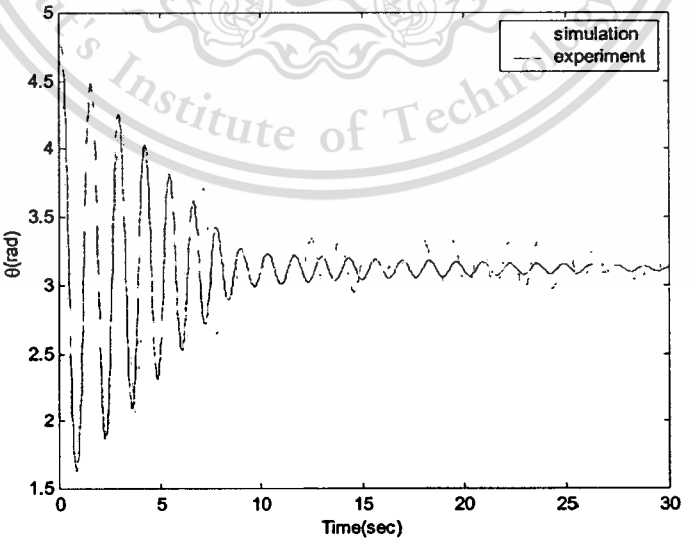

Figure 5.1 Open-loop response comparison

Table 5.1 Parameters of the rotational inverted pendulum

Pendulum mass (m)	0.05 kg
Pendulum length (l)	0.48 m
Arm length (R)	0.47 m
Moment of inertia (J)	0.03264 $kg \cdot m^2$
Viscous coefficient (b)	0.00351 $kg \cdot m^2 / s$
Coulomb friction constant (F_c)	0.04 $kg \cdot m^2 / s^2$
Stiction friction constant (F_s)	0.12 $kg \cdot m^2 / s^2$

The experimental apparatus is depicted in Fig. 5.2. It consists of three main parts: the inverted pendulum system, the interfaces and the digital controller. The pendulum system composes of pendulum, rotating-arm, a high torque permanent magnet DC motor and two angular positions sensors to detect the pendulum angle θ and the arm position angle β. The interface devices are two microcontrollers PIC16C55 to filter the quadrature signal from each encoder, one microcontroller 89C1051 as a sampling clock generator, one eight-bit D/A converter and servo amplifier. A personal computer with Intel Pentium II 350 MHz processor is used as the digital controller. The control program is written in C language and the sampling period is set at 25 milliseconds.

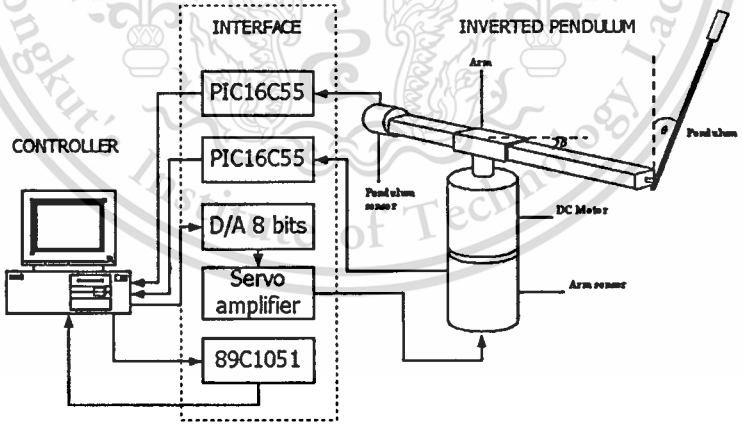

Figure 5.2 Experimental apparatus [7]

5.2 Simulation Results

The simulation has been done as previously mentioned in Chapter 1 as an easy way to check the effectiveness of the controller as well as to avoid unnecessary action in developing the control system. In order to perform the simulation, the nonlinear pendulum model in (3.26) was

used with its parameters depicted in Table. 5.1. Then the first order ODE model in Matlab can be composed for simulation. The goal of using its nonlinear model is to achieve the most precise results compared to the real situations.

5.2.1 Responses of the System without Integrator

The feedback gains of the system without integrator are found by setting the standard stability index $\gamma_1 = 2.5, \gamma_2 = \gamma_3 = 2$. Even though the equivalent time constant τ can almost be selected freely in theory, it must still be experimentally practical. Therefore, in this thesis, the value of the equivalent time constant τ is set to be 0.8 second, which is found from the closed-loop system using the feedback gains stated in reference [7]. The state feedback gains K then can be found to be $[4.0270 \quad 0.8183 \quad 0.4916 \quad 0.3960]$. The response of the system is then depicted in Fig. 5.3. It is seen that the system can be stabilized around upright position and the arm angle can also be brought back to the original position. When compared the results obtained by simulation to the experimental results shown in Fig. 5.14, later the results are not consistent as in the real situation steady-state error occurred in the controlling arm angle. However, this can be considered as uncertainty or disturbance entering the system. By introducing a constant step disturbance in model (3.26) as

$$\dot{x} = f(x,u) + [0 \quad 0 \quad d \quad 0]^T \tag{5.1}$$

where d is a constant, then the responses of the system without integrator using the modified model can be viewed in Fig. 5.4 which is having steady-state error.

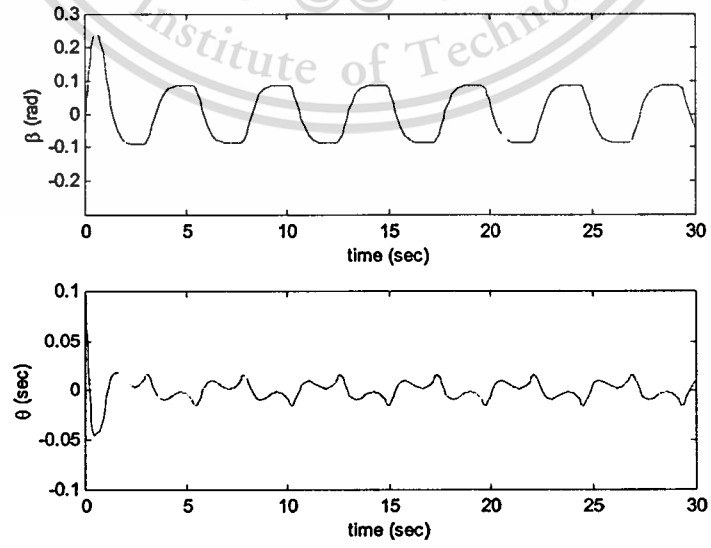

Figure 5.3 System responses without integrator from the original model

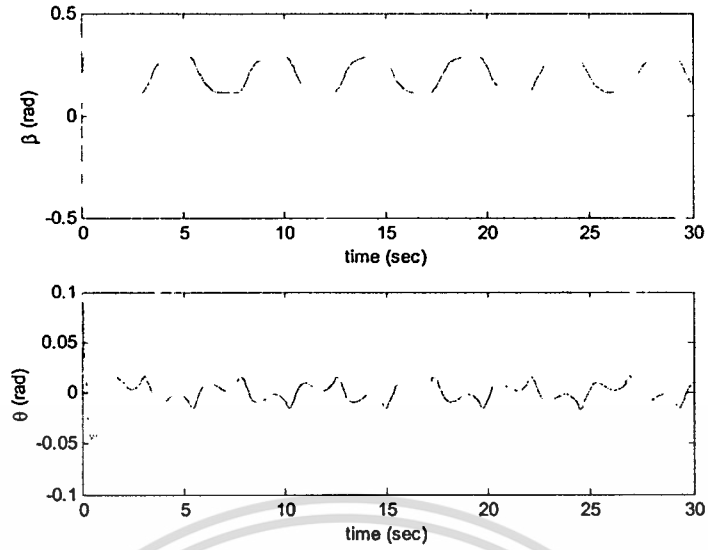

Figure 5.4 System responses without integrator from the modified model

5.2.2 Responses of the System with Integrator

The standard stability index $\gamma_1 = 2.5, \gamma_2 = \gamma_3 = \gamma_4 = 2$ and equivalent time constant $\tau = 2.8$ seconds, which is also from the results of reference [7], are used in order to find the state feedback gains and integral gain. According to the design method described in Chapter 4 the state feedback gains and integral gain can be found to be $K_a = [-1.8298 \quad -0.3141 \quad -0.0653 \quad -0.0777 \vdots \quad 0.0233]$. After adding the integrator the steady-state error seen in Fig. 5.4 can be rejected as shown in Fig. 5.5. However, the amplitude of oscillation of the arm angle by using the same stability index and equivalent time constant is greater and is not desired. The easiest way to decrease the oscillation amplitude is by decreasing the equivalent time constant τ. Another method to decrease the amplitude of oscillation is using friction compensator as described in Chapter 4. However, the effect of the friction compensation cannot be simulated as the friction itself remains unknown while the compensation is just only an approximate to counter attack the friction. Figure 5.6 is the result when we decrease the equivalent time constant τ to 1.2 seconds.

Table 5.2 Comparison of system with and without integrator

System	Amplitude of Oscillation (beta)	Amplitude of Oscillation (theta)
Without integrator	0.09 *rad*	0.02 *rad*
With integrator	1.2 *rad*	0.1 *rad*

For comparison, the performances of system responses of the system with and without integrator can be seen in Table 5.2.

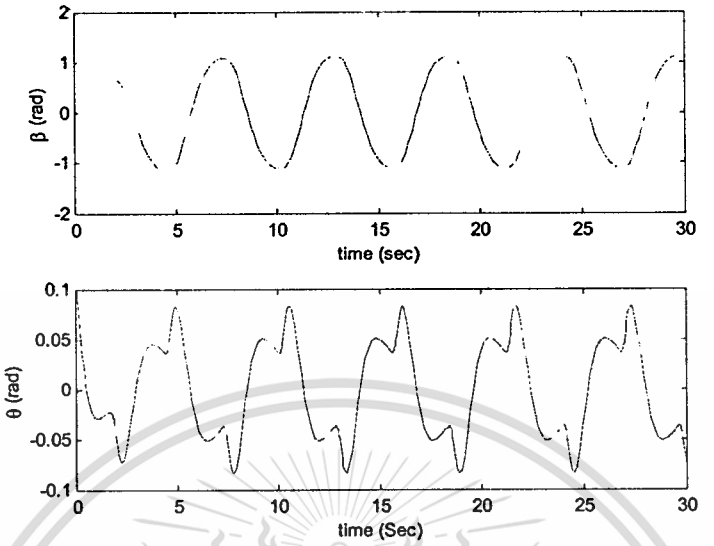

Figure 5.5 Responses of the system with integrator when $\tau = 2.8$ seconds

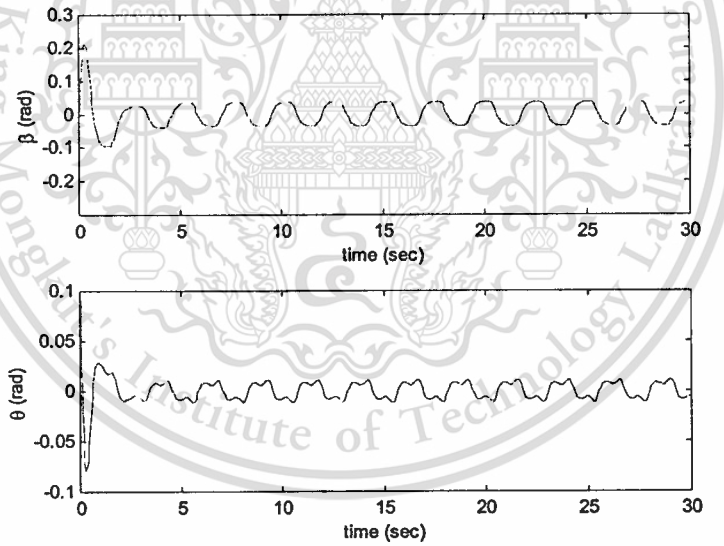

Figure 5.6 Responses of the system with integrator when $\tau = 1.2$ seconds

5.2.3 Tracking Capability

In this subsection, the tracking capability is going to be observed. For this purpose, a changed reference of the rotating arm angle from 0 rad to 1 rad of which each time interval will be applied at $t = 10$ seconds. The results depicted in Fig. 5.7. It is shown that the rotating arm angle can track the given reference while the pendulum angle can still be stabilized around the upright position. Despite an overshoot in the pendulum angle occurs during stepping period, the

overall responses show the good tracking capability with zero steady-state error at the steady state.

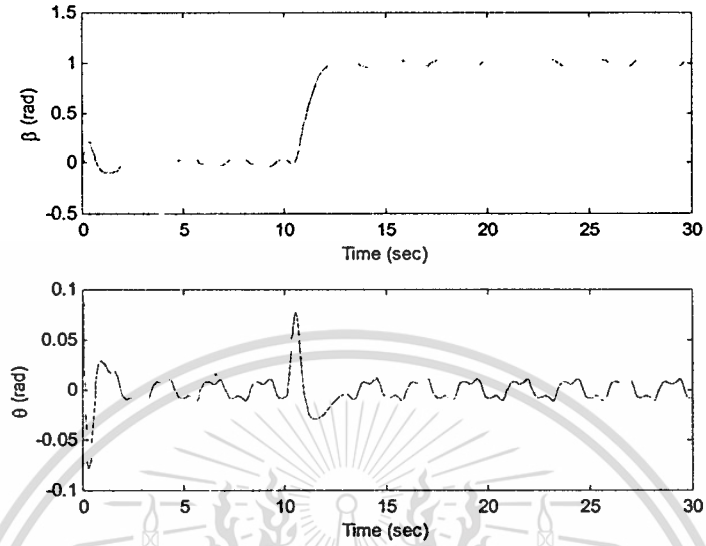

Figure 5.7 Responses of tracking capability

5.2.4 Parameters Variation

The following subsection presents the response of the system when the length of the pendulum is varied. The aim is to show the robustness of the controller under the parameter perturbation. For this purpose, the pendulum length will be increased or decreased 6 cms, and then the closed-loop poles investigation will be done to observe the effect of the parameter variations.

The responses of the system using the nominal value of 48 cms can be seen in Fig. 5.6 while the responses of the system when the pendulum length is increased and decreased by 6 cms are respectively depicted in Fig. 5.8 and Fig.5.9. It is seen that all of the three figures has similar system responses which means the robustness of the controller.

The closed-loop pole movements of the perturbed system are summarized in Fig. 5.10 and Table 5.3. By observing their poles movements we can conclude that the longer the pendulum the more stable the system will be achieved as the dominant closed-loop poles move to the left. On the other hand, for the shorter pendulum the system tends to be unstable as the dominant closed-loop poles move to the right.

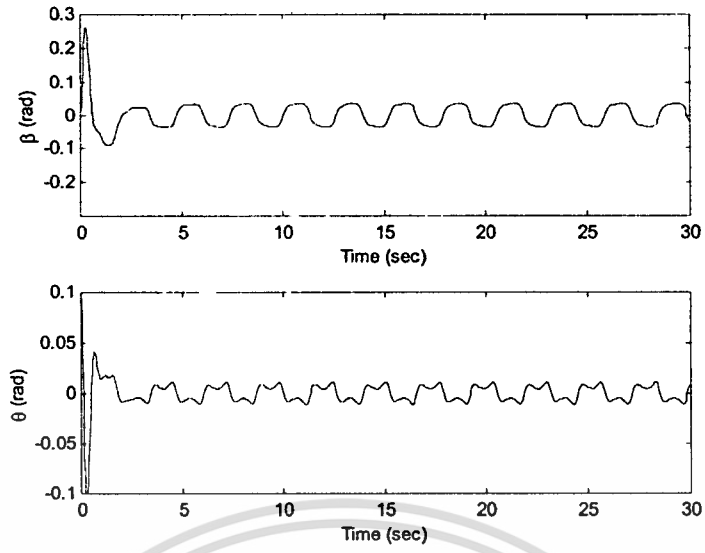

Figure 5.8 System responses when $l = 54$ cms

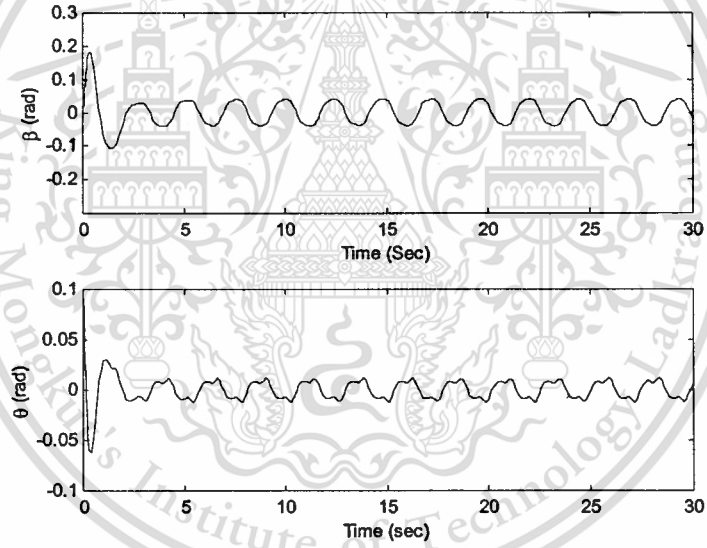

Figure 5.9 System responses when $l = 42$ cms

Table 5.3 Closed-loop poles of the system due to length variation

Pendulum length (cms)	Closed-loop poles				
42	-0.2118 + 2.9389j	-0.2118 - 2.9389j	-1.1182	-4.5824	-25.8088
45	-0.2415 + 2.9930j	-0.2415 - 2.9930j	-1.1168	-4.8705	-21.8494
48	-0.2757 + 3.0513j	-0.2757 - 3.0513j	-1.1155	-5.2643	-18.2272
51	-0.3153 + 3.1143j	-0.3153 - 3.1143j	-1.1141	-5.8711	-14.7528
54	-0.3619 + 3.1829j	-0.3619 - 3.1829j	-1.1128	-7.2178	-10.8347

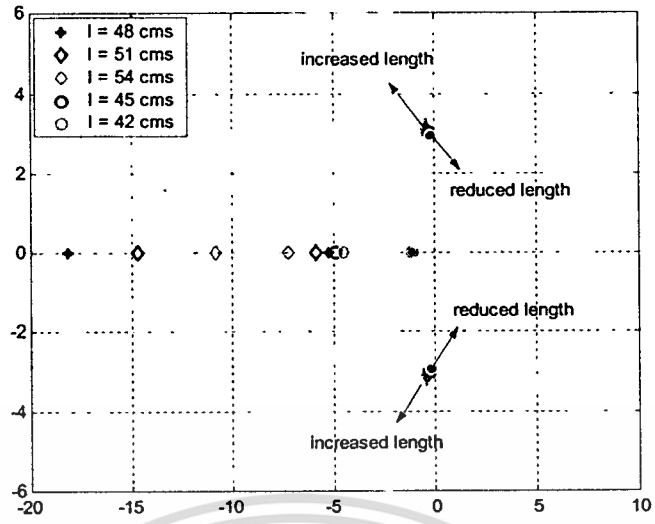

Figure 5.10 Closed-loop poles movement due to length variation

5.2.5 Effect of Stability Index γ_i

The system responses corresponding to the variation of stability index will be observed. By varying the stability index from the standard stability index $\gamma_1 = 2.5, \gamma_2 = \gamma_3 = \gamma_4 = 2$ to $\gamma_1 = \gamma_2 = \gamma_3 = \gamma_4 = 2$ and to $\gamma_1 = \gamma_2 = \gamma_3 = \gamma_4 = 2.2$ then their corresponding gain K_a of the augmented system for $\tau = 1.2$ seconds can be obtained as mentioned in Table 5.4.

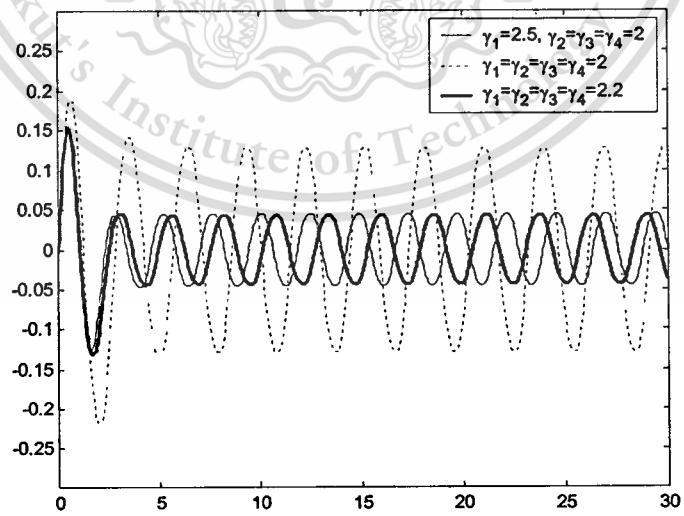

(a) Rotating arm angle β

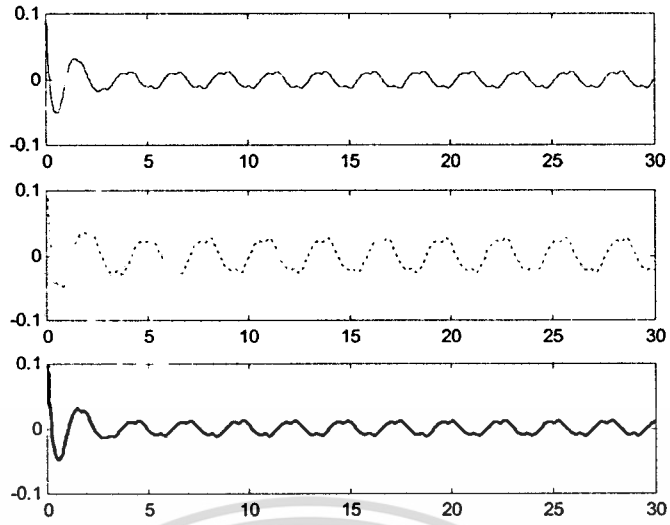

(b) Pendulum angle θ

Figure 5.11 Effect of stability index

As depicted in Fig. 5.11 the dark line, the light line and the dashed line respectively show their simulation results. It is shown that the responses of the system with different values of stability index oscillate around the zero radian line, which means that the integrator added to the arm angle of the rotational inverted pendulum can reject the steady-state error. The control signal of the system with different stability index depicted in Fig. 5.12 show that the lower the oscillation amplitude, the smaller the control signal will be.

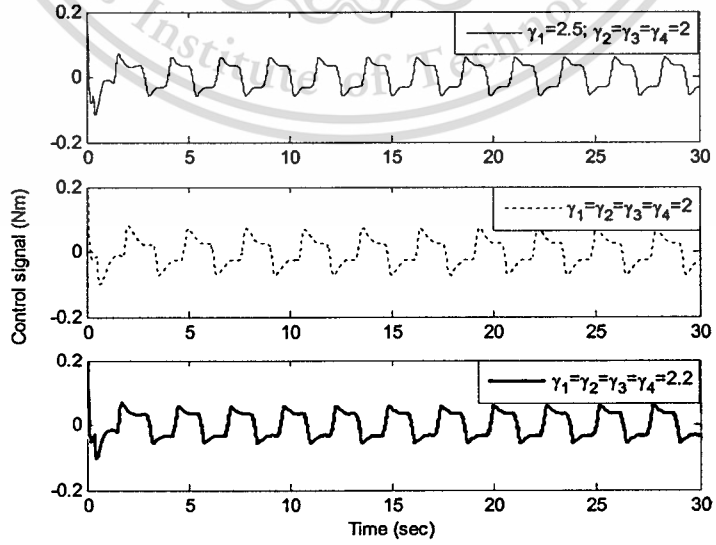

Figure 5.12 Control signal of the system with different stability index

Table 5.4 State feedback gains and integral gains of various γ_i

γ_i	K_a
$[2.5 \quad 2 \quad 2 \quad 2]$	$[-7.5092 \quad -1.5808 \quad -1.9274 \quad -1.0074 \quad 1.6062]$
$[2 \quad 2 \quad 2 \quad 2]$	$[-4.6803 \quad -0.9611 \quad -0.7895 \quad -0.5094 \quad 0.6579]$
$[2.2 \quad 2.2 \quad 2.2 \quad 2.2]$	$[-8.7764 \quad -1.8768 \quad -2.0477 \quad -1.2040 \quad 1.7064]$

5.3 Experimental Results

In order to verify the effectiveness of the controller the experiments in controlling the pendulum angle θ and the arm angle β has also been done. The photograph of the rotational inverted pendulum is depicted in Fig. 5.13. The results of the experiment are summarized in the following sub-sections.

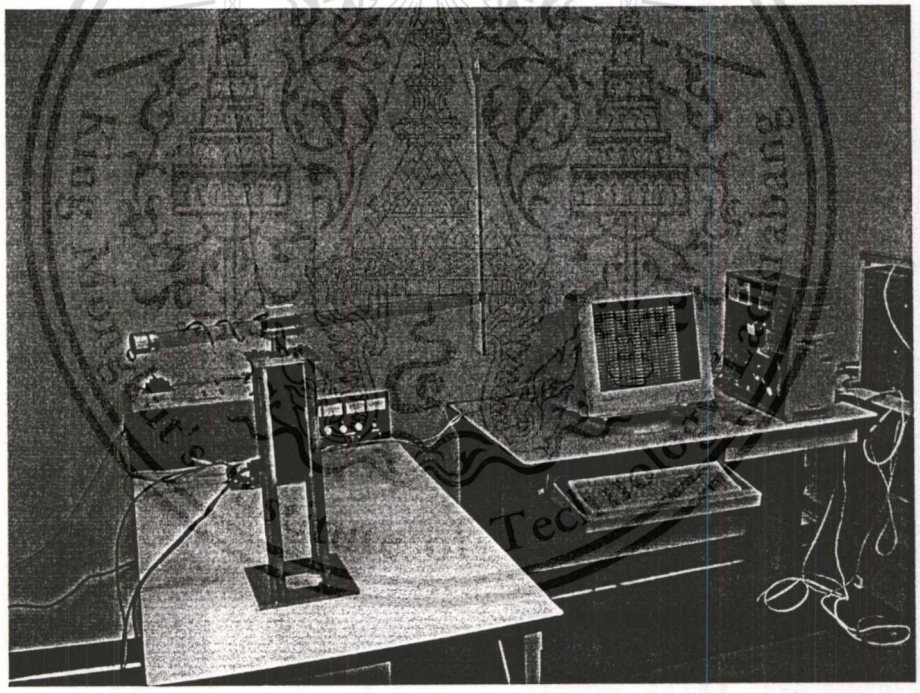

Figure 5.13 Inverted pendulum used in laboratory

5.3.1 Responses of the System with and without Integrator

The responses of the system without any integrator are displayed in Fig. 5.14. For both systems using the standard stability index, the equivalent time constants are set to be 0.8 second and 2.8 seconds respectively. It is seen that the steady-state error occurred at both the pendulum angle and the rotating arm angle. In reality, however, the offset at the pendulum angle is never

occurred as it is impossible to keep the pendulum forever using finite energy other than in its equilibrium points. Therefore, the offset is nothing other than the measurement error. In contrast to the offset in the pendulum angle, the offset or steady-state error in the arm angle needs to be rejected by introducing an integrator. It has been demonstrated by the simulation as shown in Fig. 5.5. The results were also consistent with those obtained by simulation assuming that the steady-state error due to the external disturbance.

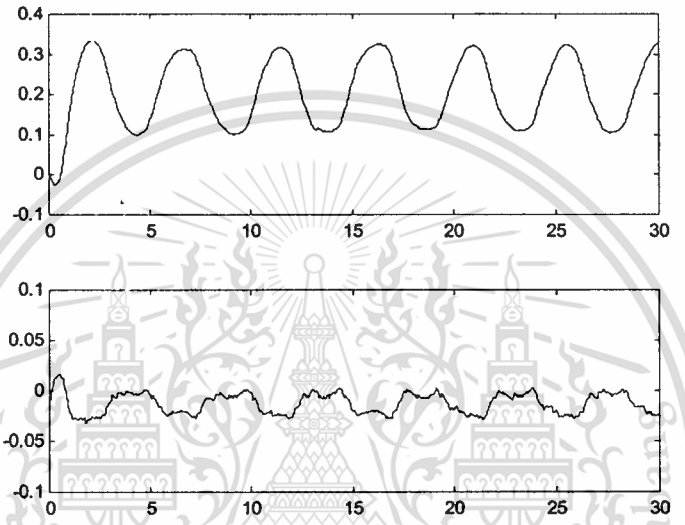

Figure 5.14 Responses of the system without integrator when $\tau = 0.8$ second

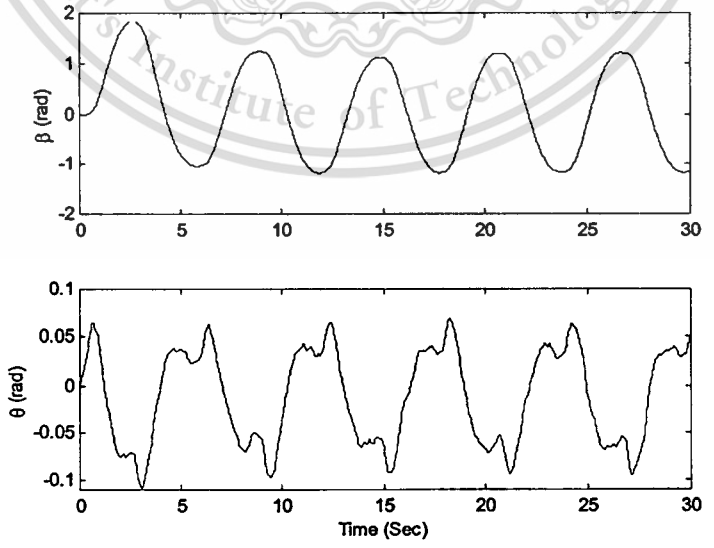

Figure 5.15 Responses of the system with integrator when $\tau = 2.8$ seconds

When the integrator is augmented the error can be successfully removed as shown in Fig. 5.15 but the amplitude of oscillation will be greater than those of the system without integrator using the same stability index. These phenomenons are well predicted by the simulations. Referring to the simulation results in Fig. 5.6, it is seen that decreasing the equivalent time constant τ to 1.2 seconds will decrease the amplitude of oscillation; the similar results in the experiment are also obtained as depicted in Fig. 5.16.

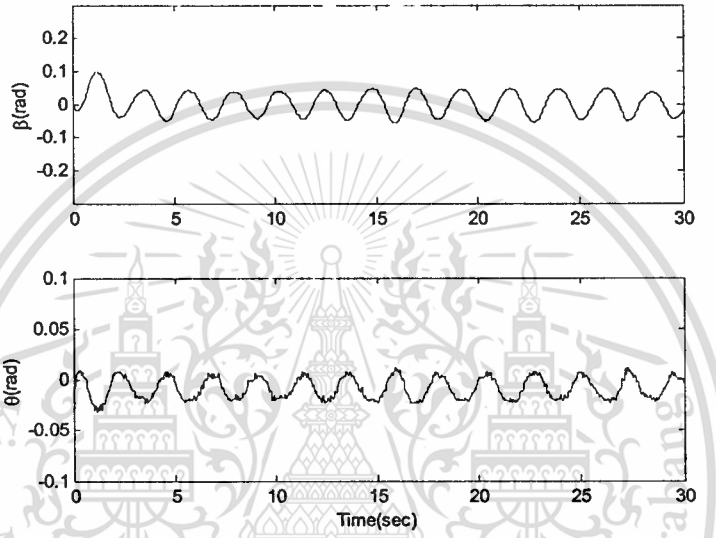

Figure 5.16 Responses of the system with integrator when $\tau = 1.2$ seconds

5.3.2 Parameters Variation

In experiments the length of the inverted pendulum can only be increased or decreased approximately 6 cms. There are two reasons for this. First, when the length of the pendulum increases the more vibration in the responses due to un-modelled dynamics will occur. It leads to harm the apparatus and the safety in doing the experiments. Second, in the laboratory the pendulum rod with different length is not available. The experiment is done by using the single rod by shifting the rod either up or down the pivot. Therefore, when decreasing the pendulum length in one point there will be a balance in mass for upper and lower part of the pivot implies to the lost of controllability.

The effects of the length variation are depicted in Fig. 5.17 and 5.18 respectively. It is seen that that the experimental results behave like the simulation results. The inverted pendulum still can be stabilized and their responses are also similar which means the robustness in stability and performance of the controller with respect to the inverted pendulum length perturbation.

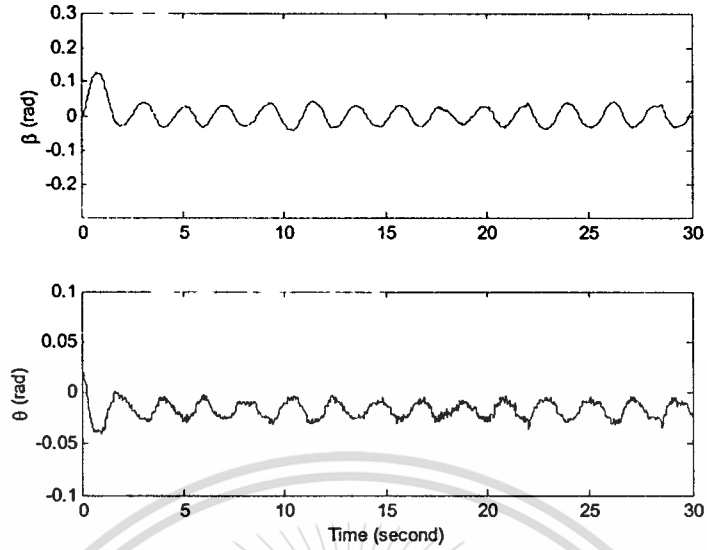

Figure 5.17 System responses when $l = 54$ cms

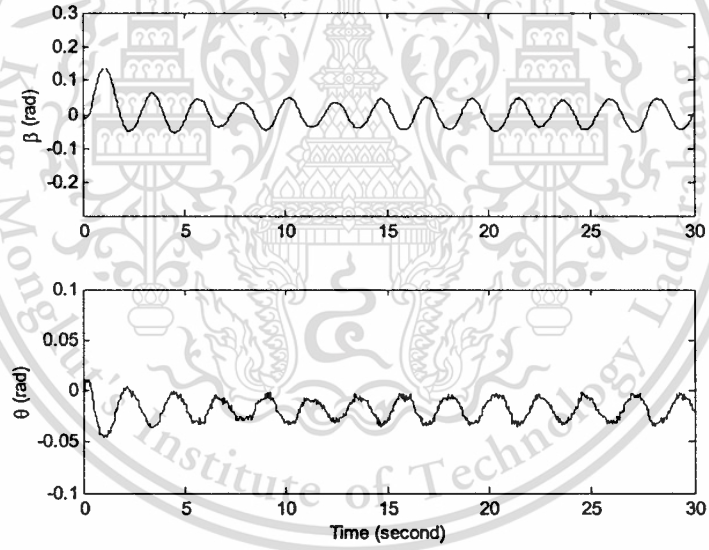

Figure 5.18 System responses when $l = 42$ cms

5.3.3 Effect of Stability Index γ_i

The experimental results of the system with varying stability index from the standard stability index $\gamma_1 = 2.5, \gamma_2 = \gamma_3 = \gamma_4 = 2$ to $\gamma_1 = \gamma_2 = \gamma_3 = \gamma_4 = 2$ and to $\gamma_1 = \gamma_2 = \gamma_3 = \gamma_4 = 2.2$ for τ =1.2 seconds are depicted in Fig. 5.19. In the same way to the simulation results, the experimental results are also shown by the dark line, the light line and the dashed line respectively. It is shown that the responses of the system with different values of stability index behave like the simulations do. They are oscillating around the zero radian line, which means that

the integrator added to the arm angle of the rotational inverted pendulum can reject the steady-state error.

In contrast with the simulation results, however, the lower amplitude of oscillation implies to the higher control signal as shown in Fig. 5.20. It is also shown that the control signals are chattering due to approximation of the velocity by backward difference as described in Chapter. 4.

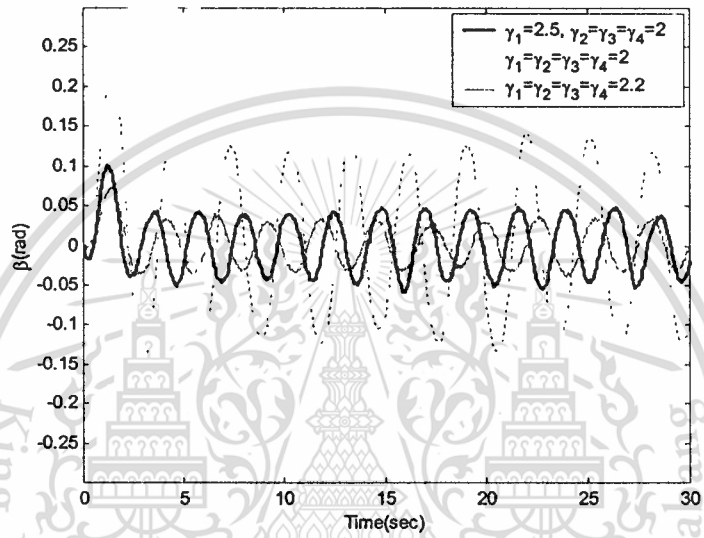

(a) Arm angle

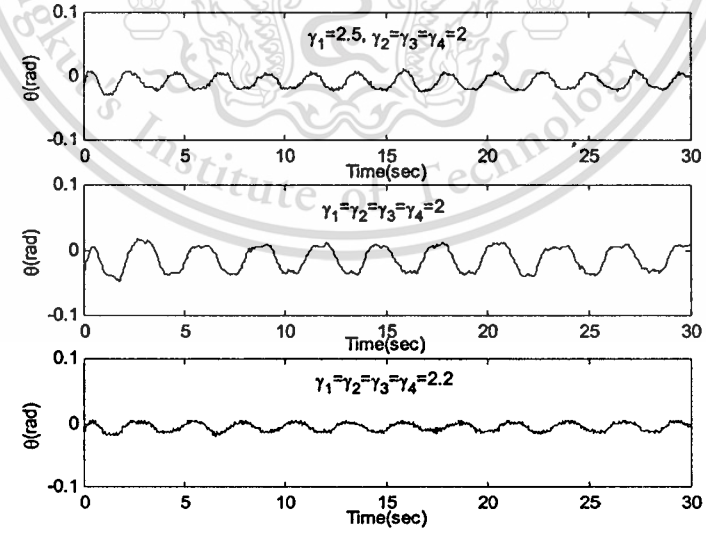

(b) Pendulum angle

Figure 5.19 System responses when the stability index is varied

The coefficient diagram of the proposed control system with varying stability index is shown in Fig. 5.21. As described in Chapter 2, if the curvature of the coefficient of the characteristic polynomial a_i becomes larger, the control system become more stable, corresponding to larger stability index γ_i. By relating the responses in Fig. 5.19 to its coefficient diagram in Fig. 5.21, one can infer that the greater curvature of the coefficient diagrams implies to the smaller oscillation of its corresponding system responses. On the other words, the more stable system will lead to the smaller oscillation.

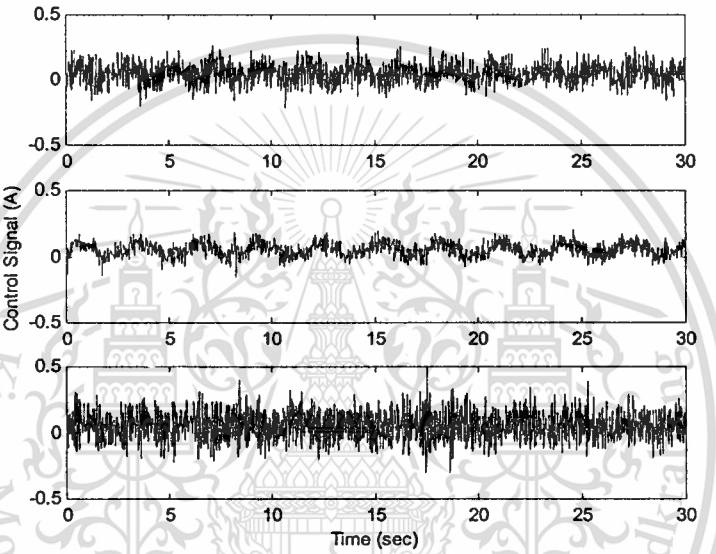

Figure 5.20 Control signal of system with different stability index

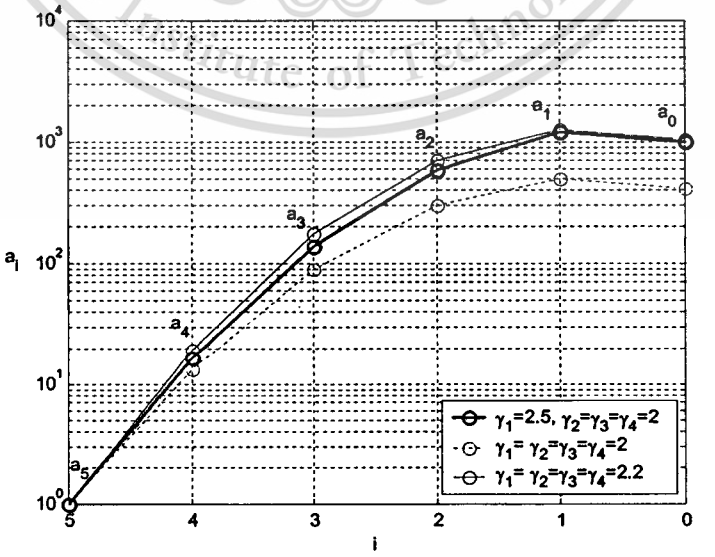

Figure 5.21 Coefficient diagrams of system with different stability index

5.3.4 Effect of Friction Compensation

Indeed increasing the stability index can reduce the amplitude of oscillation. However, the control signal will be high which is undesirable. Therefore, simple model based friction compensation using Coulomb friction with stiction is developed and then is applied to the system at t =10 seconds. Fig. 5.22 shows the responses of the inverted pendulum when the standard stability index γ_i and equivalent time constant τ =1.2 seconds are used. It is seen that the oscillation amplitude of the arm angle β can be reduced significantly.

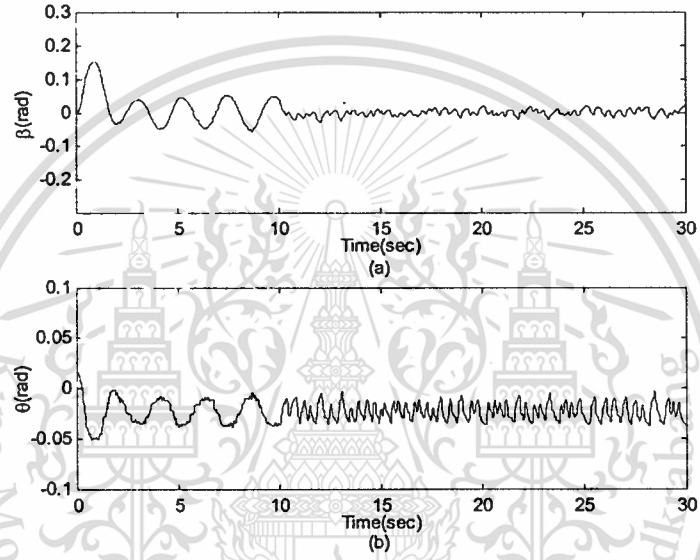

Figure 5.22 System responses when friction compensation is applied

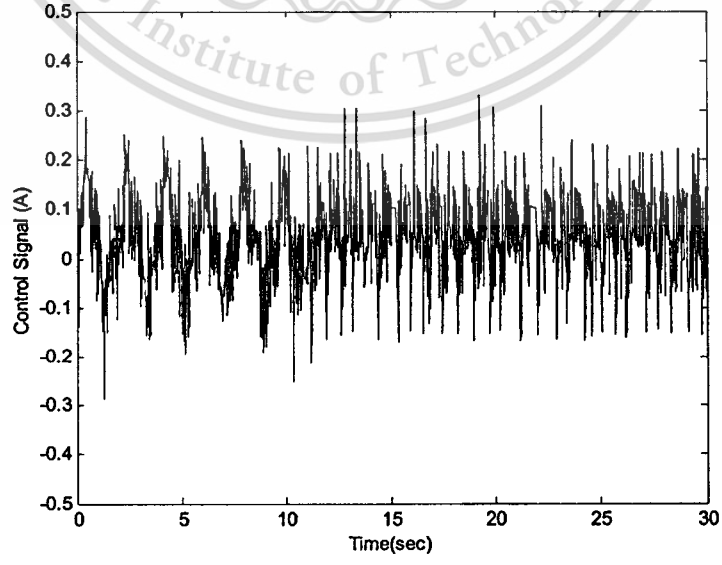

Figure 5.23 Control signal when friction compensation is applied

The control signal of the friction compensation effect is depicted in Fig. 5.23. It is seen that the envelope of the control signal of the system without any friction compensation is approximately the same magnitude with that of when the friction compensation is applied, in spite of more chattering.

5.3.5 Tracking Capability

In order to show the tracking capability, the reference input of the arm angle is changed from zero radian to one radian at 10 seconds for equivalent time constant τ=1.2 seconds. The result depicted in Fig. 5.24 shows that the output arm angle can track the constant reference input and oscillates around the one radian line, while the effect of the step change in arm angle does not affect the oscillatory behavior of the steady-state response. It can also be observed that the rotational inverted pendulum angle is still almost unaffected at the steady-state.

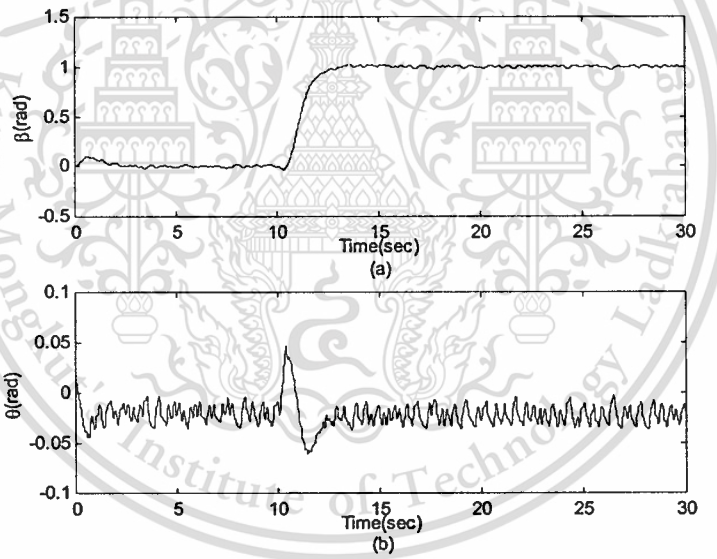

Figure 5.24 Responses of tracking capability

5.3.6 Swinging-up Control

In order to swing the pendulum up as soon as possible, the response of the position control of the arm angle must be fast enough. This requirement implies to the small choice of the equivalent time constant of the position control. However, the choice of an unnecessarily fast equivalent time constant of the position control will make the position control being superior over the energy control. It means that the energy cannot be pumped to the system even though the direction of energy has not changed its sign yet. Therefore, the choice of the equivalent time

constant of the position control is also constrained.

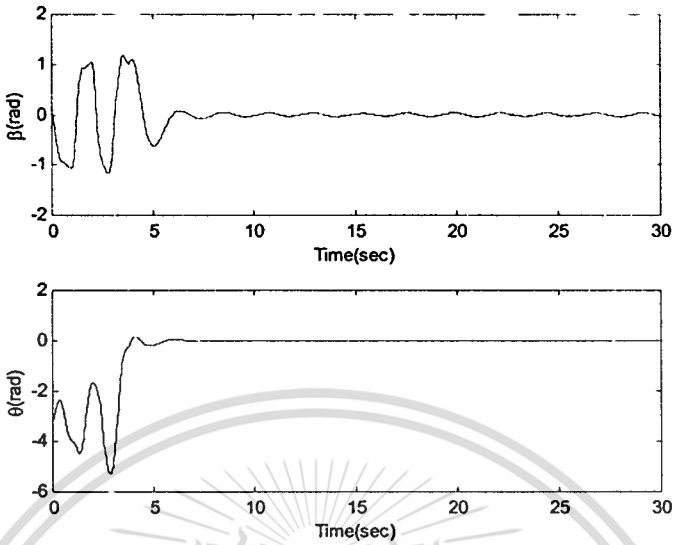

Figure 5.25 Responses of swinging-up control

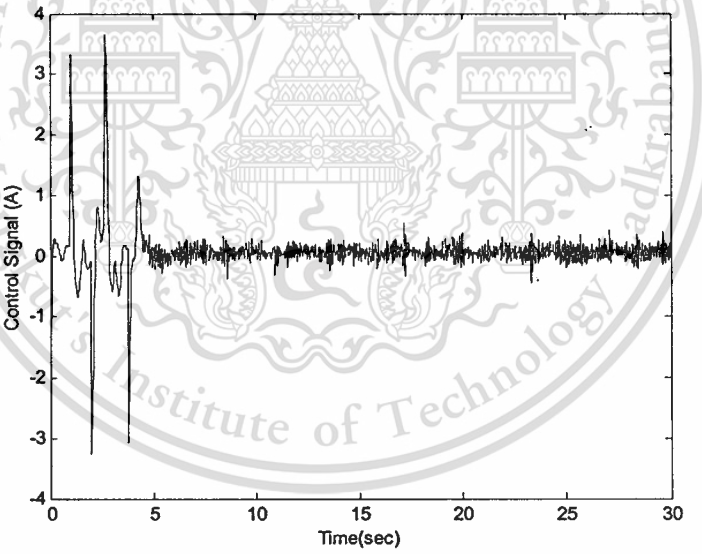

Figure 5.26 Control signal of swinging-up control

Based on those considerations, in this experiment the equivalent time constant τ and the stability index γ_1 of the arm angle position controller is set to be 0.25 second and 2.5 respectively. Then the proportional gain k_p and the derivative gain k_d are found to be -1.3056 and -0.3299 respectively. The reference constant r_c is set to be 1 radian and the condition for the control switching is chosen such that $\theta = 0.2$ radian. For the stabilizing controller the equivalent time

constant is chosen as 1.2 seconds and using the standard stability index. Consequently, the state feedback gains and the integral gain can be seen in Table 5.4. The swinging-up results are depicted in Fig. 5.25 and its control signal is shown in Fig. 5.26. It is seen that the pendulum can be brought to the upright position in approximately 5 seconds and the arm angle can also be brought back to zero radian line. Moreover, during the swinging-up period the arm angle is restricted in the 1 radian sector angle around the zero radian line. As depicted in Fig. 5.26, during the swinging-up period, the control signal is normally higher than that during the stabilization period.

Chapter 6

Conclusion and Future Works

6.1 Conclusion

In conclusion, the controller designed by CDM incorporating simple friction compensation for a servo type system which is a rotational inverted pendulum with an integrator added to its arm have been proposed. First the simulation is done to verify the effectiveness of the controller. Then the controller is implemented to control the system. It is shown that the responses of the control system are well predicted by the simulation results. Both the experimental and simulation results show that the satisfied performances have been achieved. The good capabilities of angle position error rejection and tracking can also be obtained and shown. In addition, the coefficient diagram used for investigating system stability due to the variation of stability index γ_i has also been shown. Moreover, the swing-up control has also been done.

The friction compensation using the simple model of coulomb friction with stiction is also built to attenuate the effect of the friction in the control system. It is seen that the amplitude of oscillation due to the friction can be substantially rejected.

6.2 Future Works

In the future the friction model should be given more emphasis. A better model of the friction will reduce the amplitude of oscillation generated by the friction more significantly.

The CDM concept applied in this thesis is focused to linear system without considering the uncertainty. The analysis of the uncertainty either structured or non-structured in the plant still cannot be coped by using the method developed so far in this thesis. However, it is an interesting research topic on the robustness of the control system to be dealt in the next works.

The development of an observer is also needed in the next research. It is shown that the control signal and the angular velocity are chattering due to rough approximation which is undesirable.

Finally the swing-up procedures; an improvement of swing-up procedures is keenly needed. Instead of trial and error method, optimization of the gains of the position control which is designed by CDM should be done in order to achieve the minimum swing-up time.

REFERENCES

[1] K. Crisman, "An Alternative Inverted Pendulum Apparatus for Education," Proceedings of ACC1996, Seattle, pp. 554~558. June 1996

[2] H. Morimoto, S. Kawamoto, "Nonlinear Control Based on Equilibrium Point Analysis for Inverted Pendulum," Proceedings of SICE 2002, Osaka, Japan, 2002

[3] W. T. Pomales and O.R. Gonzalez, "Nonlinear Control of Swing-up Inverted Pendulum," Proceedings of the 1996 ICCA, Dearborn, MI, September 15-18, 1996

[4] A. Ohsumi and T. Izumikawa, "Noninear Control of Swing-up and stabilization of an Inverted Pendulum," Proceedings of 34th Conference on Decision and Control, New Orleans, LA, December, 1995

[5] K. J. Astrom and K. Furuta, "Swinging up a Pendulum by Energy Control," Proceedings of IFAC 13th world Congress, San Francisco, California, 1996

[6] S. Renou and L. Saydy, "Real Time Control of an Inverted Pendulum based on Approximate Linearization," Proceedings of CCECE'96, Canada, 1996

[7] N. Chanapan, S. Panaudomsup, J. Ngamwiwit. and N. Komine., "Experimental Study of Rotational Inverted Pendulum," Proceedings of KACC 2000, Korea, October 2000

[8] J. Akesson, K. J. Astrom "Safe Manual Control of the Furuta Pendulum," Proceedings of ICCA 2001, Mexico City, pp. 890~895, 2001

[9] C. Canudas, H. Olsson, K. J. Astrom, "Dynamic Model Based Friction Compensation on the Furuta Pendulum," IEEE Transaction on Automatic Control, Vol 40, No. 3, March 1995

[10] D. Kumpanya, T. Benjanarasuth, J. Ngamwiwit and N. Komine, "FFC Design for PI Flow Control System Design by CDM", Proceedings of ICASS 2001, Jeju, Korea, pp. 1022-1025, October 2001

[11] A. Ucar, S. E. Hamamci, "A Controller Based on Coefficient Diagram Method for the Robotics Manipulator", Proceedings of ICECS 2000, Lebanon, vol. 2, December 2000

[12] A. Numsomran, W. Sriratana, P. Julsereewong, V. Kongratana, and K. Tirasesth, "I-PDA Controller Designed by CDM," Proceedings of KACC'99, pp. E-284 – E-287, 1999

[13] A.I. Cahyadi, N. Khuakoonatt, T. Benjanarasuth, J. Ngamwiwit and N. Komine, "Design of I-PDA Controller Incorporating FFC for Flow Control Systems," Proceedings of

ICCAS 2003, Gyeong-Ju, Korea , 2003

[14] S. Manabe, " Comparison of H-Inf and Coefficient Diagram Method in Aerospace," Proceedings of 19th Gudance and Control Symposium, Tokyo, November 14-15, 2002

[15] S.E. Hamamci and M. Koksal, "Robust Controller Design for TITO Processes with Coefficient Diagram Method," Proceedings of ICCA, Turkey, vol. 1, June 2003

[16] H. Olsson, K. J. Astrom, "Friction Generated Limit Cycles ¹," ICCA 2001, Mexico City, pp. 798~803, 2001

[17] L. Fang, W.J. Chen, S.U Cheang, "Friction Compensation for Double Inverted Pendulum," Proceedings of the 1996 IEEE Conference on Control Applications, Mexico City, Mexico, September 5-7, 2001

[18] S. Manabe, "Coefficient Diagram Method", 14th IFAC Symposium in Aerospace, 1998

[19] S. Manabe, "Brief Tutorial of Coefficient Diagram Method", proceedings of the 4th Asian Control Conference, Singapore, September 25-27, 2002

[20] S. Manabe, "Importance of Coefficient Diagram in polynomial method", proceedings of 42nd IEEE Conference on Decision and Control, Hawaii USA, 2003

[21] N. komine, K shibata, T. Benjanarasuth and J. Ngamwiwit, "Weighting Matrix Selection of Derivative State Constrained Control by CDM," The 4th Asian Control Conference, Singapore, September 25-27, 2002

[22] M. Gafvert, "Modelling of the Furuta Pendulum," Dissertation report, Department of Automatic Control Lund institute of Technology, April 1998

[23] A.I. Cahyadi, T. Benjanarasuth, D. Isarakorn, J. Ngamwiwit and N. Komine, "Application of Coefficient Diagram Method for Rotational Inverted Pendulum Control," Proceedings of ICARCV 2004, Kunming, Peoples Republic of China, pp.1769-1773, December, 2004

[24] A.I. Cahyadi, T. Benjanarasuth, D. Isarakorn, J. Ngamwiwit and N. Komine, "CDM Controller Incorporating Friction Compensation for Rotational Inverted Pendulum," Proceedings of ICCAS2004, Bangkok, pp.1901-1905, August, 2004

[25] K. Ogata, Modern Control Engineering, Second Edition, Prentice-Hall international, Inc., 1990

[26] H. Khalil, Nonlinear Systems, Third Edition, Prentice-Hall Inc, Pearson Education International, 2000

Appendix A

Listing programs

A.1 First order ordinary differential equation (ODE) model

Type : Matlab's m-file

File name : mypendulum1.m

```
function dxdt=mypendulum1(t,x)

%parameters of the inverted pendulum obtained from optimization
%-------------------------------------------------------------

m=0.05;
l=0.48;
R=0.47;
g=9.8;
J=0.0234;
b=0.0034;

u=0;

%friction model using coulomb friction with stiction
%---------------------------------------------------
Fs=0.12; Fc=0.04;
if x(4)>0
   tauf=Fc;
elseif x(4)<0
   tauf=-Fc;
elseif (x(4)==0 & abs(u)<Fs)
   tauf=u;
elseif u>0
   tauf=Fs;
else
   tauf=-Fs;
end;


% The first order ODE
%-------------------------------------------------

A=m*R^2;
B=m*l^2;
C=m*R*l;
D=m*R*g;
E=sin(x(1)); F=cos(x(1)); G=(J+(m*l^2+m*R^2)*sin(x(1))^2);

dxdt(1)= x(2);
dxdt(2)= ((J+A+B*E^2)*F*E*x(4)^2-2*C*F^2*E*x(4)*x(2)-...
         A*E*F*x(2)^2+(g/l)*(J+A+B*E^2)*E-(R/l)*F*(u-b*x(4)-tauf))/G;
dxdt(3)= x(4);
```

```
dxdt(4)= (-C*F^2*E*x(4)^2-2*B*F*E*x(4)*x(2)+C*E*x(2)^2-…
         D*F*E+u-b*x(4)-tauf)/G;
dxdt=    dxdt';
```

```
%enter this command in the command line

>> options = odeset('RelTol',1e-3,'AbsTol',1e-3);
>> [t,x1,=ode23('mypendulum1',[0 30],[0.1 0 0 0],options);
>> plot(t,x1(:,1));
>> figure; plot(t,x1(:,2));
>> figure; plot(t,x1(:,3));
>> figure; plot(t,x1(:,4));
```

A.2 The linearized model

Type : Matlab's m-file

File name : linearized model.m

```
%linearized model of the pendulum

%parameters of the inverted pendulum obtained from optimization
%-----------------------------------------------------------------
m=0.005;
l=0.48+0.06;
R=0.47;
J=0.03264;
b=0.351;
g=9.8;


% the linearized model is dx/dt=Ax+Bu,
% The augmented system is
% Ahat=[  A  0]
%      [ -H  0]
%
% Bhat=[ B ]
%      [ 0 ]
%-----------------------------------------------------------------

A=[0 1 0 0;
   g*(J+m*R^2)/(J*l) 0 0 R*b/(J*l);
   0 0 0 1;
   -m*R*g/J 0 0 -b/J];

Ahat=[A zeros(4,1);-[0 0 1 0] 0];
eig(A);

B=[0;-R/(J*l);0;1/J];

Bhat=[B;0];

K=[-7.5092 -1.5808 -1.9274 -1.0777 1.6061];
```

```
Acl=Ahat-Bhat*K;

eig(Acl)          the closed-loop poles


poles=poly(Acl);

plot([0 1 2 3 4 5],poles,'k');  plot of CDM in linear scaling
```

A.3 Parameters optimization

Type : Matlab's m-file

File name : optim_the_param.m

```
function F = optim_the_param1(initi,xdata)

%globa_ ydata;
J=initi(1);
b=initi(2);
Fc=initi(3);
Fs=initi(4);
%xdat=xdata;
[sza szb]=size(xdata);
%timespan=xdata(sza,1);
%tolerance=0.001;
%xdat=[(0::15)' xdata];
xdat=xdata;
R=0.47;
l=0.48;
m=0.05;

L=J+m*R^2;
M=m*l^2;
N=M*R*l;
O=M*0.98*l;


% Choose solver and set model workspace to this function
opt = simset('solver','ode5','SrcWorkspace','Current','AbsTol',1e-
10,'FixedStep',0.025);
%[tout,xout,yout] = sim('pendulum_optim_par',[0 1261],opt);
[tout,xout,yout] = sim('pendulum_optim_par1',[],opt,xdat);
size(tout);
tout;
%size(ydata);
global ydata;
F =yout-ydata;
szf=size(F);
size(xout);
```

A.4 Simulink model

Type : Matlab's simulink model

File name : pendulum_with_fric.mdl

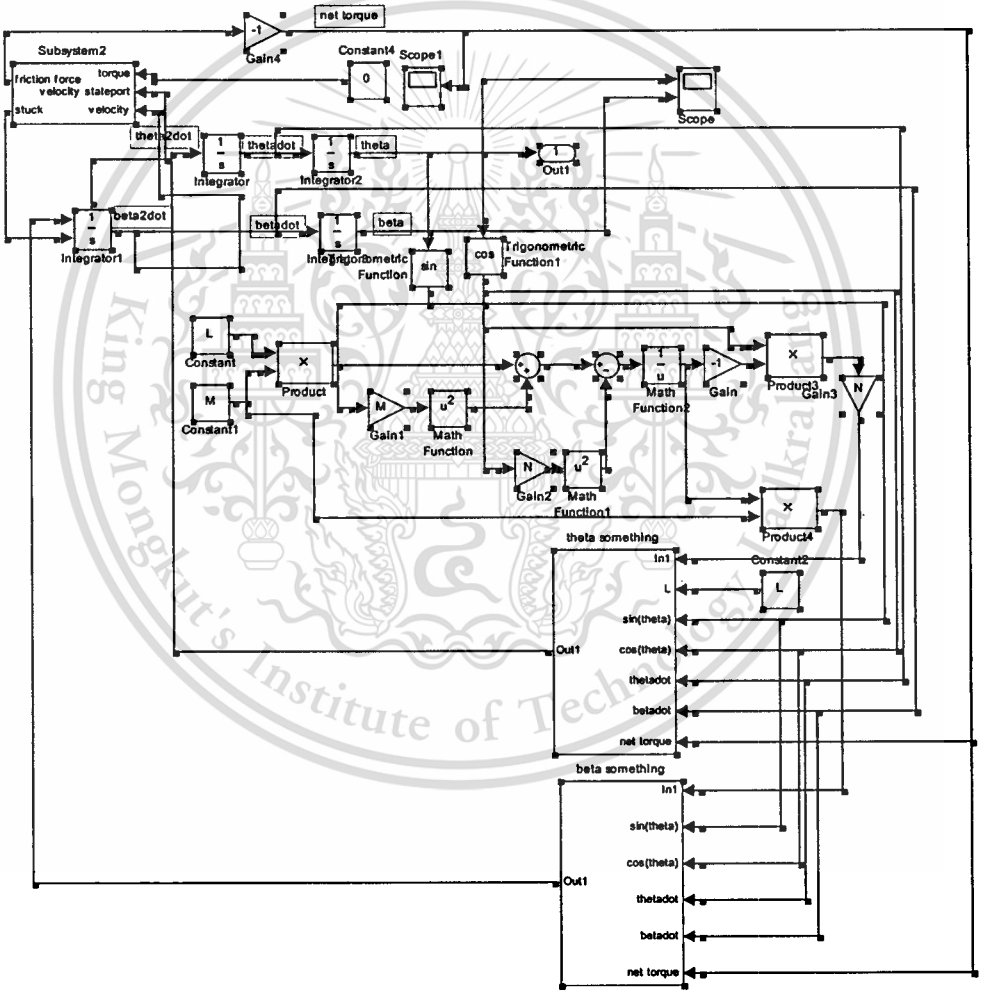

block #1

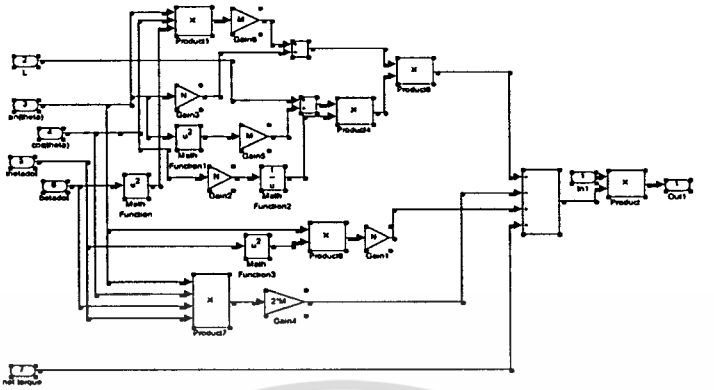

block #2

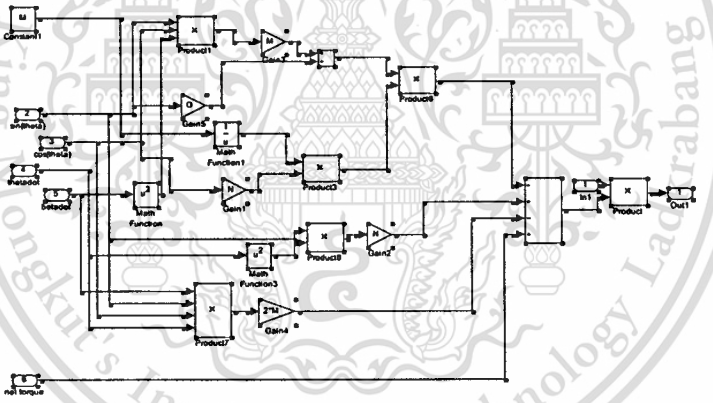

A.5 To find the gains without integrator

Type : : Matlab m-file

File name : : without integ.m

```
% Model of the inverted pendulum
format short
syms s
```

```
g1=2.5;
g2=2;
g3=2;
tau=2.8;

d0=(g3*g2^2*g1^3)/(tau^4);
d1=d0*tau;
d2=(d1*tau)/g1;
d3=(d1*tau^2)/(g2*g1^2);
d4=(d1*tau^3)/(g3*g2^2*g1^3);

Kcdm=[d4 d3 d2 d1 d0];
roots(Kcdm);

%The system from pe' Tao
%-------------------------
A= [  0         1      0      0      ;
      27.3254   0      0      0.1053      ;
      0         0      0      1      ;
    -7.0558     0      0      -0.1075  ]  ;
B= [  0  ;
      -29.9990 ;
      0  ;
     30.6373   ];
C= [0 0  1  0];
D= [ 0 0 0 0];

M=[B A*B A^2*B A^3*B];
a=poly(A);
a0=a(5);a1=a(4);a2=a(3);a3=a(2);a4=a(1);

%The results
%SS=s*eye(5)-A1
%det(SS)
%s^5+43/400*s^4-7691416328609359/2814749767106560*s^3-
38606136013276480313417/17592186044416000000000*s^2
%s^5+0.1075s^4-27.3254s^3-2.1945*s^2

W=[a1 a2 a3 1
   a2 a3 1  0
   a3 1  0  0
   1  0  0  0];

T=M*W
That=inv(T);
contrl=That*A*T
K=[d0-a0 d1-a1 d2-a2 d3-a3];
KK=K*That
```

A.6 To find the gain with integrator

Type : : Matlab m-file

File name : : with integ.m

```
% Model of invert pendulum
format short
syms s
g1=2.5;
g2=2;
g3=2;
g4=2;
tau=2.8;

a0=(g4*g3^2*g2^3*g1^4)/(tau^5);
a1=a0*tau;
a2=(a1*tau)/g1;
a3=(a1*tau^2)/(g2*g1^2);
a4=(a1*tau^3)/(g3*g2^2*g1^3);
a5=(a1*tau^4)/(g4*g3^2*g2^3*g1^4);

Kcdm=[a5 a4 a3 a2 a1 a0];
roots(Kcdm);
% of the inverted pendulum system just designed
%Enter neccessary matrices
A= [  0        1     0     0      ;
      27.3254  0     0     0.1053      ;
      0        0     0     1      ;
    -7.0558    0     0     -0.1075  ]  ;
B= [  0  ;
      -29.9990 ;
      0  ;
     30.6373   ];
C= [0 0  1  0];
D= [ 0 0 0 0];

A1=[A zeros(4,1);
   -C zeros(1,1)];
B1=[B;0];

M=[B1 A1*B1 A1^2*B1 A1^3*B1 A1^4*B1];
%SS=s*eye(5)-A1
%det(SS)
%s^5+43/400*s^4-7691416328609359/281474976710656*s^3-
3860613601327648031341/1759218604441600000000*s^2
%s^5+0.1075s^4-27.3254s^3-2.1945*s^2
W=[   0        -2.1945     -27.3254   0.1075   1;
      -2.1945  -27.3254    0.1075        1     0;
   -27.3254       0.1075     1          0     0;
      0.1075      1          0          0     0;
      1           0          0          0     0];


T=M*W
That=inv(T);
contrl=That*A1*T;

K=[a0 a1 a2+2.1945 a3+27.3254 a4-0.1075];
KK=K*That
KKK=[KK(1) KK(2) KK(3) KK(4)];
ki=-KK(5);
%the closed-loop system
AA=[A-B*KKK B*ki;
     -C      0];
```

```
BB=[0;
   0;
   0;
   0;
   0.2];     % Input to the linearized model using r=0.2 rad
CC=[C 0];
DD=[0];


t=0:0.02:6;
[y,x,t]=step(AA,BB,CC,DD,1,t);
plot(t,x);grid
title(' Response Curves x1, x2, x3, x4, x5 versus t')
xlabel('t Sec')
ylabel('x1, x2, x3, x4, x5')


text(1.3,0.04,'x1')
text(1.5,-0.34,'x2')
text(1.5,0.44,'x3')
text(2.33,0.26,'x4')
text(1.2,1.3,'x5')


figure
x1=[1 0 0 0 0]*x';
x2=[0 1 0 0 0]*x';
x3=[0 0 1 0 0]*x';
x4=[0 0 0 1 0]*x';
x5=[0 0 0 0 1]*x';


subplot(3,2,1);
plot(t,x1);grid
title('x1 versus t')
xlabel('t Sec')
ylabel('x1')

subplot(3,2,2);
plot(t,x2);grid
title('x2 versus t')
xlabel('t Sec')
ylabel('x2')

subplot(3,2,3);
plot(t,x3);grid
title('x3 versus t')
xlabel('t Sec')
ylabel('x3')

subplot(3,2,4);
plot(t,x4);grid
title('x4 versus t')
xlabel('t Sec')
ylabel('x4')

subplot(3,2,5);
plot(t,x5);grid
title('x5 versus t')
xlabel('t Sec')
ylabel('x5')
```

A.7 To find the CDM equivalent parameters from LQR method

Type : : Matlab m-file

File name : : equivalent mr tao.m

```
format short
syms s

  Model of the inverted pendulum
 ---------------------------------

%original system
A= [  0         1      0      0      ;
      27.3254   0      0      0.1053      ;
      0         0      0      1      ;
    -7.0558     0      0      -0.1075  ]  ;
B= [  0  ;
      -29.9990 ;
      0  ;
     30.6373   ];
C= [0 0  1  0];
D= [ 0 0 0 0];

%augmented system
A1=[A zeros(4,1);
   -C zeros(1,1)];
B1=[B;0];


% Retrieval of tau
%-------------------
KK=[-5.6365466e+000 -1.1788850e+000 -8.8440400e-001 -6.0777473e-001
3.1622777e-001]; % gain from LQR method

KKK=[KK(1) KK(2) KK(3) KK(4)];
ki=-KK(5);
AA=[A-B*KKK B*ki;
     -C      0];

BB=[0;
   0;
   0;
   0;
   0.2];

CC=[C 0];
DD=[0];

% Characteristic polynomial of pe' Tao
%---------------------------------------
a=poly(AA)
a0=a(6);a1=a(5);a2=a(4);a3=a(3);a4=a(2);a5=a(1);
tau=a1/a0 %the tau
g1=a1^2/(a0*a2)
```

```
g2=a2^2/(a1*a3)
g3=a3^2/(a2*a4)
g4=a4^2/(a3*a5)

%Reverse the order
 ----------------------
a0=(g4*g3^2*g2^3*g1^4)/(tau^5);
a1=a0*tau;
a2=(a1*tau)/g1;
a3=(a1*tau^2)/(g2*g1^2);
a4=(a1*tau^3)/(g3*g2^2*g1^3);
a5=(a1*tau^4)/(g4*g3^2*g2^3*g1^4);

Klqrbycdm=[a5 a4 a3 a2 a1 a0]
M=[B1 A1*B1 A1^2*B1 A1^3*B1 A1^4*B1];

%the result is …
%s^5+0.1075s^4-27.3254s^3-2.1945*s^2

W=[   0         -2.1945     -27.3254    0.1075    1;
      -2.1945   -27.3254    0.1075        1       0;
   -27.3254       0.1075       1          0       0;
      0.1075      1            0          0       0;
      1           0            0          0       0];

T=M*W;
That=inv(T);
That*A1*T;
K=[a0 a1 a2+2.1945 a3+27.3254 a4-0.1075];
KK2=K*That
KK

if KK2-KK<0.001
   disp('correct!!');
else
   disp('your computation is totally wrong');
end
```

A.8 Control source codes

Type : : C/C++ file

File name : : wfric3.c

```
#include <DOS.H>
#include <STDIO.H>

#define TCK 0x0d
#define DATA 1200

void interrupt (*Old_ISR)();

volatile int port300,port301,port302,port303;
```

```
volatile int sp1,sp2,encoder_p,encoder_m,i;

volatile float theta,theta_t,thetadot,beta,beta_t,betadot;
volatile float Ktheta,Kthetadot,Kbeta,Kbetadot,Ki,Mi,R;
volatile float fb1,fb1dot,fb2,fb2dot,output,t=0.025;
volatile float Fbar,Fs,Fc,Fhat;          //for the friction model

//interrupt for stabilizing controller using friction compensation
void interrupt My_ISR()
{
        disable();

        port300 = inportb(0x300);
        port301 = inportb(0x301);
        port302 = inportb(0x302);

        encoder_p=(port302*16)+((port301&0xf0)/16);
        encoder_m=((port301&0xf)*256)+port300;

        theta=((float)(encoder_p-sp1))*0.001571;
        thetadot=(theta-theta_t)/t;

        beta=((float)(encoder_m-sp2))*0.001571;
        betadot=(beta-beta_t)/t;

        theta_t=theta;
        beta_t=beta;

        fb1=Ktheta*theta;
        fb1dot=Kthetadot*thetadot;
        fb2=Kbeta*beta;
        fb2dot=Kbetadot*betadot;

        Mi=Mi+((-Ki)*(0-beta)*t);
        // friction compensator
        //added on 8-4-2547

        Fbar=-7.0558*theta-0.1075*betadot+30.6373*output;
        Fc=0.15;
        Fs=0.18;
        if(betadot==0)
        {if(Fbar>0)
        Fhat=Fs;
        else
        Fhat=-Fs;
        }
        else
        {if(betadot>0)
        Fhat=Fc;
        else
```

```
        Fhat=-Fc;
        }

        output=Mi-fb1-fb1dot-fb2-fb2dot+Fhat;

        output=output/(0.3*0.181);
        port303=output+0x7f;
        outportb(0x303,port303);
        outportb(0x20,0x20);  /* End of Interrupt */
        i=i++;
        enable();
}

//interrupt for swinging-up and stabilizing controller
/*
void interrupt My_ISR()
{
        disable();

        port300 = inportb(0x300);
        port301 = inportb(0x301);
        port302 = inportb(0x302);

        encoder_p=(port302*16)+((port301&0xf0)/16);
        encoder_m=((port301&0xf)*256)+port300;

        theta=((float)(encoder_p-sp1))*0.001571;
        thetadot=(theta-theta_t)/t;

        beta=((float)(encoder_m-sp2))*0.001571;
        if (beta>3.14)
         beta=beta-6.28;
        if (beta<-3.14)
         beta=beta+6.28;

        betadot=(beta-beta_t)/t;

        theta_t=theta;
        beta_t=beta;

        if (fabs(theta)>0.2)
        {
                Ec=thetadot*cos(theta);  //rate of pumped of the energy
            //  refb=0.4;
            //  Ec=thetadot;

                if (fabs(Ec)<0.1&fabs(beta)>0.0005)
                 CoE=-1;
                else
            //  if (fabs(Ec)>0.01&fabs(beta)>0.005)
```

```
                CoE=1;

                r=r*CoE;
               // refb=r;
                output=+1.3*(r-beta)-0.33*betadot;  //PD controller for arm postion

                output=output/(0.3*0.181);
                port303=0x7f+output;
                outportb(0x303,port303);
        }

        if(fabs(theta)<0.2)
        {
                fb1=Ktheta*theta;
                fb1dot=Kthetadot*thetadot;
                fb2=Kbeta*beta;
                fb2dot=Kbetadot*betadot;

                Mi=Mi+((-Ki)*(0-beta)*t);
                output=Mi-fb1-fb1dot-fb2-fb2dot;//Fhat;

                output=output/(0.3*0.181);
                port303=0x7f+output;
                outportb(0x303,port303);
        }

        i=i++;
        outportb(0x20,0x20); /* End of Interrupt */
        enable();
}
*/

void main()
{
FILE   *fpw1,*fpw2,*fpw3,*fpr1;

        clrscr();
        if((fpw1 = fopen("theta55.m","w"))==NULL)
                {
                puts("cannot open file theta.m\n");
                exit(1);
                }
        fprintf(fpw1,"a = [ ");

        if((fpw2 = fopen("beta55.m","w"))==NULL)
                {
                puts("cannot open file beta.m\n");
                exit(1);
                }
        fprintf(fpw2,"a = [ ");
```

```
if((fpw3 = fopen("output55.m";"w"))==NULL)
        {
        puts("cannot open file output.m\n");
        exit(1);
        }
fprintf(fpw3,"a = [ ");

if((fpr1 = fopen("gia1c2.dat","r"))!=NULL)
        {
fscanf(fpr1,"%e %e %e %e%e",&Ktheta,&Kthetadot,&Kbeta,&Kbetadot,&Ki);
        fclose(fpr1);
        }
else printf("Coudn't open the file \"gain.dat\"\n");

sp1=2000;
sp2=0;
Mi=0;
outportb(0x305,0x04);          /* Clear All PIC Microcontroller */
delay(5);
outportb(0x305,0x07);  /* Enable Encoder Microcontrollers */
outportb(0x303,0x7f);  /* Stop Motor */

while (!kbhit())
        {
        port300 = inportb(0x300);
        port301 = inportb(0x301);
        port302 = inportb(0x302);
        encoder_p=(port302*16)+((port301&0xf0)/16);
        encoder_m=((port301&0xf)*256)+port300;
        theta=((float)(encoder_p-sp1))*0.001571;
        beta=((float)(encoder_m-sp2))*0.001571;
        gotoxy(24,12);
        printf("theta=%f beta=%f",theta,beta);
        }
getch();
theta_t=theta;
sp2=encoder_m;
beta=((float)(encoder_m-sp2))*0.001571;
beta_t=beta;
i=0;

outportb(0x304,0x34);  /* Set Samping Period */
outportb(0x305,0x03);  /* Enable Sampling Clock Microcontrollers */
Old_ISR = getvect(TCK); /* Recieve Interrupt Vector */
setvect(TCK,My_ISR);   /* Set Interrupt Vector to My ISR */
outportb(0x21,(inportb(0x21) & 0xdf)); /* Enable IRQ5 */

while (!kbhit() & encoder_p <2200 & encoder_p >1800 & i<DATA)
        {
```

```
                gotoxy(7,14);
                printf("theta=%f thetadot=%f beta=%f
betadot=%f",theta,thetadot,beta,betadot);
                fprintf(fpw1,"%f %f;\n",t*i,theta);
                fprintf(fpw2,"%f %f;\n",t*i,beta);
                fprintf(fpw3,"%f %f;\n",t*i,output);
                }

        outportb(0x21,(inportb(0x21) | 0x20)); /* Disable IRQ5 */
        setvect(TCK,Old_ISR);   /* Return Interrupt Vector to Old ISR */
        outportb(0x303,0x7f);/* Stop Motor */
        outportb(0x305,0x04);          /* Clear All PIC Microcontroller */

        fprintf(fpw1,"%f %f];\n",t*i,theta);
        fprintf(fpw2,"%f %f];\n",t*i,beta);
        fprintf(fpw3,"%f %f];\n",t*i,output);

        fprintf(fpw1,"x = a(:, 1);\n");
        fprintf(fpw2,"x = a(:, 1);\n");
        fprintf(fpw3,"x = a(:, 1);\n");

        fprintf(fpw1,"y = a(:, 2);\n");
        fprintf(fpw2,"y = a(:, 2);\n");
        fprintf(fpw3,"y = a(:, 2);\n");

        fprintf(fpw1,"figure(1)\n");
        fprintf(fpw2,"figure(2)\n");
        fprintf(fpw3,"figure(3)\n");

        fprintf(fpw1,"plot(x,y)\n");
        fprintf(fpw2,"plot(x,y)\n");
        fprintf(fpw3,"plot(x,y)\n");

        fprintf(fpw1,"xlabel('Time(sec)')\n");
        fprintf(fpw1,"ylabel('Theta(rad)')\n");
                fprintf(fpw2,"xlabel('Time(sec)')\n");
        fprintf(fpw2,"ylabel('Beta(rad)')\n");
        fprintf(fpw3,"xlabel('Time(sec)')\n");
        fprintf(fpw3,"ylabel('Control Signal')\n");

        fprintf(fpw1,"title('Graph of Theta(Pendulum)')\n");
        fprintf(fpw2,"title('Graph of Beta(Base)')\n");
        fprintf(fpw3,"title('Graph of Control Signal')\n");

        fclose(fpw1);
        fclose(fpw2);
        fclose(fpw3);

}
```

Appendix B

Derivation of Equation 4.21

The Characteristic polynomial of the designed system is

$$P(s) = a_0\left[\left\{\sum_{i=2}^{n}\left(\prod_{j=1}^{i-1}\frac{1}{\gamma_{i-j}^{j}}\right)(\tau s)^i\right\} + \tau s + 1\right] \tag{B.1}$$

As the characteristic polynomial must be monic then

$$1 = a_0\prod_{j=1}^{n-1}\frac{\tau^n}{\gamma_{n-j}^{j}}\ , \tag{B.2}$$

on the other word

$$a_0 = \prod_{j=1}^{n-1}\frac{\gamma_{n-j}^{j}}{\tau^n}\ . \tag{B.3}$$

Multiplying to all term then we get

$$\begin{aligned} a_1 &= a_0\tau \\ &= \tau\prod_{j=1}^{n-1}\frac{\gamma_{n-j}^{j}}{\tau^n} = \prod_{j=1}^{n-1}\frac{\gamma_{n-j}^{j}}{\tau^{n-1}} \end{aligned} \tag{B.4}$$

$$\begin{aligned} a_2 + \cdots + a_{n-1} &= a_0\left\{\sum_{i=2}^{n-1}\left(\prod_{j=1}^{i-1}\frac{1}{\gamma_{i-j}^{j}}\right)\tau^i\right\} \\ &= \left\{\sum_{i=2}^{n-1}\left(\prod_{j=1}^{i-1}\frac{1}{\gamma_{i-j}^{j}}\right)\tau^i\right\}\prod_{k=1}^{n-1}\frac{\gamma_{n-k}^{k}}{\tau^n} \\ &= \sum_{i=2}^{n-1}\prod_{j=1}^{n-1}\frac{\gamma_{n-j}^{j}}{\tau^{n-i}}\prod_{k=1}^{i-1}\frac{1}{\gamma_{i-k}^{k}}\ . \end{aligned} \tag{B.5}$$

Therefore, in the compact form, the characteristic polynomial can be rewritten as

$$P(s) = s^n + \sum_{i=2}^{n-1}\left(\prod_{j=i}^{n-1}\gamma_j^{n-j}\prod_{k=1}^{i-1}\gamma_k^{n-i}\frac{1}{\tau^{n-i}}s^i\right) + \sum_{i=0}^{1}\left(\prod_{j=1}^{n-1}\gamma_{n-j}^{j}\frac{1}{\tau^{n-i}}s^i\right)\ . \tag{B.6}$$

APPENDIX C

Swinging-up the Inverted Pendulum by Energy Control [5]

Let consider again the inverted pendulum shown in Fig. 4.4. To be convenient it is depicted again in Fig. C.1. We have shown before that the energy and the rate of energy expressions are respectively described as

$$E = \frac{1}{2} J_p \dot{\theta}^2 + mgl\cos\theta . \tag{C.1}$$

$$\dot{E} = J_p \dot{\theta}\ddot{\theta} - mgl\dot{\theta}\sin\theta = -mal\dot{\theta}\cos\theta . \tag{C.1}$$

Figure C.1 Inverted pendulum when the base is fixed to its arm

Therefore, instead of controlling the original equation of motion, we can control its energy. The last equation tells us that the energy can be pumped to the system when the arm acceleration a is in the opposite direction of $\dot{\theta}\cos\theta$. A control strategy can be designed from Lyapunov method. Consider this choice of control law

$$u = mRa \tag{C.3}$$

such that the arm acceleration a is

$$a = \Psi(E - E_d)\cdot\dot{\theta}\cos\theta . \tag{C.4}$$

Using $V = \frac{1}{2}(E - E_d)^2$ as Lyapunov function candidate then we can find

$$\dot{V} = -ml\Psi\left(\frac{1}{2}(E - E_d)\dot{\theta}\cos\theta\right)^2 \tag{C.5}$$

which is negative semi-definite. This Lyapunov function decreases as long as $\dot{\theta} \neq 0$ and $\cos\theta \neq 0$. Since the pendulum cannot maintain a stationary position with $\dot{\theta} = \pm\frac{\pi}{2}$, therefore the control law (C.3) will drive the inverted pendulum toward its desired value E_d. To change the

energy as soon as possible the control signal should be as large as possible. This is achieved by the following control law

$$u = a = \tau_{m\max}\,\mathrm{sgn}\left((E - E_d)\cdot\dot{\theta}\cos\theta\right), \tag{C.6}$$

where $\tau_{\max}$ is the maximum torque could be generated by the DC motor. However it may result the chattering. Therefore, it motivates the following choice of control law

$$u = sat(\Psi(E - E_d)\cdot\mathrm{sgn}(\dot{\theta}\cos\theta)) \tag{C.7}$$

where Ψ is a constant gain, E_d is the desired energy level, sgn is the sign function and sat is the saturation function given as

$$sat(x) = \begin{cases} \tau_{m\max} & (x > 0) \\ 0 & (x = 0) \\ -\tau_{m\max} & (x < 0) \end{cases}. \tag{C.8}$$

APPENDIX D

Related Publications

[1] A.I. Cahyadi, T. Benjanarasuth, D. Isarakorn, J. Ngamwiwit and N. Komine, "CDM Controller Incorporating Friction Compensation for Rotational Inverted Pendulum," Proceedings of International Conference on Control, Automation and Systems (ICCAS2004), Bangkok, pp.1901-1905, August, 2004

[2] A.I. Cahyadi, D. Isarakorn, T. Benjanarasuth, J. Ngamwiwit and N. Komine, "Application of Coefficient Diagram Method for Rotational Inverted Pendulum Control," Proceedings of 8th International Conference on Control, Automation, Robotics and Vision (ICARCV 2004), Kunming, Peoples Republic of China, pp.1769-1773, December, 2004

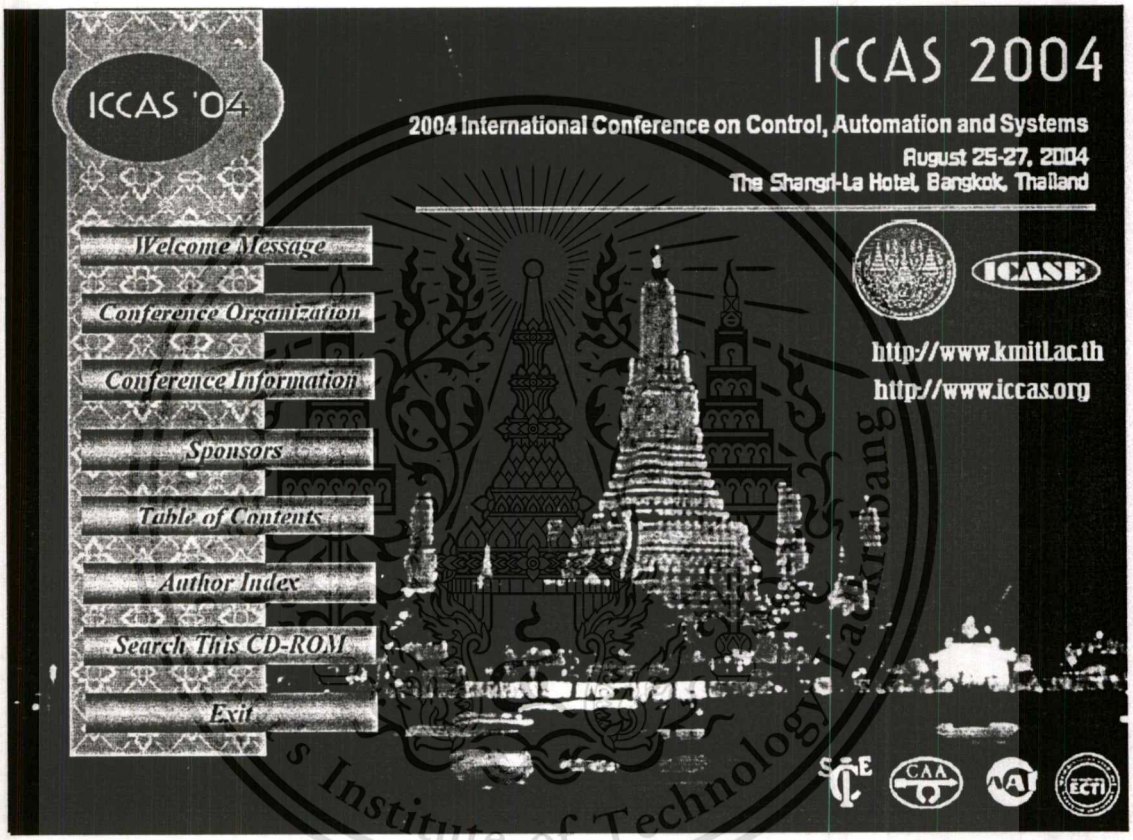

ICCAS2004 August 25-27, The Shangri-La Hotel, Bangkok, THAILAND

CDM Controller Incorporating Friction Compensation for Rotational Inverted Pendulum

Adha I. Cahyadi*, Taworn Benjanarasuth*, Don Isarakorn*, Jongkol Ngamwiwit* and Noriyuki Komine**

* Faculty of Engineering and Research Center for Communications and Information Technology
King Mongkut's Institute of Technology Ladkrabang, Bangkok 10520, Thailand
(Tel : +66-232-64-221, Fax: +66-232-64-225, E-mail: knjongko@kmitl.ac.th)

** Dept. of Applied Computer Engineering, School of Information Technology and Electronics
Tokai University, Hiratsuka-Shi,Kanagawa-Ken 259-1292, Japan
(Tel : +81-463-58-1211, Fax: +81-463-50-2240, E-mail: komine@keyaki.cc.u-tokai.ac.jp)

Abstract: A controller designed by CDM for a servo type system which is an augmented system constructed from a rotational inverted pendulum with an integrator added to its arm, is presented in this paper. In order to be able to apply the CDM concept, the augmented system must be linearized and converted into controllable canonical form. Then, the controller consisting of the state feedback gain matrix and an integral gain in the sense of CDM can be obtained. This shows that design procedure for the proposed controller is easy. The experimental results obtained from the rotational inverted pendulum controlled by the proposed controller show that the system response has no steady-state error, however, the oscillation amplitude of the arm angle is still significant. Therefore, in this paper, the friction compensation using Coulomb friction with stiction is also added to the controller. The oscillation amplitude of the arm angle that can be reduced remarkably is also shown in the experimental results.

Keywords: Rotational inverted pendulum, coefficient diagram method, state feedback, friction compensation

1. INTRODUCTION

Inverted pendulum is a famous tool for testing the effectiveness of many control schemes. Owing to their nonlinearity and unstable characteristic, the controller development had been a great interest of many researchers [1-6]. So far, many controllers had been implemented either linear or nonlinear controllers. The nonlinear controllers guarantee a wide range operation and overcome the hard nonlinearity [2-3]. In spite of having some drawbacks, a linear controller, however, is easier to be designed and implemented [4-6]. As proposed in [4], a linear controller based on linear quadratic regulator (LQR) with an integrator augmented to the rotating arm angle can satisfy the required specification. The integrator was needed to reject the steady-state error in controlling the inverted pendulum system due to the noise generated by the hardware. Unfortunately the choice in selecting the proper weighting matrix was still trial and error. Furthermore, when the inverted pendulum is linearized by neglecting the friction simply, it will lead to limit cycles, which implies to somewhat an oscillatory result [7-8]. As reported in [9], coefficient diagram method (CDM) can satisfy time domain specification and the design is simple. In CDM the stability and speed of the closed-loop system are related to the stability index and the equivalent time constant respectively. Then, the desired characteristic polynomial based on these parameters can be composed.

In this paper, a design of a controller to stabilize the inverted pendulum in upright position while maintaining the arm position angle in certain position using CDM will be presented. As the responses exhibit significant oscillation, friction compensation using Coulomb friction with stiction will also be introduced.

The rotational inverted pendulum shown in Fig. 2 is a SIMO system with motor torque input and two outputs i.e. the pendulum angle θ and the arm angle β. By employing the Newton-Euler formulation, a nonlinear model of the inverted pendulum system can be obtained. As a linear controller will be designed, the model must be linearized about upright position. After representing the linear model including one augmented integrator in state space form, it will be transformed into controllable canonical form utilizing a transformation matrix [10] so that the CDM concept can be applied. Then, each element of the state feedback gain matrix and the integral gain can be designed by matching the closed-loop characteristic polynomial of the system to those obtained from the CDM concept.

The experimental results of the proposed control system with and without friction compensation are also shown.

2. PLANT AND CDM CONCEPT

2.1 Overview of the plant

After applying Newton-Euler formulation, the inverted pendulum model is derived as the nonlinear equation as follows [4]

$$\dot{x} = f(x(t)) + g(x(t))u, \tag{1}$$

where

$$f(x) = \begin{bmatrix} x_2 \\ -\left(\frac{R\cos(x_1)}{mlR^2\sin^2 x_1 + Jl}\right)\left(mlRx_2^2\sin x_1 - bx_4 - \frac{(J+mR^2)g\sin x_1}{R\cos x_1}\right) \\ x_4 \\ \frac{1}{J+mR^2\sin^2 x_1}\left(-mRg\cos x_1\sin x_1 + mlRx_2^2\sin x_1 - bx_4\right) \end{bmatrix}$$

$$g(x) = \begin{bmatrix} 0 \\ -\left(\frac{R\cos(x_1)}{mlR^2\sin^2 x_1 + Jl}\right) \\ 0 \\ \frac{1}{J+mR^2\sin^2 x_1} \end{bmatrix},$$

and where $[x_1 \quad x_2 \quad x_3 \quad x_4]^T = [\theta \quad \dot{\theta} \quad \beta \quad \dot{\beta}]^T$, $u = \tau_m$, τ_m is the torque applied to the pivot, θ is the pendulum angle, β is the arm angle, m is the mass of the pendulum, l is the distance from the pivot point to the center of mass of the pendulum, R is the length of the rotating arm, J and b are the moment of inertia of the rotating arm and the pivot's friction coefficient respectively.

The equilibrium points which satisfy the following equation

$$0 = f(x(t)) + g(x(t))u \tag{2}$$

are $x_{ss} = [0 \quad 0 \quad c \quad 0]^T$ or $x_{ss} = [\pi \quad 0 \quad c \quad 0]^T$ and $u_{ss} = 0$ where c is any constant. First equilibrium point corresponds to the upright position which is unstable, while the second is the hanging position. Linearizing about its upright position we have

$$\dot{x}(t) = Ax(t) + Bu(t) \tag{3}$$

where

$$A = \begin{bmatrix} 0 & 1 & 0 & 0 \\ \frac{Jg + mgR^2}{Jl} & 0 & 0 & \frac{bR}{Jl} \\ 0 & 0 & 0 & 1 \\ \frac{-mgR}{J} & 0 & 0 & \frac{-b}{J} \end{bmatrix} \text{ and } B = \begin{bmatrix} 0 \\ \frac{-R}{Jl} \\ 0 \\ \frac{1}{J} \end{bmatrix}.$$

As our main interests are the arm angle β and the pendulum angle θ, the output equation is

$$y(t) = Cx(t), \tag{4}$$

where $C = \begin{bmatrix} 1 & 0 & 0 & 0 \\ 0 & 0 & 1 & 0 \end{bmatrix}$.

2.2 Concept of CDM

In CDM, the characteristic polynomial is given in the following form

$$P(s) = a_n s^n + \cdots + a_1 s^1 + a_0 = \sum_{i=0}^{n} a_i s^i . \tag{5}$$

Based on Eq. (5) the performance specification known as stability index γ_i, equivalent time constant τ and stability limit γ_i^* can be synthesized as these equations

$$\gamma_i = \frac{a_i^2}{a_{i-1}a_{i+1}}, \qquad (i = 1,2,\cdots,n-1) \tag{6}$$

$$\tau = \frac{a_1}{a_0}, \tag{7}$$

$$\gamma_i^* = \frac{1}{\gamma_{i-1}} + \frac{1}{\gamma_{i+1}}, \tag{8}$$

where $i = 1 \sim n-1$, $\gamma_1 = \gamma_n = \infty$.

Then the characteristic polynomial in term of γ_i, τ and a_0 can be expressed back as follows

$$P_m(s) = a_0 \left[\left\{ \sum_{i=2}^{n} \left(\prod_{j=1}^{i-1} \frac{1}{\gamma_{i-j}^{j}} \right) (\tau s)^i \right\} + \tau s + 1 \right]. \tag{9}$$

The choice of stability index γ_i due to the control design specifications must satisfy the following inequality

$$\gamma_i > 1.5\gamma_i^*, \tag{10}$$

and τ normally can be chosen from settling time specification as

$$\tau = t_s / (2.5 \sim 3). \tag{11}$$

However, in general the stability index known as standard stability index is recommended as

$$\gamma_{n-1} = \ldots = \gamma_3 = \gamma_2 = 2, \gamma_1 = 2.5. \tag{12}$$

3. CONTROL SYSTEM STRUCTURE

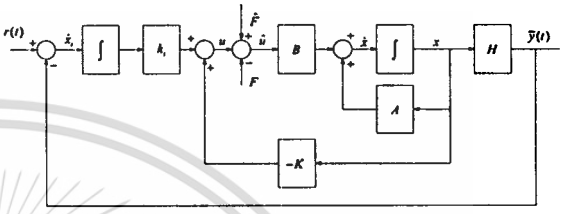

Fig. 1 Control system structure.

In this section, the CDM controller design procedure and friction compensation will be described respectively. Since an integrator is added to the arm of rotational inverted pendulum system for rejecting the steady-state error, the augmented system can be constructed as shown in Fig.1, and

$$\dot{x}_a(t) = A_a x_a(t) + B_a u(t) + G r(t) \tag{13}$$

$$y(t) = C_a x_a(t), \tag{14}$$

$$\dot{x}_i(t) = r(t) - Hx(t) \tag{15}$$

can also be obtained, where

$$x_a = \begin{bmatrix} x \\ x_i \end{bmatrix}, A_a = \begin{bmatrix} A & 0 \\ -H & 0 \end{bmatrix}, B_a = \begin{bmatrix} B \\ 0 \end{bmatrix}, G = \begin{bmatrix} 0 \\ 1 \end{bmatrix} \text{ and } C_a = \begin{bmatrix} C \\ 0 \end{bmatrix}^T$$

and where $r(t)$ is the reference signal to the arm angle, $H = [0 \quad 0 \quad 1 \quad 0]$ is derived from second row of C matrix and $x_i(t)$ is the state variable obtained by augmenting an integrator to the arm angle.

If the pair of A and B in Eq. (3) is controllable and $A_a = \begin{bmatrix} A & B \\ -H & 0 \end{bmatrix}$ is full rank, then the augmented system is completely state controllable. Therefore, the control law $u(t)$ can be assigned as

$$u(t) = -K_a x_a(t) \tag{16}$$

where $K_a = [K \quad -k_i]$, and where $K = [k_1 \quad k_2 \quad \ldots \quad k_{n-2} \quad k_{n-1}]$ is the state feedback gains matrix and $k_i = -k_n$ is the integral gain. Then the following relation can be derived as

$$\dot{x}_a(t) = (A_a - B_a K_a) x_a(t) + G r(t) = A_{cl} x_a(t) + G r(t). \tag{17}$$

3.1 CDM controller

In this sub-section, the design procedure for assigning the feedback gain matrix K and integral gain k_i of the system

shown in Fig. 1 by CDM is proposed. It can be done by matching the closed-loop characteristic polynomial of Eq. (17) to the characteristic polynomial obtained from CDM as the following procedure:

1. Transform the closed-loop system (17) into controllable canonical form as

$$\dot{z}(t) = T^{-1}A_{cl}Tz(t) + Gr(t) \tag{18}$$

by introducing a new state $z(t) = T^{-1}x_a(t)$. The transformation matrix T is defined as $T = MW$, where M and W are given by [10]

$$M = \begin{bmatrix} B_a & A_aB_a & A_a^2B_a & \cdots & A_a^{n-1}B_a \end{bmatrix}$$

$$W = \begin{bmatrix} \delta_1 & \delta_2 & \cdots & \delta_{n-1} & 1 \\ \delta_2 & \delta_3 & \cdots & 1 & 0 \\ \vdots & \vdots & & 0 & 0 \\ \delta_{n-1} & 1 & \cdots & 0 & 0 \\ 1 & 0 & \cdots & 0 & 0 \end{bmatrix},$$

and where $\delta_{n-1}, \delta_{n-2}, \ldots, \delta_1$ are the coefficient of the open-loop characteristic polynomial

$$P_a(s) = |sI - A_a| = s^n + \delta_{n-1}s^{n-1} + \ldots + \delta_1 s + \delta_0 .$$

2. Find the closed-loop characteristic polynomial of system (18) as

$$P_a(s) = |sI - T^{-1}A_{cl}T|$$
$$= s^n + (\delta_{n-1} + \hat{k}_n)s^{n-1} + (\delta_{n-2} + \hat{k}_{n-1})s^{n-2} + \ldots + (\delta_0 + \hat{k}_1), \tag{19}$$

where

$$K_aT = \begin{bmatrix} \hat{k}_1 & \hat{k}_2 & \cdots & \hat{k}_{n-1} & \hat{k}_n \end{bmatrix}. \tag{20}$$

3. Choose the equivalent time constant τ and the stability index γ_i and derive the desired characteristic polynomial

$$P(s) = s^n + \sum_{i=2}^{n-1}\left(\prod_{j=i}^{n-1}\gamma_j^{n-j}\prod_{k=1}^{i-1}\gamma_k^{n-i}\frac{1}{\tau^{n-i}}s^i\right) + \sum_{i=0}^{1}\left(\prod_{j=1}^{n-i}\gamma_{n-j}^{j}\frac{1}{\tau^{n-i}}s^i\right)$$
$$= s^n + a_{n-1}s^{n-1} + \cdots + a_1 s^1 + a_0 \tag{21}$$

from the characteristic polynomial (9) which is assumed to be monic (i.e. $a_n = 1$) so that $a_0 = (\prod_{j=1}^{n-1}\gamma_{n-j}^{j})/\tau^n$.

4. Equate the closed-loop characteristic polynomial (19) with the desired characteristic polynomial (21) to obtain

$$K_a = \begin{bmatrix} a_0 - \delta_0 & a_1 - \delta_1 & \ldots & a_{n-2} - \delta_{n-2} & a_{n-1} - \delta_{n-1} \end{bmatrix}T^{-1}. \tag{22}$$

3.2 Friction compensation

The friction compensation is introduced because of the ineligible limit cycles generated mainly by motor driving the arm. Some methods for friction compensation have been described in [8]. However, a simple method of Coulomb friction with stiction $\hat{F}$ which can effectively reduce the oscillation amplitude is employed and expressed as

$$\hat{F} = \begin{cases} F_c\,\mathrm{sgn}(\dot{\beta}) & \text{if } \dot{\beta} \neq 0, \\ \bar{F} & \text{if } \dot{\beta} = 0 \text{ and } |\bar{F}| < F_s, \\ F_s\,\mathrm{sgn}(\bar{F}) & \text{otherwise} \end{cases} \tag{23}$$

where F_c is the coulomb friction constant, F_s is the stiction constant and $\bar{F}$ is the resultant forces acting on the slip ring. In this case $\bar{F} = \frac{-mgR}{J}x_1(t) + \frac{-b}{J}x_4(t) + \frac{1}{J}u(t)$.

The friction compensation added to the system is shown in Fig. 1 and then is applied to the control law as

$$\hat{u} = K_a x_a + \hat{F}. \tag{24}$$

4. EXPERIMENTS

4.1 Experimental setup

In order to verify the effectiveness of the controller the experiments in controlling the pendulum angle θ and the arm angle β has been done. The physical parameters of the rotational inverted pendulum used in the experiments are shown in Table 1.

Table 1 Parameters of the inverted pendulum.

Pendulum mass (m)	0.05 kg
Pendulum length (l)	0.48 m
Arm length (R)	0.47 m
Moment of inertia (J)	0.03264 $kg \cdot m^2$
Viscous coefficient (b)	0.00351 $kg \cdot m^2/s$

As shown in Fig 2, the experimental apparatus consists of three main parts: the inverted pendulum system, the interfaces and the digital controller. The pendulum system composes of pendulum, rotating-arm, a high torque permanent magnet DC motor and two angular positions sensors to detect the pendulum angle θ and the arm position angle β. The interface devices are two microcontrollers PIC16C55 to filter the quadrature signal from each encoder, one microcontroller 89C1051 as a sampling clock generator, one eight-bit D/A converter and servo amplifier. A personal computer with Intel Pentium II 350 MHz processor is used as the digital controller. The control program is written in C language and the sampling period is set at 25 milliseconds.

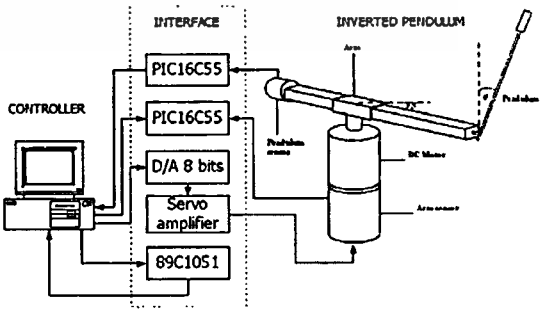

Fig. 2 Experimental apparatus.

4.2 Effect of stability index γ_i

First, the system responses corresponding to the variation of stability index will be observed. By varying the stability index from the standard stability index $\gamma_1 = 2.5, \gamma_2 = \gamma_3 = \gamma_4 = 2$ to $\gamma_1 = \gamma_2 = \gamma_3 = \gamma_4 = 2$ and to $\gamma_1 = \gamma_2 = \gamma_3 = \gamma_4 = 2.2$ then their corresponding gain K_a of the augmented system for $\tau = 1.2$ seconds can be obtained. As depicted in Fig. 3 the dark line, the light line and the dashed line respectively show their experimental results. It is shown that the responses of the system with different values of stability index oscillate around the zero radian line, which means that the integrator added to the arm angle of the rotational inverted pendulum can reject the steady-state error.

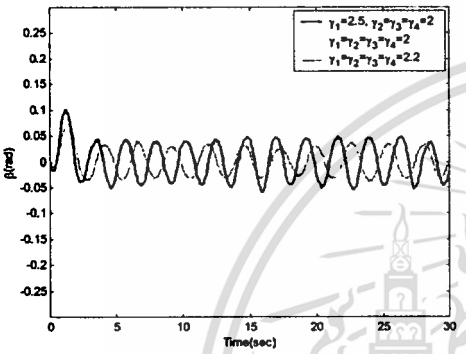

(a) Arm angle

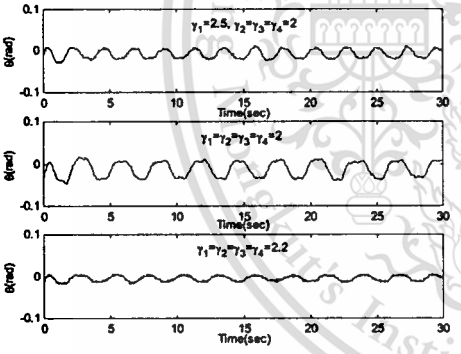

(b) Pendulum angle

Fig. 3 System responses when the stability index is varied.

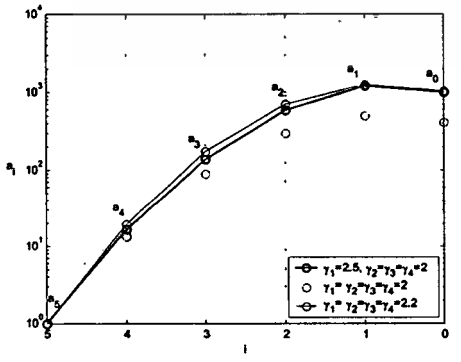

Fig. 4 Coefficient diagrams.

As reported in [9] the stability in CDM can be qualitatively observed visually using graphical interpretation known as coefficient diagram. The coefficient diagram of the proposed control system with varying stability index is shown in Fig. 4. By relating the responses in Fig. 3 to its coefficient diagram in Fig. 4, one can infer that the greater curvature of the coefficient diagrams implies to the smaller oscillation of its corresponding system responses. On the other words, the more stable system will lead to the smaller oscillation.

4.3 Effect of friction compensation

Indeed increasing the stability index can reduce the amplitude of oscillation. However, the control signal will be high which is undesirable. Therefore, simple model based friction compensation using Coulomb friction with stiction is developed and then is applied to the system at $t = 10$ seconds. Fig. 5 shows the responses of the inverted pendulum when the standard stability index γ_i and equivalent time constant $\tau = 1.2$ seconds are used. It is seen that the oscillation amplitude of the arm angle β can be reduced significantly.

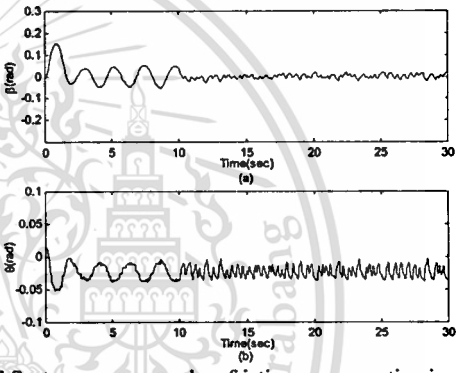

Fig.5 System responses when friction compensation is applied.

4.4 Tracking capability

In order to show the tracking capability, the reference input of the arm angle is changed from zero radian to one radian at 10 seconds for equivalent time constant $\tau = 1.2$ seconds. The result depicted in Fig. 6, shows that the output arm angle can track the constant reference input and oscillates around the one radian line, while the effect of the step change in arm angle does not affect the oscillatory behavior of the steady state response. It can also be observed that the rotational inverted pendulum angle is still almost unaffected at the steady state.

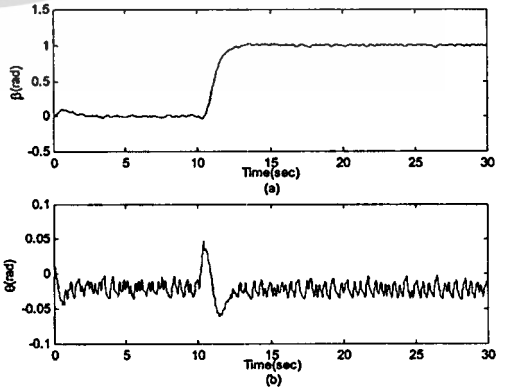

Fig. 6 Tracking capability response.

5. CONCLUSION

In conclusion, the controller designed by CDM incorporating simple friction compensation for a servo type system which is a rotational inverted pendulum with an integrator added to its arm have been proposed. The controller is implemented to control the system and the satisfied performances have been achieved. The good capabilities of angle position error rejection and tracking can be obtained as shown in the experiments. Furthermore, the coefficient diagram used for investigating system stability due to variation of stability index γ_1 has also been shown.

REFERENCES

[1] K. Chrisman and J. Vagners, "An Alternative Inverted Pendulum Apparatus for Education," *Proceedings of the* American *Control Conference 1995*, Vol. 1, pp. 554~558, USA, 21-23 June 1995.

[2] H. Morimoto, S. Kawamoto, "Nonlinear Control Based on Equilibrium Point Analysis for Inverted Pendulum," *Proceedings of the 41st SICE Annual Conference,* Vol. 1, pp 238 – 242, 5-7 Aug. 2002.

[3] M. Bugeja, "Non-Linear Swing-Up and stabilizing Control of an Inverted Pendulum System," *EUROCON 2003*, Vol. 2, pp. 437~441, 2003.

[4] N. Chanapan, S. Panaudomsup, J. Ngamwiwit. and N. Komine., "Experimental Study of Rotational Inverted Pendulum," *KACC 2000*, Korea, October 2000.

[5] J. Akesson, K. J. Astrom "Safe Manual Control of the Furuta Pendulum," *Proceedings of the 2001 IEEE International Conference Control Applications*, pp. 890~895, Mexico, 2001.

[6] S. Renou and L. Saydy, "Real Time Control of an Inverted Pendulum based on Approximate Linearization," *Canadian Conference on Electrical and Computer Engineering*, Vol. 2, pp. 502 – 504, Canada, 1996.

[7] H. Olsson, K. J. Astrom, "Friction Generated Limit Cycles 1," *Proceedings of the 2001 IEEE International Conference Control Applications*, pp. 798~803, Mexico, 2001.

[8] C. Canudas, H. Olsson, K. J. Astrom, "Dynamic Model Based Friction Compensation on the Furuta Pendulum," *IEEE Transaction on Automatic Control*, Vol. 40, No. 3, March 1995.

[9] S. Manabe, "Coefficient Diagram Method", *14th IFAC Symposium in Aerospace*, 1998.

[10] K. Ogata, Modern Control Engineering, Second Edition, Prentice-Hall international, Inc., 1990.

2004 8th International Conference on
Control, Automation, Robotics and Vision
Kunming, China, 6-9th December 2004

Application of Coefficient Diagram Method for Rotational Inverted Pendulum Control

A. I. Cahyadi[1], D. Isarakorn[1], T. Benjanarasuth[1], J. Ngamwiwit[1] and N. Komine[2]

[1] Faculty of Engineering and Research Center for Communication and Information Technology
King Mongkut's Institute of Technology Ladkrabang, Bangkok 10520, Thailand
Email: knjongko@kmitl.ac.th

[2] School of Information Technology and Electronics, Tokai University
Kitakaname, Hiratsuka-Shi, Kanagawa-Ken, 1117, Japan 1292-259
Email: komine@keyaki.cc.u-tokai.ac.jp

Abstract

In this paper, a design of the augmented state feedback controller by using the concept of Coefficient Diagram Method (CDM) for a servo type of the rotational inverted pendulum system is presented. An Integrator is augmented to the system due to the responses exhibiting steady-state error. In order to apply the CDM method, the augmented system must be firstly linearized and converted into controllable canonical form by a transform matrix. Then a feedback gain matrix in sense of CDM can be obtained. One can observe that the design procedure of the proposed controller is easy compared to other methods. The experimental results are shown in order to verify the effectiveness of the controller.

1 Introduction

An inverted pendulum is a nonlinear and unstable system and the developments of its controller have been a great interest for many researchers [1]-[6]. So far many kinds of inverted pendulum were implemented such as inverted pendulum on cart and rotational inverted pendulum. Some authors proposed nonlinear controller especially for those having strong non-linearity [2],[3]. Also, some issues on linearization method of the inverted pendulum such as approximate linearization were raised [4], [5].

In the contrary to the nonlinear controller, a linear controller is easier to be designed and implemented. As proposed in [6], a linear controller based on LQR with an integrator augmented to the rotating arm angle can satisfy the design specification. The integrator is needed to reject the steady-state error in controlling the inverted pendulum system due to the hardware of the system. Unfortunately the choice of the weighting matrix was still trial and error.

Coefficient Diagram Method, however, as reported in [7] can satisfy time domain specification. Thus, this paper will employ the CDM concept to design the state feedback gains and the integral gain of the inverted pendulum servo system instead of LQR. In CDM the stability and speed of the closed-loop system are related to the stability index γ_i and the equivalent time constant τ respectively. Then based on these parameters, the desired characteristic polynomial can be composed.

In order to apply the CDM concept, the system has to be linearized and transformed into the controllable canonical form by a transformation matrix. Then each element of the gain matrix can be designed by matching the closed-loop characteristic polynomial of the system to that obtained from the CDM concept.

2 Model of the Inverted Pendulum

From [6] the dynamic behavior of the system represented in Fig. 2 is described by

$$\tau_m = mlR\ddot{\theta}\cos\theta - mlR\dot{\theta}^2\sin\theta + b\dot{\beta} + (J + mR^2)\ddot{\beta} \quad (1)$$

$$mg\sin\theta = mR\ddot{\beta}\cos\theta + ml\ddot{\theta} \quad (2)$$

where τ_m is the torque applied to the pivot, θ is the pendulum angle, β is the arm position angle, m is the mass of the pendulum, l represents the distance from the pivot point to the center of mass of the pendulum, R is the length of the rotating arm, J and b are the moment of inertia of the rotating arm and the pivot's viscous friction coefficient respectively.

By linearizing the above equations about upright position, the state and the output equations of the rotational inverted pendulum system can be obtained as follows

$$\dot{x}(t) = Ax(t) + Bu(t) \quad (3)$$

$$y(t) = Cx(t) \quad (4)$$

where

$$A = \begin{bmatrix} 0 & 1 & 0 & 0 \\ \frac{mgR^2 + Jg}{Jl} & 0 & 0 & \frac{bR}{Jl} \\ 0 & 0 & 0 & 1 \\ -\frac{mgR}{J} & 0 & 0 & -\frac{b}{J} \end{bmatrix}, \quad B = \begin{bmatrix} 0 \\ -\frac{R}{Jl} \\ 0 \\ \frac{1}{J} \end{bmatrix} \quad \text{and} \quad C = \begin{bmatrix} 1 & 0 \\ 0 & 0 \\ 0 & 1 \\ 0 & 0 \end{bmatrix}^T.$$

0-7803-8653-1/04/$20.00 © 2004 IEEE

The input control signal $u(t)$ is the input torque τ_m proportional to input voltage of DC motor current driver, the output $y_1(t)$ is the inverted pendulum angle θ and $y_2(t)$ is the arm angle β, and the state variables are $x_1(t)=\theta$, $x_2(t)=\dot{\theta}$, $x_3(t)=\beta$ and $x_4(t)=\dot{\beta}$.

2.1 Augmented System

In this subsection, an integrator is augmented to the system of equation (3) and (4) in order to reject the steady-state error at the arm angle. Since the pendulum angle θ will be naturally kept around zero radian, only the arm angle β is used for the augmented system. Thus, the output matrix C is reduced to $H=[0\ \ 0\ \ 1\ \ 0]$. The block diagram of the linearized augmented system is illustrated in Fig. 1.

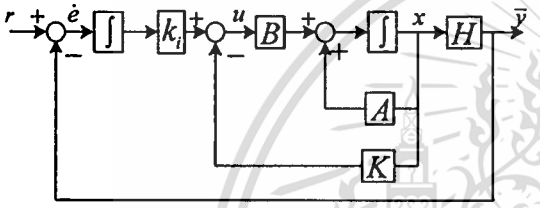

Figure 1. Augmented system

The state equation and output equation of the augmented system shown in Fig. 1 are given as follows

$$\dot{x}_a(t)=A_a x_a(t)+B_a u(t)+Fr(t) \tag{5}$$

$$\bar{y}(t)=H_a x_a(t) \tag{6}$$

where $\bar{y}(t)$ is the controlled output arm angle $y_2(t)$, $r(t)$ is the arm angle reference signal of the rotational inverted pendulum system and $e(t)$ is the augmented state variable for the arm angle output, and

$$A_a=\begin{bmatrix} A & 0 \\ -H & 0 \end{bmatrix}, B_a=\begin{bmatrix} B \\ 0 \end{bmatrix}, H_a=[H\ \ 0], F=\begin{bmatrix} 0 \\ 1 \end{bmatrix}$$

$$x_a(t)=\begin{bmatrix} x(t) \\ e(t) \end{bmatrix}.$$

If the pair of A and B of equation (3) is controllable and $\begin{bmatrix} A & B \\ -H & 0 \end{bmatrix}$ is full rank, then the system in equation (5) becomes completely state controllable. Therefore, the control law $u(t)$ can be assigned as given by

$$\begin{aligned} u(t) &= -K_a x_a(t) = -\begin{bmatrix} K & -k_i \end{bmatrix} x_a(t) \\ &= -\begin{bmatrix} k_1 & k_2 & \cdots & k_{n-1} & | & k_n \end{bmatrix} x_a(t) \end{aligned} \tag{7}$$

where K and k_i are state feedback gains and integral gain respectively. Therefore, the closed-loop system of the augmented system (5) and (6) with the control law (7) is

$$\dot{x}_a(t)=(A_a-B_aK_a)x_a(t)+Fr(t). \tag{8}$$

The state feedback gains and integral gain of the control law will be designed by CDM later.

3 Concept of CDM

In CDM, the controllers are designed based on the stability index known as γ_i and the equivalent time constant known as τ which are synthesized from the characteristic polynomial of the closed-loop transfer function.

$$P(s)=a_n s^n+a_{n-1}s^{n-1}+\cdots+a_1 s+a_0. \tag{9}$$

From the characteristic polynomial $P(s)$ given in (9), the stability index γ_i and the equivalent time constant τ are respectively described in general term as the following equations [7]

$$\gamma_i=\frac{a_i^2}{a_{i-1}a_{i+1}}, \quad (i=1,2,\cdots,n-1) \tag{10}$$

$$\tau=\frac{a_1}{a_0}. \tag{11}$$

In order to meet the specifications, the equivalent time constant τ and the stability index γ_i are normally chosen as

$$\tau=\frac{t_s}{2.5}\sim\frac{t_s}{3} \tag{12}$$

$$\gamma_i > 1.5\gamma_i^* \tag{13}$$

where t_s is the specified settling time and γ_i^* is the stability limit defined as

$$\gamma_i^*=\frac{1}{\gamma_{i+1}}+\frac{1}{\gamma_{i-1}} \quad ; \quad \gamma_0,\gamma_n=\infty. \tag{14}$$

In general the stability index is recommended as

$$\gamma_{n-1}=\ldots=\gamma_3=\gamma_2=2,\gamma_1=2.5 \tag{15}$$

known as standard stability index.

Finally the characteristic polynomial known as the desired characteristic polynomial can be expressed as

$$\begin{aligned} P_m(s) &= a_0\left[\left\{\sum_{i=2}^{n}\left(\prod_{j=1}^{i-1}\frac{1}{\gamma_{i-j}^{j}}\right)(\tau s)^i\right\}+\tau s+1\right] \\ &= a_n s^n+a_{n-1}s^{n-1}+\ldots+a_1 s+a_0, \end{aligned} \tag{16}$$

where $a_n, a_{n-1}, \cdots, a_0$ are the coefficients of the desired characteristic polynomial.

4 Controller Design

The open-loop polynomial of the augmented system (5) is given by

$$P_{ol}(s) = |sI - A_a| = s^n + \delta_{n-1}s^{n-1} + \ldots + \delta_1 s + \delta_0, \quad (17)$$

where $\delta_{n-1}, \ldots, \delta_0$ are the coefficients of the polynomial.

In order to be able to apply the concept of CDM, the state variable controllable form of the augmented system (5) must be obtained via the transformation matrix T given by

$$T = MW \quad (18)$$

where M and W from [8] are given by

$$M = \begin{bmatrix} B & AB & A^2B & \cdots & A^{n-1}B \end{bmatrix} \quad (19)$$

and

$$W = \begin{bmatrix} \delta_1 & \delta_2 & \cdots & \delta_{n-1} & 1 \\ \delta_2 & \delta_3 & \cdots & 1 & 0 \\ \vdots & \vdots & & \vdots & \vdots \\ \delta_{n-1} & 1 & \cdots & 0 & 0 \\ 1 & 0 & \cdots & 0 & 0 \end{bmatrix}. \quad (20)$$

By defining the relation of

$$x_a(t) = Tz(t), \quad (21)$$

system (5) can be transformed into controllable canonical form as

$$\dot{z}(t) = A_c z(t) + B_c r(t) \quad (22)$$

where $A_c = T^{-1}(A_a - B_a K_a)T$ and $B_c = T^{-1}F$. Consequently, its characteristic polynomial is

$$p(s) = |sI - A_c| = s^n + (\hat{k}_n + \delta_{n-1})s^{n-1} + \cdots + (\hat{k}_2 + \delta_1)s + (\hat{k}_1 + \delta_0) \quad (23)$$

where

$$K_a T = \begin{bmatrix} \hat{k}_1 & \hat{k}_2 & \cdots & \hat{k}_{n-1} & \hat{k}_n \end{bmatrix}.$$

Hence, state feedback gains K and integral gain k_I of the gain matrix K_a can be obtained by equating the closed-loop augmented characteristic polynomial (23) to the desired characteristic polynomial (16). Note that the desired characteristic polynomial must be monic (that is $a_n = 1$), which implies to $a_0 = (\prod_{j=1}^{n-1} \gamma_{n-j}^j)/\tau^n$. Finally, the gain matrix K_a for the augmented system (5) can be found as

$$K_a = \begin{bmatrix} a_0 - \delta_0 & \cdots & a_{n-2} - \delta_1 & | & a_{n-1} - \delta_{n-1} \end{bmatrix} T^{-1}. \quad (24)$$

5 Experiments

5.1 Outline of the System

The experiments have been done in order to show the effectiveness of the controller. As shown in Fig. 2, the experimental apparatus consists of three main parts: the inverted pendulum system, the interfaces and the digital controller.

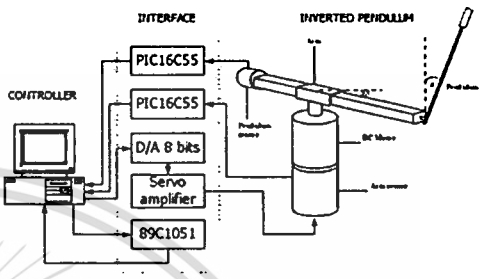

Figure 2. Rotational inverted pendulum system

The pendulum system composes of pendulum, rotating-arm, a high torque permanent magnet DC motor and two angular position sensors to detect the pendulum angle θ and the arm position angle β. The interface devices are two microcontrollers PIC16C55 to filter the quadrature signal from each encoder, one microcontroller 89C1051 as a sampling clock generator, one eight-bit D/A converter and servo amplifier. A personal computer with Intel Pentium II 350 MHz processor is used as the digital controller and the sampling time is set to be 25 milliseconds. The physical parameters of the rotational inverted pendulum system in the laboratory can be found in Table 1.

Pendulum mass (m)	0.05 kg
Pendulum length (l)	48 cms
Arm length (R)	57 cms
Moment of inertia (J)	0.03264 $kg \cdot m^2$
Friction coefficient (b)	0.00351 $kg \cdot m^2/s$

Table 1. Parameters of the inverted pendulum

5.2 Response of the Augmented System

By assigning the equivalent time constant τ to be 1.2 seconds and varying the stability index γ_i from $\gamma_1 = 2.5$, $\gamma_2 = \gamma_3 = \gamma_4 = 2$ to $\gamma_1 = \gamma_2 = \gamma_3 = \gamma_4 = 2$ and to $\gamma_1 = \gamma_2 = \gamma_3 = \gamma_4 = 2.2$, then the corresponding feedback gains and integral gains K_a of the augmented system can be obtained as summarized in Table 2. The experimental results when the constant reference input of the arm angle is zero radian are depicted in Fig. 3. as shown by dark solid line, dash line and light solid line respectively. It is seen from Fig. 3 that the responses of

the system with different values of stability index γ_i oscillate around the zero radian line. This means that the effectiveness of the integrator, which is added to the rotational inverted pendulum arm, can reject the steady-state error.

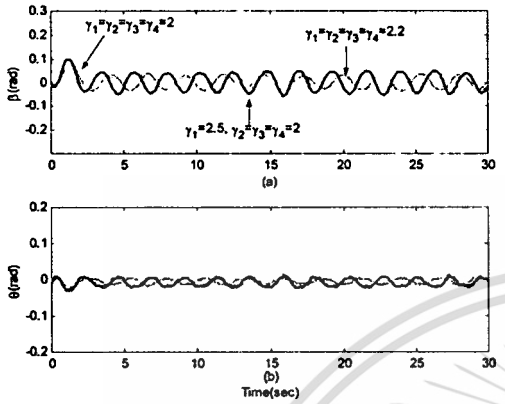

(a) Arm angle, (b) Inverted pendulum angle

Figure 3. System responses with various γ_i

The system stability can be evaluated by using the coefficient diagram as shown in Fig. 4 [7]. In CDM, the greater curvature of the coefficient diagrams implies to the more stable system. The light solid line shown in Fig. 4 has the most curvature, therefore, this system is the most stable when compared to the dark solid line and the dash line. As demonstrated in Fig. 3, the more stable system implies to the smaller amplitude of oscillation.

γ_i	K_a
[2.5 2 2 2]	[-7.5092 -1.5808 -1.9274 -1.0074 1.6062]
[2 2 2 2]	[-4.6803 -0.9611 -0.7895 -0.5094 0.6579]
[2.2 2.2 2.2 2.2]	[-8.7764 -1.8768 -2.0477 -1.2040 1.7064]

Table 2. State feedback gains and integral gains of various γ_i

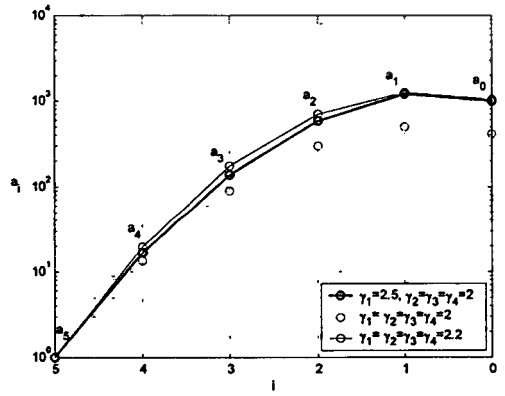

Figure 4. Coefficient diagram of various γ_i

5.3 Tracking Capability

In this subsection, the responses of the arm angle and the rotational inverted pendulum angle when the reference input of the arm angle changes from zero radian to one radian at 10 seconds will be investigated. In this experiment the same controller designed by $\tau =$ 1.2 seconds and standard stability index will be employed. The experimental results are shown in Fig. 5. One can observe from the response shown in Fig. 5(a) that the output arm angle can track the changed reference input properly. Furthermore, the response of the arm angle still oscillates around the one radian line, while the effect of the step change in arm angle does not affect the oscillatory behavior of the steady state response. It can be also observed from Fig. 5(b) that the rotational inverted pendulum angle is still almost unaffected except at the point of the step change occurred.

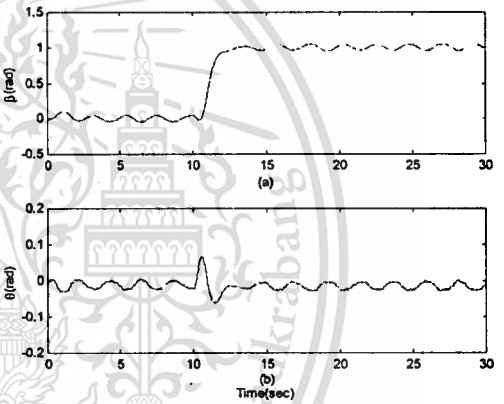

(a) Arm angle, (b) Inverted pendulum angle

Figure 5. Responses to the step change

6 Conclusions

An augmented state feedback controller based on CDM for controlling the rotational inverted pendulum servo system has been proposed in this paper. The controller has been implemented to control the system and the satisfied performances have been achieved. The results have shown that the proposed controller can reject the angle position error of the arm. It is also observed that choosing the stability index γ_i appropriately can increase the system stability. Furthermore the output of the system can still track the changed reference input without the error at the steady state.

7 Acknowledgements

This works received the financial assistance from AUN-SEED/Net program which is supported by JICA and ASEAN foundation. The authors would like to thank for their kind support.

References

[1] K. Crisman and J. Vagners, "An Alternative Inverted Pendulum Apparatus for Education," *Proceedings of American Control Conference 1995*, Seattle, pp. 554-558. June 1995.

[2] B. Codrons, F. D. Bruyne, M. D. Wan, and M. Gevers, "Iterative Feedback Tuning of a Nonlinear Controller for an Inverted Pendulum with a Flexible Transmission," *ICCA1998*, Italy, 1998

[3] H. Morimoto, S. Kawamoto, "Nonlinear Control Based on Equilibrium Point Analysis for Inverted Pendulum," *Proceedings of the 41st SICE Annual Conference,* Vol. 1, pp 238-242, Osaka, Japan, 2002

[4] T. Sugie, K. Fujimoto, "control of The Inverted Pendulum Systems based on Approximate Linearization: Design and Experiment," *Proceedings of 33rd Conference on Decision and Control*, 1994

[5] S. Renou and L. Saydy, "Real Time Control of an Inverted Pendulum based on Approximate Linearization," *Canadian Conference on Electrical and Computer Engineering*, Vol. 2, pp. 502-504 Canada, 1996

[6] N. Chanapan, S. Panaudomsup, J. Ngamwiwit. and N. Komine., "Experimental Study of Rotational Inverted Pendulum," *KACC2000*, Korea, October 2000.

[7] S. Manabe, "Coefficient Diagram Method", *14th IFAC Symposium in Aerospace*, 1998.

[8] K. Ogata, Modern Control Engineering, Second Edition, Prentice-Hall international, Inc., 1990.

Author Biography

Adha Imam Cahyadi was born in Jakarta, Indonesia, on November 02, 1979. He obtained his bachelor degree in Electrical Engineering, Major in Control System from Gadjah Mada University (UGM), Jogjakarta, Indonesia in 2002. After graduated, he worked in Matsushita Kotobuki Electronics and Halliburton Energy Services in Indonesia as an engineer from September 2002 to February 2003. His job was dealt with electronic devices and troubleshooting. Since May 2003 he has been joining with Department of Control Engineering, King Mongkut's Institute of Technology Ladkrabang (KMITL) in Bangkok, Thailand as Master Student of the AUN-SEED/Net project under the JICA program. There he is being a student member of Control and Mechatronics Laboratory, Research Centre for Communication and Information Technology (ReCCIT) and Electrical Engineering/Electronics, Computer, Telecommunication, and Information Technology (ECTI) Thailand.

His research area is the design of servo system for rotational inverted pendulum using CDM approach toward his master degree.